

**PETROGRAPHIC ANALYSIS  
OF MIXED CARBONATE-CLASTIC  
HYDROSTRATIGRAPHIC UNITS IN  
THE GENERAL SEPARATIONS AREA (GSA),  
SAVANNAH RIVER SITE (SRS),  
AIKEN, SOUTH CAROLINA (U)**

Paul A. Thayer, Anrew D. Smits, Wayne H. Parker, Karen R. Conner, Mary K. Harris, and  
Mark B. Amidon,

Publication Date: December 17, 1993

Westinghouse Savannah River Company  
Environmental Restoration Department  
Savannah River Site  
Aiken, SC 29808

---

**PETROGRAPHIC ANALYSIS  
OF MIXED CARBONATE-CLASTIC  
HYDROSTRATIGRAPHIC UNITS IN  
THE GENERAL SEPARATIONS AREA (GSA),  
SAVANNAH RIVER SITE (SRS),  
AIKEN, SOUTH CAROLINA (U)**

**Westinghouse Savannah River Company  
Environmental Restoration Department  
Savannah River Site  
Aiken, SC 29808**

**Prepared By:  
Science Applications International Corporation  
360 Bay Street, Suite 200  
Augusta, GA 30901**

**WSRC Contract Number AA46324P  
Task Order 8**

## **ABSTRACT**

---

Petrographic study of several hundred samples collected from hydrostratigraphic units including the "calcareous zone" in the General Separations Area at the SRS indicates that aquifer unit IIA, confining unit IIA-IIB, and aquifer zone IIB<sub>1</sub> are divisible into eight microfacies: quartz sand and sandstone; terrigenous mud and mudstone; skeletal lime mudstone; skeletal wackestone; skeletal packstone; skeletal grainstone; microsparite; and siliceous mudstone. All the carbonate microfacies contain appreciable amounts of terrigenous mud and quartz sand. Foraminifers, and worn and abraded byozoans, echinoderms, and molluscs are the dominant skeletal allochems.

The depositional model proposed for these units is a shallow marine shelf that received variable amounts of terrigenous sediment input. Diagenetic pathways for the carbonate sediment typically included: (1) marine phreatic — skeletal micritization and rare fibrous cementation within foraminiferal tests; (2) meteoric vadose — minor leaching of aragonitic skeletal grains; and (3) meteoric phreatic — neomorphism of micrite to microspar and pseudospar, wholesale dissolution of opal-A and aragonitic skeletal grains, formation of equant low-Mg calcite spar, and development of syntaxial calcite overgrowths on echinoderm fragments. Minor opal-CT and fibrous chalcedony cements are ubiquitous in all microfacies. The source of the silica was dissolution of biogenic opal-A from sponge spicules and diatom valves.

The dominant porosity types in the carbonate microfacies are secondary moldic and vug, with subordinate channel, interparticle, intraparticle, and intercrystal. Interparticle is the dominant pore type in the sand and sandstone microfacies. Moldic pores formed chiefly from dissolution of aragonitic pelecypods and gastropods. Solution-enlargement of molds produced vug and channel pores. Minor cementation by low-Mg calcite spar has locally reduced moldic, vug, and interparticle pores. Permeability of the carbonate microfacies is controlled by allochem composition and packing, volume of micrite and terrigenous mud, and amount of secondary dissolution and cementation.

## TABLE OF CONTENTS

---

<b>ABSTRACT .....</b>	<b>ii</b>
<b>LIST OF FIGURES .....</b>	<b>vi</b>
<b>LIST OF TABLES .....</b>	<b>viii</b>
<b>LIST OF APPENDICES .....</b>	<b>ix</b>
<b>1.0 INTRODUCTION .....</b>	<b>1</b>
<b>1.1 General .....</b>	<b>1</b>
<b>1.2 Hydrostratigraphy .....</b>	<b>3</b>
<b>1.3 Materials and Methods .....</b>	<b>5</b>
<b>2.0 PETROLOGY .....</b>	<b>8</b>
<b>2.1 General .....</b>	<b>8</b>
<b>2.2 Aquifer Unit IIA .....</b>	<b>10</b>
<b>2.2.1 General .....</b>	<b>10</b>
<b>2.2.2 Terrigenous Mud .....</b>	<b>10</b>
<b>2.2.2.1 Description .....</b>	<b>10</b>
<b>2.2.2.2 Interpretation .....</b>	<b>11</b>
<b>2.2.3 Terrigenous Sand and Sandstone .....</b>	<b>11</b>
<b>2.2.3.1 Description .....</b>	<b>11</b>
<b>2.2.3.2 Interpretation .....</b>	<b>13</b>
<b>2.3 Confining Unit IIA-IIB .....</b>	<b>14</b>
<b>2.3.1 General .....</b>	<b>14</b>
<b>2.3.2 Lime Mud .....</b>	<b>14</b>
<b>2.3.2.1 Description .....</b>	<b>14</b>
<b>2.3.2.2 Interpretation .....</b>	<b>15</b>
<b>2.3.3 Siliceous Mudstone .....</b>	<b>17</b>
<b>2.3.3.1 Description .....</b>	<b>17</b>
<b>2.3.3.2 Interpretation .....</b>	<b>18</b>

## TABLE OF CONTENTS (Continued)

---

2.3.4	<i>Sandy Terrigenous Mud</i>	20
2.3.4.1	<u>Description</u>	20
2.3.4.2	<u>Interpretation</u>	20
2.3.5	<i>Terrigenous Sand and Sandstone</i>	21
2.3.5.1	<u>Description</u>	21
2.3.5.2	<u>Interpretation</u>	22
2.4	<i>Aquifer Zone IIB<sub>1</sub></i>	24
2.4.1	<i>General</i>	24
2.4.2	<i>Lime Mud</i>	25
2.4.2.1	<u>Description</u>	25
2.4.2.2	<u>Interpretation</u>	26
2.4.3	<i>Skeletal Wackestone</i>	27
2.4.3.1	<u>Description</u>	27
2.4.3.2	<u>Interpretation</u>	29
2.4.4	<i>Skeletal Packstone</i>	31
2.4.4.1	<u>Description</u>	31
2.4.4.2	<u>Interpretation</u>	32
2.4.5	<i>Skeletal Grainstone</i>	33
2.4.5.1	<u>Description</u>	33
2.4.5.2	<u>Interpretation</u>	34
2.4.6	<i>Microsparite</i>	34
2.4.6.1	<u>Description</u>	34
2.4.6.2	<u>Interpretation</u>	36
2.4.7	<i>Siliceous Mudstone</i>	37
2.4.7.1	<u>Description</u>	37
2.4.7.2	<u>Interpretation</u>	38

## **TABLE OF CONTENTS (Continued)**

---

2.4.8 <i>Terrigenous Mud</i> .....	39
2.3.8.1 <u>Description</u> .....	39
2.3.8.2 <u>Interpretation</u> .....	40
2.4.9 <i>Terrigenous Sand and Sandstone</i> .....	40
2.4.9.1 <u>Description</u> .....	40
2.4.9.2 <u>Interpretation</u> .....	41
3.0 SUMMARY AND CONCLUSIONS .....	42
REFERENCES .....	44
APPENDIX A	
APPENDIX B	

## LIST OF FIGURES

---

1	Location of the General Separations Area, Savannah River Site, South Carolina .....	53
2	Lithostratigraphic and Hydrostratigraphic Nomenclature for the General Separations Area .....	54
3	Wells and Boreholes in the General Separations Area that Penetrate Carbonate Sediment or Rock .....	55
4	Computed Percentage of Carbonate for 396 Samples in the General Separations Area, SRS .....	56
5	Summary of Insoluble Residue Data for Well BGO-9AA, General Separations Area, SRS .....	57
6	Summary of Insoluble Residue Data for Well FSB-116C, General Separations Area, SRS .....	58
7	Summary of Insoluble Residue Data for Well HPT-2A, General Separations Area, SRS .....	59
8	Summary of Insoluble Residue Data for Well HSB TB, General Separations Area, SRS .....	60
9	Summary of Insoluble Residue Data for Well YSC-5A, General Separations Area, SRS .....	61
10	Classification of "Calcareous Zone" Sediments and Sedimentary Rocks according to Folk's (1980) Classification .....	62
11	Photomicrograph of Unconsolidated Mud from Terrigenous Mud Microfacies, Aquifer Unit IIA .....	63
12	Photomicrograph of Muddy Sand from Terrigenous Sand and Sandstone Microfacies, Aquifer Unit IIA .....	63
13	Photomicrograph of Chalcedony-Cemented Quartzarenite from Terrigenous Sand and Sandstone Microfacies, Aquifer Unit IIA .....	64
14	Photomicrograph of Unconsolidated Lime Mud, Lime Mud Microfacies, Confining Unit IIA-IIB .....	64
15	Photomicrograph of Sandy, Siliceous Mudstone, Siliceous Mudstone Microfacies, Confining Unit IIA-IIB .....	65
16	Photomicrograph of Sandy, Skeletal Siliceous Mudstone, Siliceous Mudstone Microfacies, Confining Unit IIA-IIB .....	65
17	Photomicrograph of Quartz-Rich Mud, Terrigenous Mud Microfacies, Confining Unit IIA-IIB .....	66

## LIST OF FIGURES (Continued)

18	Photomicrograph of Unconsolidated Muddy Sand, Terrigenous Sand and Sandstone Microfacies, Confining Unit IIA-IIB .....	66
19	Photomicrograph of Chalcedony-Cemented Quartzarenite from Terrigenous Sand and Sandstone Microfacies, Confining Unit IIA-IIB .....	67
20	Composition of 148 Sediment and Rock Samples from the General Separations Area according to Lindholm's (1987) Modified Classification. ....	68
21	Ternary Diagram after Folk (1962) Showing Composition of Carbonate Sediment Samples from Aquifer Zone IIB <sub>1</sub> , General Separations Area, SRS .....	69
22	Ternary Diagram Showing Proportion of Skeletal Allochems in Carbonate Sediment Samples from Aquifer Zone IIB <sub>1</sub> , General Separations Area, SRS .....	70
23	Composition of 103 Thin-Section Samples Collected from Aquifer Zone IIB <sub>1</sub> , General Separations Area, SRS .....	71
24	Photomicrograph of Quartz-Rich Lime Mud, Lime Mud Microfacies, Aquifer Zone IIB <sub>1</sub> .....	72
25	Photomicrograph of Skeletal Wackestone, Skeletal Wackestone Microfacies, Aquifer Zone IIB <sub>1</sub> .....	72
26	Photomicrograph of Quartz-Rich Skeletal Wackestone, Skeletal Wackestone Microfacies, Aquifer Zone IIB <sub>1</sub> .....	73
27	Photomicrograph of Quartz-Rich Skeletal Packstone, Skeletal Packstone Microfacies, Aquifer Zone IIB <sub>1</sub> .....	73
28	Photomicrograph of Quartz-Rich Skeletal Grainstone, Skeletal Grainstone Microfacies, Aquifer Zone IIB <sub>1</sub> .....	74
29	Photomicrograph of Quartz-Rich Microsparite, Microsparite Microfacies, Aquifer Zone IIB <sub>1</sub> .....	74
30	Photomicrograph of Quartz-Rich Siliceous Mudstone, Siliceous Mudstone Microfacies, Aquifer Zone IIB <sub>1</sub> .....	75
31	Photomicrograph of Quartz-Rich Terrigenous Mud, Terrigenous Mud Microfacies, Aquifer Zone IIB <sub>1</sub> .....	75
32	Photomicrograph of Muddy Sand from Terrigenous Sand and Sandstone Microfacies, Aquifer Zone IIB <sub>1</sub> .....	76
33	Photomicrograph of Chalcedony-Cemented Quartzarenite, Terrigenous Sand and Sandstone Microfacies, Aquifer Zone IIB <sub>1</sub> .....	76



## LIST OF TABLES

---

1	Classifications and Terminology used in this Report .....	77
2	Composition of Skeletal Wackestone, Aquifer Zone IIB <sub>1</sub> .....	78
3	Composition of Quartz-Rich Skeletal Wackestone, Aquifer Zone IIB <sub>1</sub> .....	79
4	Composition of Quartz-Rich Skeletal Packstone, Aquifer Zone IIB <sub>1</sub> .....	80
5	Composition of Quartz-Rich Microsparite, Aquifer Zone IIB <sub>1</sub> .....	81
6	Composition of Quartz-Rich Siliceous Mudstone, Aquifer Zone IIB <sub>1</sub> .....	82
7	Composition of Quartz-Rich Terrigenous Mudstone, Aquifer Zone IIB <sub>1</sub> .....	83

## **LIST OF APPENDICES**

---

### **APPENDIX A**

- A-1 Grain Size Terminology and Class Intervals for Grade Scales (from Folk, 1980)
- A-2 Formulas and Verbal Scales for Folk and Ward (1957) Sedimentary Grain Size Parameters
- A-3 Ninety-five Percent Confidence Limits for Constituent Proportions, where  $n$  is the Total Number of Points Counted and  $p$  is the Estimated Proportion of a Particular Constituent (Modified from van der Plas and Tobi, 1965)
- A-4 Formula and Nomogram for Calculating Dryden's (1931) Probable Error at 95.4% for Number Percentages Obtained from the Line Method of Point Counting (Modified from Galehouse, 1971)
- A-5 Sorting Images of Folk (1980)
- A-6 Sorting Images of Harrell (1984)
- A-7 Sorting Images of Longiaru (1986)
- A-8 Roundness Images and Classes. Columns Show Grains of Similar Roundness but Different Sphericity (Modified from Powers, 1953)
- A-9 Comparison Chart for Describing the Roundness of Carbonate Bioclasts (Modified from Pilkey and others, 1967)
- A-10 Description of Particle Packing and Particle Contacts (modified from Taylor, 1951; Flügel, 1982)
- A-11 Classification of Carbonate-Terrigenous Sediment Mixtures (Modified from Lindholm, 1987)
- A-12 Classification of Carbonate Sediments and Rocks According to Depositional Texture (from Dunham, 1962)
- A-13 Classification of Sand and Sandstone (from Folk, 1980)
- A-14 Grain-Size Scale for Carbonate Sediments and Rocks (Modified from Folk, 1962)
- A-15 Textural Terminology for Gravel-Bearing Terrigenous Sediments (Modified from Folk, 1954)
- A-16 Textural Terminology for Gravel-Free Terrigenous Sediments (Modified from Folk, 1954)
- A-17 Flow Chart for Determining Textural Maturity of Terrigenous Sand (Modified from Folk, 1951)
- A-18 Porosity Classification of Choquette and Pray (1970)
- A-19 Porosity Classification of Choquette and Pray (1970)

## **LIST OF APPENDICES (Continued)**

---

### **APPENDIX B**

- B-1 Abbreviations for Microfacies Used in this Report.
- B-2 Point Count Data for Samples from Aquifer Unit IIA in the General Separations Area, Savannah River Site
- B-3 Point Count Data for Samples from Confining Unit IIA-IIB in the General Separations Area, Savannah River Site
- B-4 Point Count Data for Samples from Aquifer Zone IIB<sub>1</sub> in the General Separations Area, Savannah River Site
- B-5 Textural Data for Samples from Aquifer Unit IIA in the General Separations Area, Savannah River Site
- B-6 Textural Data for Samples from Confining Unit IIA-IIB in the General Separations Area, Savannah River Site
- B-7 Textural Data for Samples from Aquifer Zone IIB<sub>1</sub> in the General Separations Area, Savannah River Site
- B-8 Acid Insoluble Residue Data for General Separations Area "Calcareous Zone" Samples
- B-9 Acid Insoluble Residue Data and Folk and Ward (1957) Grain-Size Statistics for the Greater than 62  $\mu\text{m}$  Insoluble Fraction of "Calcareous Zone" Samples from the General Separations Area, Savannah River Site (after Richardson, 1991)

**PETROGRAPHIC ANALYSIS  
OF MIXED CARBONATE-CLASTIC  
HYDROSTRATIGRAPHIC UNITS  
IN THE GENERAL SEPARATIONS AREA (GSA),  
SAVANNAH RIVER SITE (SRS),  
AIKEN, SOUTH CAROLINA (U)**

**December 17, 1993**

**1.0 INTRODUCTION**

**1.1 General**

The Savannah River Site (SRS), a Department of Energy (DOE) facility that produces nuclear materials for national defense, covers approximately 300 mi<sup>2</sup> in the upper Atlantic Coastal Plain of southwestern South Carolina (Figure 1), and lies about 20 mi southeast of the Piedmont physiographic province. Sediment underlying the SRS forms a wedge of sedimentary strata that thickens from about 700 ft in the northwest to almost 1400 ft at the southeastern boundary of the site. Regional dip is to the southeast and decreases from about 48 ft/mi at the base of the Cretaceous-aged sediment to about 15 ft/mi at the top of middle Eocene-aged strata (Snipes and others, 1993).

The stratigraphy of the central Savannah River area has been the focus of numerous, and often conflicting studies, including those of Sloan (1908), Veatch and Stephenson (1911), Cooke (1936), LaMoreaux (1946a, 1946b), Cooke and McNeil (1952), Siple (1967), Colquhoun and Johnson (1968), Baum and others (1979), Huddlestun and Hetrick (1979, 1981), Powell and Baum (1982), Colquhoun and others (1983), Powell (1984), Prowell and others (1985), Steele (1985), Laws and others (1987), Gohn (1988), Harris and Zullo (1988, 1990, and 1992), Nystrom and others (1989, 1991), Price and others (1992), Fallaw and others (1992), and Fallaw and Price (1992).

Studies related to the hydrogeology of the SRS area include Siple (1967), Colquhoun and others (1982, 1983), Brooks and others (1985), Clark and others (1985), Gorday (1985), Miller (1986), Aucott and others (1987), Aucott (1988), Dennehy and others (1989), Krause and Randolph (1989), Logan and Euler (1989), Aadland (1990), Clark and others (1990), Aadland and others (1991), Aadland and others (1992a, 1992b), Harris and others (1992), Strom and Kaback (1992), Thayer and others (1992), Thayer and others (1993), and Newcome (1993).

The purpose of this report is to describe the lithofacies, petrology, diagenesis, depositional environments, and pore-system characteristics of sedimentary strata that constitute the "calcareous zone" beneath the General Separations Area (GSA) at the SRS (Figure 1). The "calcareous zone" was first recognized and described by the U.S. Army Corps of Engineers (1952) during subsurface investigations related to foundation grouting in the GSA. The Corps of Engineers 1952 report noted the presence of numerous surface sinkholes in the vicinity of the GSA. These were attributed to the solution of subsurface carbonate sediment. During drilling operations in the GSA, the Corps of Engineers (1952) reported "abundant voids and areas of excessive water and drilling mud loss" in and just above the "calcareous zone." The lithostratigraphic and hydrostratigraphic position of the "calcareous zone" was first documented in a U.S. Department of Energy (DOE) 1990 application for a hazardous waste post-closure permit for H-Area (Figure 2). The DOE report (1990) listed all wells and boreholes penetrating carbonate strata in the GSA, and provided isopach maps of the "calcareous zone's" upper and lower divisions relative to hydrostratigraphic units in the area. The isopach maps in the DOE (1990) report indicate an irregular areal distribution of the "calcareous zone" in the GSA. Recent work by Grant Richardson (in progress) confirms the irregular distribution of calcareous strata in the GSA and suggests that the distribution results from post-depositional, subsurface leaching of carbonate sediment.

The "calcareous zone" in the GSA includes calcareous strata belonging to the Warley Hill Formation, McBean (Santee) Formation, and Griffins Landing Member of the Dry Branch Formation (Figure 2). The McBean (Santee) Formation forms most of the "calcareous zone" within the GSA (Harris and others, 1992). According to Harris and others (1992), the calcareous sediment consists of calcareous sand, calcareous mud, limestone, sandy limestone, muddy limestone, and sandy muddy limestone.

Harris and others (1992) also demonstrated that the calcareous sediment in the GSA is laterally and vertically discontinuous, and informally divided it into lower and upper zones. The lower zone is present in three separate areas of the GSA and follows a northeast-southwest trend. Beds within this zone thicken and thin over short distances. The lower zone includes parts of aquifer unit IIA, confining unit IIA-IIB, and aquifer zone IIB<sub>1</sub> of aquifer unit IIB (Harris and others, 1992) (Figure 2). Most of the calcareous strata in the lower zone of the GSA are present within aquifer zone IIB<sub>1</sub>. The upper calcareous zone is very thin and discontinuous, and is located within the upper part of aquifer zone IIB<sub>1</sub>.

The stratigraphic relationships of Eocene-aged carbonate strata in the SRS region have been reviewed by Powell (1984), Huddlestun and Hetrick (1979, 1985), Prowell and others (1985), Nystrom and others (1989, 1991), Fallaw and others (1992), Fallaw and Price (1992), and Harris and Zullo (1992). Papers concerned primarily with petrology and diagenesis of carbonate strata in this area include Powell and Baum (1981), Powell (1984), Thayer and Miller (1988), Thayer and others (1988), and Thayer and Harris (1992). Papers dealing with petrographic and diagenetic aspects of aquifer limestone of the southeastern U.S. Coastal Plain include those by Textoris (1967), Textoris and others (1972), and Thayer and Textoris (1972, 1977).

## 1.2 Hydrostratigraphy

Aadland and others (1991) and Harris and others (1992) applied Aadland's (1990) alphanumeric hydrostratigraphic nomenclature to subsurface units in the GSA. Figure 2 shows the subdivision of hydrostratigraphic units of Tertiary age in the GSA after Harris and others (1992) and correlates them to lithostratigraphic units recognized in the SRS (Fallaw and others, 1992). Detailed descriptions of the hydrostratigraphic units in the GSA are beyond the scope of this report, but are available in Aadland and others (1991), Harris and others (1992), and Thayer and others (1993). Hence, only a brief summary is given here as it pertains to the calcareous sediment within the hydrostratigraphic units.

The lowermost unit of concern in this report is aquifer unit IIA, which is equivalent to the Gordon aquifer of Aadland and others (1992a, 1992b). Aquifer unit IIA consists mainly of sand and muddy sand with thin, minor interbeds of mud, muddy sand, and calcareous sand. Twenty-three wells and borings that penetrate the aquifer in the GSA show that the unit

averages  $82 \pm 19$ -ft thick and ranges from 58 to 129-ft thick. Rare beds of calcareous sediment, usually less than 2-ft thick, are found near the top of the unit. Beneath the GSA, aquifer unit IIA overlies confining system I-II of Harris and others (1992). Confining system I-II is equivalent to the Meyers Branch confining system of Aadland and others (1992a, 1992b).

Confining unit IIA-IIB separates aquifer unit IIA from aquifer unit IIB (Figure 2). The unit is commonly referred to as the "green clay" in previous SRS reports and is equivalent to the Gordon confining unit of Aadland and others (1992a, 1992b). Confining unit IIA-IIB consists of sediment belonging to the Warley Hill Formation, and includes fine-grained, silty and clayey sand, sandy clay, and clay. The clay is stiff to hard and sometimes fissile. Glauconite is common and imparts a distinctive greenish color to these sediments, hence the informal name "green clay" for the unit. Zones of silica-cemented sand, mud, and "shell hash" or coquina are present in some GSA cores. Confining unit IIA-IIB in the GSA also includes minor, discontinuous calcareous beds, primarily lime mud, sandy lime mud, clayey lime mud, and calcareous mud. Ninety wells and borings penetrate confining unit IIA-IIB in the GSA. The unit varies from 1 to 16-ft thick and has an average thickness of  $6 \pm 3$  ft in the GSA. An isopach map of calcareous sediment within confining unit IIA-IIB by Thayer and others (1993, Figure 16) shows seven, small isolated patches of carbonate sediment within the GSA; most are less than 5 feet in thickness. For the most part confining unit IIA-IIB is barren of carbonate sediment beneath the GSA.

Aquifer unit IIB includes all sediment from the water table down to the top of confining unit IIA-IIB (Figure 2) (Aadland and others, 1991; Harris and others, 1992). In the GSA, aquifer unit IIB is equivalent to the Upper Three Runs aquifer of Aadland and others (1992a, 1992b), and includes part of the part of the "upland" unit, Tobacco Road Sand, Dry Branch Formation, and McBean (Santee) Formation. Beneath the GSA, aquifer unit IIB is divided into three hydrostratigraphic zones. Confining zone IIB<sub>1</sub>-IIB<sub>2</sub> separates aquifer zone IIB into "lower" and "upper" zones (R. K. Aadland, personal communication, 1992). Confining zone IIB<sub>1</sub>-IIB<sub>2</sub> is equivalent to the "tan clay" zone referred to in previous SRS reports. Confining zone IIB<sub>1</sub>-IIB<sub>2</sub> consists of light yellowish tan to orange clay and sandy clay interbedded with clayey sand and sand within the Dry Branch Formation. The clay is lithologically similar to the Twiggs Clay Member of the Dry Branch Formation, but is present at different intervals and is not laterally continuous over long distances (Harris and others, 1992). Based on data from one hundred and fifteen wells and borings which penetrate confining zone IIB<sub>1</sub>-IIB<sub>2</sub>,

average thickness is  $11 \pm 6$  ft. Calcareous sediment has not been found within confining zone IIB<sub>1</sub>-IIB<sub>2</sub>.

Aquifer zone IIB<sub>1</sub> (Aadland and others, 1991; Harris and others, 1992) comprises the dominantly fine-grained, well sorted sand and muddy sand of the McBean Formation (Santee Limestone) and the part of the Dry Branch Formation beneath confining zone IIB<sub>1</sub>-IIB<sub>2</sub> ("tan clay"). The "lower" aquifer zone of the Upper Three Runs aquifer of Aadland and others (1992a, 1992b) is equivalent to aquifer zone IIB<sub>1</sub>. Thickness of aquifer zone IIB<sub>1</sub> ranges from 40 ft to 89 ft southeast of the Burial Grounds (Thayer and others, 1993); the zone has a mean thickness of  $63 \pm 12$  ft. Most of the calcareous sediment beneath the GSA is included in aquifer zone IIB<sub>1</sub>. Fifty-nine wells and borings penetrate calcareous sediment within aquifer zone IIB<sub>1</sub>, and thickness of the carbonate ranges from near zero to a maximum of 43 ft near the Mixed Waste Management Facility. Descriptions of drill core from the GSA indicate that the calcareous sediment is usually mixed with varying proportions of terrigenous sand and mud, and consists mainly of limestone, sandy limestone, calcareous sand, slightly calcareous muddy sand, and slightly calcareous sand; muddy limestone and calcareous mud are present in minor amounts. An isopach map of calcareous sediment within aquifer zone IIB<sub>1</sub> (Thayer and others, 1993, Figure 23) shows that the carbonate strata are laterally discontinuous and are present as isolated patches in the central, eastern, and western parts of the GSA.

### 1.3 Materials and Methods

Lithologic logs prepared by SRS subcontractors for 90 wells and boreholes penetrating the "calcareous zone" in the GSA were examined for this study. The logs incorporate binocular microscope descriptions of the cores on a foot-by-foot basis, including amount of recovery, degree of induration, color, texture, fabric, sedimentary structures, carbonate content, percent porosity, pore type and size, fossil content, and composition. Total thickness of the described core intervals is 8,040 ft of which 5,519 ft is from aquifer zone IIB<sub>1</sub>, 569 ft is from confining unit IIA-IIB, and 1,952 ft is from aquifer unit IIA. Figure 3 shows the location of wells and boreholes that penetrated carbonate sediment in the GSA.

Thirty GSA cores were selected for detailed study after careful review of the 90 "calcareous zone" core logs. Two-hundred and seventy-five representative samples were collected from these cores for thin section, insoluble residue, grain size, and scanning electron microscopy



studies. All samples were examined with a stereo binocular microscope for texture, color, fabric, and composition. Color was determined using the Geological Society of America rock color chart (Goddard *et al.*, 1948). Grain size (Appendix A-1) was measured directly using a calibrated micrometer ocular on the binocular microscope.

Insoluble residues were obtained from 202 samples by dissolving between 43 and 190 g of sample in dilute hydrochloric acid following Ireland's 1971 procedure. Grain size of the insoluble fraction was determined by wet-sieve analysis. Samples were first dispersed by soaking for 12-24 hours in 200 ml of distilled water to which 50 ml of 10% sodium hexametaphosphate (Calgon) was added. The sediment-water mixture was placed in a soil dispersion cup and stirred for 5 minutes on a milk-shake machine. The dispersed sediment was poured onto a 62.5  $\mu\text{m}$  (U.S. # 230) stainless-steel screen and wet sieved to separate sand from mud. The sand fraction was dried and split to obtain enough sample for dry-sieve analysis. The split sample was sieved on optically calibrated screens at 1/2 phi-unit intervals for 15 minutes on a Ro-Tap machine (Ingram, 1971). Sand and mud percentages were determined by computer and cumulative frequency curves drawn on arithmetic probability paper. Phi percentiles interpolated from the curves were used to calculate Folk and Ward (1957) grain size parameters. Appendix A-2 gives formulas used for calculation of Folk and Ward (1957) grain size statistics.

Blue-dyed, epoxy-impregnated thin sections (standard- and over-sized) were prepared from 130 "calcareous zone" samples cut perpendicular to bedding. The samples were collected from 26 boreholes in the GSA (Appendices B2-B7; Figure 3) and are considered representative of the hydrostratigraphic units comprising the "calcareous zone." All thin sections were etched with dilute hydrochloric acid and stained with alizarin red-S to facilitate identification of carbonate mineralogy (Friedman, 1971). Volume percent composition of thin sections with undisturbed fabric, including pore types, was determined by counting 300 points per thin section using the Glagolev-Chayes point counting method (Galehouse, 1971). The point distance used for the counts was chosen according to the grain size of the sample; the distance selected was always slightly greater than the largest grain on the slide (Dennison and Shea, 1966). At the 95 percent confidence level the maximum error is probably less than  $\pm 4$  percent of the real value of any constituent (van der Plas and Tobi, 1965) (Appendix A-3). In a few cases, the allochem grain size of carbonate samples was so large that fewer than 300 points were counted per thin section, thus increasing the probable error (Appendix A-3).

The fabric of some soft, unconsolidated sediment samples was disrupted during thin section preparation, making it impossible to reliably point count pore spaces using the Glagolev-Chayes method. These thin sections were treated as grain mounts and counted quantitatively using the line method, which yields a number rather than volume percentage (Galehouse, 1971). Generally, a total of 300 framework grains plus matrix (terrigenous and carbonate) were counted per thin section. The probable error (Dryden, 1931; Appendix A-4) at the 95% confidence level for a line method count of 300 is: 1) less than  $\pm 1$  percent for constituents present in amounts less than 5 percent or greater than 95%; 2) between  $\pm 1$ -2 percent for constituents forming 5-10 or 90-95 percent of the total sample; 3) between  $\pm 2$ -4 percent for constituents forming 10-20 or 80-90 percent of the total; and  $\pm 4$ -8 percent for constituents forming 20-40 or 60-80 percent of the total.

In addition to quantitative compositional analysis, all thin sections were studied for sedimentary structures, texture (grain size, sorting, and roundness), fabric (grain orientation and packing), pore type and size, and diagenetic features (compaction, cementation and replacement, and dissolution of grains or cement). The average and maximum grain size of the terrigenous fraction of each sample was determined by measuring the apparent long diameter of quartz grains in thin section using a calibrated micrometer ocular. The average and maximum size of skeletal allochems was measured in a similar manner. Thin section size was converted to equivalent sieve size using the empirical conversion equations of Harrell and Eriksson (1979). Sorting of the terrigenous sand fraction was estimated by visual comparison with charts given in Folk (1980), Harrell (1984), and Longiaru (1986). For reference, copies of these sorting comparators are included as Appendices A-5, A-6 and A-7 of this report. Quartz grain roundness in thin section was estimated visually using the chart of Powers (1953) (Appendix A-8). The chart of Pilkey and others (1967) shown in Appendix A-9, which is based on empirical observations of modern shelf sediments, was used to describe the roundness of carbonate shell fragments (bioclasts) in thin section. Fabric and packing were estimated by visual comparison with the chart of Taylor (1950) (Appendix A-10) as well as photomicrographs and diagrams given in Flügel (1982).

Sub-samples prepared for SEM examination were fractured cleanly, dusted with canned air, coated with an equal mixture of gold-palladium, and observed in an ISI-SX-40 instrument at accelerating voltages ranging from 10 to 30 kV. Energy dispersive X-ray (EDX) analyses of the same fracture surfaces used for SEM were done on an ISI-DS-130 SEM equipped with a Tracor Northern 5500 energy-dispersive fluorescence X-ray system using a 20 kV

accelerating potential. Identification of detrital and authigenic mineral phases in the samples was based on grain morphology and EDX pattern (Welton, 1984).

Table 1 gives the sources for terminology and classifications used in this report. Appendix A provides summaries of the most important classifications and terminologies. We use the hydrostratigraphic nomenclature proposed by Aadland (1990) for the SRS and adopted by Aadland and others (1991) and Harris and others (1992) for the GSA.

## 2.0 PETROLOGY

### 2.1 General

Appendix B presents petrographic data in tabular form for all samples analyzed in this study. Appendix B-1 lists abbreviations for microfacies types listed in Tables B-2 through B-7. Appendices B-2, B-3, and B-4 provide thin-section point count data for samples from aquifer unit IIA, confining unit IIA-IIB, and aquifer zone IIB<sub>1</sub>. Appendices B-5, B-6, and B-7 furnish thin-section textural data for samples from aquifer unit IIA, confining unit IIA-IIB, and aquifer zone IIB<sub>1</sub>. Insoluble residue data for GSA "calcareous zone" samples are given in Appendices B-8 and B-9. Appendix B-9 gives the percentage of terrigenous sand, terrigenous mud, and carbonate for 195 "calcareous zone" samples as well as Folk and Ward (1957) grain size statistics for the greater than 62  $\mu\text{m}$  insoluble fraction.

Figure 4 shows the computed percentage of carbonate content (weight percent) for 396 insoluble residue samples from the GSA "calcareous zone." Slightly more than one-third of the samples contain less than 10 percent carbonate material by weight, and nearly 80 percent of them contain less than 50 weight percent carbonate material. The average weight percent carbonate content for the sample set is  $29.1 \pm 2.6\%$  with a standard deviation of 24.6%. Percent carbonate content ranges from zero to a maximum of 86.7% (Appendices B-8 and B-9) and is skewed toward lower values (Figure 4).

Plots showing the vertical distribution of weight percent carbonate material in GSA wells BGO-9AA, FSB-116C, HPT-2A, HSB-TB, and YSC-5A are given in Figures 5 through 9. These figures show that aquifer unit IIA and confining unit IIA-IIB have considerably less carbonate content than aquifer zone IIB<sub>1</sub>, although the smaller number of samples analyzed from aquifer unit IIA and confining unit IIA-IIB makes it impractical to apply rigorous

statistical tests. Also, there are no obvious vertical trends in the distribution within aquifer zone IIB<sub>1</sub> for the wells examined in this study. However, where present, the percentage of carbonate material appears to be slightly higher in the lower part of the aquifer interval (Figures 5-9). The calcareous sediments and limestones are not distinctive on natural gamma-ray curves from wells in the GSA; however, limestone with high moldic or other porosity usually has high values on the resistivity curve (Harris and others, 1992; Figures 5-9).

Figure 10 shows the fundamental classification of calcareous sediments from the GSA according to Folk's (1980) nomenclatural scheme and is based on thin-section point count data from 122 samples. Terrigenous constituents include materials derived from erosion of the land area outside the depositional basin, primarily quartz sand and mud (silt + clay). Allochemical components include all skeletal fragments, pellets, and intraclasts, which were formed and later transported within the basin of deposition. Orthochemical constituents comprise all chemically precipitated materials that have not undergone transportation, including primary precipitates (microcrystalline calcite ooze — micrite and pore-filling sparry calcite and silica cements) and replacement minerals (microspar, pseudospar, and silica replacements). Figure 10 indicates that sediments from the calcareous interval in the GSA are mixtures of the three primary end members and that orthochemical constituents are slightly more abundant than allochemical ones in these sediments and rocks. Impure allochemical (IO) sediments are the dominant lithologic type in the calcareous interval, forming slightly more than 50 percent of the total interval (Figure 10).

## 2.2 Aquifer Unit IIA

### 2.2.1 *General*

Twenty samples were analyzed for carbonate content from aquifer unit IIA (Appendices B-8 and B-9; Figures 5 through 9). Average content of calcareous material for the 20 samples is 3.1 weight percent with a standard deviation of 2.9 percent. Carbonate content ranges from zero to a maximum of 10.1 weight percent. Wet-sieve analysis of the insoluble terrigenous fraction of a subset of 13 samples indicates that the average sand plus gravel content is 88.1 percent and the mud (silt + clay) content is 8.8 percent. Data from binocular microscope and thin-section examination indicates that aquifer unit IIA is divided into two microfacies, terrigenous mud and terrigenous sand and sandstone.

### 2.2.2 *Terrigenous Mud*

#### 2.2.2.1 Description

Terrigenous mud forms a relatively small proportion of aquifer unit IIA beneath the GSA (Harris and others, 1992; Thayer and others, 1993). It consists of thin beds of tan, orange, and light gray mudstone and claystone, and contains variable amounts of fine and very fine terrigenous sand (Appendix B-2). Thin section examination indicates that the mud typically lacks laminations and often displays a "swirled" fabric, suggestive of bioturbation. The sand fraction is primarily unstrained monocrystalline quartz with minor muscovite, and opaque and heavy mineral grains (Figure 11). Based on X-ray diffraction analyses, Strom and Kaback (1992) have shown that kaolinite is the dominant clay mineral with minor illite and smectite. Minor to trace amounts of carbonate material is present as allochems (foraminifers and fine-grained, skeletal debris) and as finely crystalline sparry calcite cement within some foraminifers. Authigenic minerals present in minor to trace amounts include pyrite, clinoptilolite, cristobalite lepispheres, chert, and fibrous chalcedony. Pyrite is present as silt-sized cubes or framboids that grew displacively within the soft mud or within some foraminiferal tests. Tabular, euhedral crystals of weakly birefringent clinoptilolite that are between 5-25  $\mu\text{m}$  long partially fill some micropores and intraforam pores. Cristobalite (opal-CT of Jones and Segnit, 1971) is present as 2-5  $\mu\text{m}$  lepispheres (Wise and Weaver, 1973; Flörke and others, 1976;) that grew within foraminiferal tests or micropores. Chert and fibrous chalcedony have partially replaced Mg-calcite oyster and other pelecypod fragments.

Visual macroporosity in thin section is insignificant for this microfacies. Most pores are micro-sized, hence permeability values are extremely low (Thayer and others, 1992).

#### 2.2.2.2 Interpretation

The dominance of terrigenous mud and presence of foraminiferal and molluscan skeletal grains indicates deposition in relatively quiet-water within a marine environment (Wilson, 1975; Sellwood, 1986). The abundance of terrigenous mud and sand suggests proximity to riverine input and the paleo-shoreline. Organic debris, normally associated with closeness to shore, is sparse or lacking. This may be a result of current bypassing or consumption of the organic material by bottom-dwelling organisms. Lack of laminations and the homogeneous "swirled" fabric of the sediment suggests that burrowing organisms were active at the depositional site.

The main diagenetic events that affected the terrigenous mud include minor micritization of skeletal allochems, primarily molluscan grains, by boring algae and fungi while the sediment was exposed on the sea floor. The mud underwent slight post-depositional compaction within the first few hundred feet of burial. Pyrite formation probably occurred early in the marine phreatic realm. The iron probably entered the system as insoluble oxidized hematite adsorbed on clay-sized particles. After the sediment was buried and reducing conditions set in, the oxidized iron, in the presence of sulfate-reducing bacteria, precipitated as iron sulfide. The precipitation is most likely to have taken place in areas containing putrefying tissue or organics where sulfate-reducing bacteria were abundant (Scoffin, 1987). Equant calcite cementation within foraminiferal tests occurred in the saturated freshwater phreatic environment (Longman, 1980) during low stands of sea level (Colquhoun and Johnson, 1968; Haq and others, 1987). Timing of authigenic clinoptilolite and silica formation cannot be determined for this microfacies because neither phase is associated with other cements; hence, a "cement stratigraphy" cannot be determined.

### 2.2.3 *Terrigenous Sand and Sandstone*

#### 2.2.3.1 Description

Terrigenous sand forms the bulk of aquifer unit IIA in the GSA (Harris and others, 1992; Thayer and others, 1993). It consists of thick beds of unconsolidated quartz sand that

contains thin, discontinuous layers of mud and minor zones of opal- and chalcedony-cemented quartzarenite. The sand is yellowish to grayish orange in color and commonly contains pebbly layers and localized iron-oxide cemented zones. The sand is subangular and subrounded, and texturally immature and submature. Minor calcareous-bearing sands are found sporadically within the aquifer. Binocular examination of the calcareous sands indicates that the carbonate is present mostly as well-worn skeletal grains of molluscs, echinoderms, and foraminifers.

Thirteen samples were analyzed for carbonate content from the terrigenous sand facies of aquifer unit IIA (Appendices B-8 and B-9; Figures 5 through 9). Average carbonate content for the 13 samples is 3.5 weight percent with a standard deviation of  $\pm 3.3$  percent. Carbonate content ranges from zero to a maximum of 10.1 weight percent. Wet-sieve analysis of the insoluble terrigenous fraction of a subset of 12 samples indicates that the average sand plus gravel content is 90.5 percent and the mud (silt + clay) content is 6.1 percent. Grain size analysis of the sand plus gravel fraction shows that the mean grain size of the 12 samples is  $1.56\phi$  (wer medium sand) with a standard deviation of  $\pm 0.67\phi$ ; the samples range from upper very coarse ( $0.18\phi$ ) to upper fine ( $2.42\phi$ ) sand. (Appendix B-9). Sorting (inclusive graphic standard deviation of Folk and Ward, 1957) of the sand fraction averages  $0.87\phi$  (moderately sorted) and ranges from  $0.39\phi$  (well sorted) to  $1.37\phi$  (poorly sorted). Inclusive graphic skewness averages  $-0.02 \pm 0.16$ , which is near symmetrical according to the Folk and Ward (1957) verbal scale. Skewness ranges from  $-0.29$  (coarse skewed) to  $+0.23$  (fine skewed). Graphic kurtosis of the sand plus gravel fraction averages 1.25, which is leptokurtic on the Folk and Ward (1957) scale. Kurtosis ranges from 0.81 (platykurtic) to 2.42 (very leptokurtic).

Thin-section examination of one unconsolidated, muddy sand from this unit shows that it consists primarily of unstrained monocrystalline quartz with considerable silty clay matrix (Figure 12). Trace heavy minerals include magnetite, ilmenite, glauconite, garnet, sphene, tourmaline, and zircon. Authigenic cristobalite lepispheres and fibrous chalcedony exist as minor pore-lining and pore-filling cements.

One sample of chalcedony-cemented sandstone was examined from this facies (Appendix B-2). The thin section (HSB-140-156) consists primarily of moderately well sorted, subangular, unstrained monocrystalline quartz that is tightly cemented by fibrous chalcedony (Figure 13). The chalcedony is present as botryoidal rim cement on detrital quartz grains and almost completely occludes intergranular porosity. Moldic and intercrystal are the dominant pore

types forming 3.7 percent of the total rock. Polycrystalline quartz, feldspar, kaolin, and heavy and opaque minerals are present in minor amounts.

#### 2.2.3.2 Interpretation

The presence of glauconite and a normal, shallow-marine fossil fauna including oysters, other pelecypods, echinoderms, benthic and pelagic foraminifers, gastropods, and shark teeth indicate that aquifer unit IIA is a shallow-marine shelf deposit (Robertson, 1990; Robertson and Thayer, 1992). Robertson (1990) observed areal variations in mud content, mean grain size, and sorting, indicating increasing water depth and decreasing energy conditions in a downdip direction; that is, toward the southeastern boundary of the SRS. Plots of quartz types on a quartz provenance diagram, along with the presence of garnet, kyanite, staurolite, and sillimanite led Robertson (1990) to suggest a medium- to high-rank metamorphic provenance for most aquifer unit IIA sands. The scarcity of labile constituents, such as feldspars and rock fragments, implies intense chemical weathering in the source terrane.

Post-depositional diagenetic changes in aquifer unit IIA are usually minor, but include leaching of aragonitic skeletal grains, feldspar and unstable heavy mineral grains, such as garnet. The aluminum released during the dissolution of feldspar combined with silicon and pore water to form minor authigenic kaolinite. Cementation by opal or chalcedony is uncommon and restricted to localized areas within the aquifer, particularly near its upper contact with confining unit IIA-IIB (Robertson, 1990). Pre-cement porosity (i.e., porosity now plus cement-filled pore space) for one chalcedony-cemented sample is 38 percent (Appendix B-2). If initial porosity for the sand is assumed to be 40-45 percent (Pettijohn and others, 1987), then between 2-7 percent of the original porosity was destroyed by compaction prior to cementation. The source of silica for chalcedony cementation is enigmatic; the most likely one is dissolution of diatom and sponge spicule opal-A from confining unit IIA-IIB directly above. Wise and Weaver (1973) and Carver (1980) also suggested a biogenic source for the opal- and chalcedony-bearing Tertiary sediments of the southeastern Atlantic Coastal Plain.



## 2.3 Confining Unit IIA-IIB

### 2.3.1 *General*

Thirty-two samples were analyzed for carbonate from confining unit IIA-IIB (Appendices B-8 and B-9; Figures 5 through 9). Average carbonate content for the 32 samples is 14.3 weight percent with a standard deviation of  $\pm 16.9$  percent. Carbonate content ranges from zero to 79.6 weight percent. Wet-sieve analysis of the insoluble terrigenous fraction of a subset of 15 samples indicates that the average sand plus gravel content is 51.1 percent and the mud (silt + clay) content is 34.1 percent. Data from binocular microscope and thin-section examinations of core samples indicates that confining unit IIA-IIB is divided into four microfacies: 1) lime mud; 2) siliceous mudstone, including sandy siliceous mudstone and sandy, skeletal siliceous mudstone; 3) sandy terrigenous mud; and 4) terrigenous sand. Appendix B-3 summarizes point count data for confining unit IIA-IIB and Appendix B-6 gives textural data for the same samples.

### 2.3.2 *Lime Mud*

#### 2.3.2.1 Description

Two samples of lime mud from well BGO-9AA were analyzed petrographically (Appendix B-3 and B-6). Both samples are poorly indurated and light greenish gray in color. In thin section, the two samples lack laminations and appear homogeneous. One sample is a quartz-rich, sandy lime mud and the other is a lime mud. The lime mud consists of silt- and sand-sized subangular quartz "floating" in a micrite matrix that contains some terrigenous mud (Figure 14). Accessory constituents include trace skeletal fragments and opaque heavy minerals. Authigenic opal is present as a replacement of the micrite matrix and partially fills some foraminiferal tests.

The quartz-rich, sandy lime mud consists of sand-sized, subangular monocrystalline quartz set in a micrite matrix mixed with subordinate terrigenous mud. Accessory constituents include feldspar, detrital opaque mineral grains, lobate glauconite pellets, carbonate intraclasts, and sand-sized skeletal grains, including foraminifers, echinoderms, bryozoans, pelecypods, gastropods, and comminuted skeletal debris. Most of the skeletal grains are medium calcarenite-sized and rounded and subrounded; some contain numerous microborings, probably produced by algae and fungi (Bathurst, 1971). Authigenic framboidal pyrite formed

within foraminiferal tests and grew displacively within the lime mud matrix. Opal-CT is present as 2-5  $\mu\text{m}$  lepispheres that partially fill foraminiferal tests, molds, vugs, and micropores in the lime mud matrix. Fibrous, length-fast spherulitic chalcedony is present as a partial replacement of Mg-calcite molluscan and echinoderm shell fragments. The chalcedony is most commonly present near the center of the skeletal fragment, and appears to have grown outward toward the margin. Ghosts of original shell microstructure are rarely preserved as inclusions of fine shell that appear brown through transmitted light. The chalcedony often reaches but does not extend beyond the fossil-matrix contact. Visual porosity in thin section is low and is dominantly vug and interparticle between quartz grains; minor moldic and intraparticle porosity is present within foraminifers. Most pores are not connected, hence permeability values are very low for this microfacies.

#### 2.3.2.2 Interpretation

The presence of glauconite along with a normal marine fauna, including foraminifers, molluscs, bryozoans, and echinoderms, indicates that this facies was deposited in clear, open-marine water of normal salinity on the inner to middle shelf. The abundance of micrite indicates deposition in quiet water below normal marine wave base. The presence of abraded and well-worn skeletal grains indicates that bottom transport by currents or storm-generated waves alternated with quiet-water conditions in which fine-grained lime mud could accumulate. The lack of laminations in this microfacies probably results from homogenization by burrowing organisms shortly after deposition. It is also possible that the burrowing organisms mixed well-worn skeletal grains from layers of high-energy sedimentation with micrite from layers of low-energy sedimentation.

Post-depositional diagenetic events that have affected the lime mud microfacies occurred in the marine and freshwater phreatic environments. Events occurring in the marine phreatic environment included boring and partial micritization of bioclasts (mainly molluscs) by endolithic algae and fungi and precipitation of several cements including pyrite and rare glauconite. Framboidal pyrite is present within foraminiferal tests indicating that it formed under reducing conditions in areas containing putrefying tissue where sulfate-reducing bacteria were abundant (Scoffin, 1987).

The original unconsolidated sediment was dominated by low-Mg calcite molluscs and foraminifers and high-Mg echinoderms and bryozoans; aragonitic pelecypods were a minor constituent. The lime mud underwent minor post-depositional compaction within the first few hundred feet of burial. Following withdrawal of the sea, the sediment underwent the following changes in the subaerial freshwater phreatic environment: 1) High-Mg calcite allochems, mainly echinoderms and bryozoans, were converted to low-Mg calcite while in the solid state by leaching of  $Mg^{++}$  or solution-precipitation on a micro-scale (Bathurst, 1971; Thayer and Textoris, 1977). 2) Most of the aragonitic skeletal allochems, chiefly pelecypods, dissolved to create molds, which in turn underwent solution-enlargement to form vugs. This was not an important process in the lime mud microfacies because there were relatively few aragonitic pelecypods available for solution. In addition, none of the molds or vugs have been reduced or filled by low-Mg calcite spar suggesting that solution of the original aragonite took place too quickly to allow for reprecipitation nearby. This indicates that meteoric water moved rapidly through the original sediment in that there was not enough time to permit concurrent precipitation of low-Mg calcite within aragonitic molluscan molds (Moore, 1979). 3) Opal-CT lepispheres precipitated within intraforam pores, molds, vugs, and micropores in the lime mud matrix. Formation of lepispheres postdates solution of aragonitic allochems and micrite matrix because the lepispheres line the interiors of molds and vugs. Timing of silicification of fossils by chalcedony cannot be determined with certainty. The replacement most likely postdates solution of aragonitic allochems, but whether it took place before or after precipitation of opal-CT is unknown.

The replacement of fossils by chalcedony probably did not involve an initial opal-CT stage; rather the silica was more likely precipitated directly as chalcedony (Maliva and Siever, 1988). The silicification took place along thin solution films in which skeletal calcite dissolved and silica precipitated. According to Maliva and Siever (1988) the mechanism of replacement is controlled by the force of crystallization, whereby growth of the silica phase exerted pressure across the silica-carbonate contact, locally increasing the Gibbs free energy, and hence solubility of the shell calcite. Organic matter within the host Mg-calcite skeletons may have played an important role in the silicification process by providing nucleation sites for initial silica precipitation.

The formation of different types of authigenic silica is controlled mainly by chemistry and mineralogy of the host sediment, bulk pore-water pH, presence of organic matter, and concentrations of silica and certain ions, such as sulfate (Folk and Pittman, 1971). The

presence of different types of authigenic silica (i.e., opal-CT lepispheres and chalcedony) within the same thin section requires sequential replacement of each type of silica by water with varying silica concentration. The concentrations of silica were probably controlled by rates of silica supply, particularly in these sediments where most of the silica was derived from intraformational solution of siliceous sponge spicules and diatoms (Carver, 1980). The dissolved silica concentration would have depended on the quantity of siliceous sponges and diatoms remaining in the sediment, and kinetics of skeletal dissolution and rate of silica precipitation. The dissolved silica concentration probably varied considerably during the silicification process. Based on rates of nucleation and crystal growth, Maliva and Siever (1988) suggested that different silica phases form at varying dissolved silica concentrations: opal-CT forms at highest concentrations, chalcedony at lower values, microcrystalline quartz (subequant quartz with diameters less than 20  $\mu\text{m}$ ) at even lower values, and granular megaquartz (non-fibrous quartz with diameters greater than 20  $\mu\text{m}$ ) and quartz euhedra at lowest concentrations. Replacements took place with pore water at or close to saturation with respect to the carbonate phase. The silicification process continued until the silica supply (diatom and sponge-spicule biogenic opal-A) was exhausted.

### 2.3.3 *Siliceous Mudstone*

#### 2.3.3.1 Description

Seven thin sections of siliceous mudstone were examined from confining unit IIA-IIB. Four are from well BGX-2B, two are from BGO-9AA, and one is from well HMD-1C (Appendices B-3 and B-6). All samples are well-indurated and very light gray, light yellowish gray, or light greenish-gray colored. Two types of siliceous mudstone are present within confining unit IIA-IIB: sandy siliceous mudstone and sandy, skeletal siliceous mudstone.

Sandy siliceous mudstone is present in well BGX-2B (Appendix B-3 and B-6) between 152 and 156 ft. It consists of fine, subangular to angular, monocrystalline quartz ( $\bar{x}$  = 19 percent) "floating" without preferred orientation in a light brown, felted matrix of coalesced opal-CT lepispheres (Figure 15). The opal matrix averages 58.6 percent of whole-rock volume and appears structureless in transmitted light. Minor accessory constituents include glauconite pellets, heavy and opaque minerals, partially dissolved sponge spicules, organic debris, collophane, and authigenic pyrite and chalcedony. Relict sponge spicules with intact axial canals are rare but ubiquitous components. More common, however, are sponge spicule

molds that are lined or filled with fibrous chalcedony. Porosity averages nearly 16 percent and is dominantly mesomoldic and mesovug. Many of the molds were originally aragonitic pelecypod valves that were leached prior to silicification; others formed by sponge spicule dissolution. The vugs most likely formed by solution enlargement of pelecypod molds.

Sandy, skeletal siliceous mudstone (Figure 16) is present in well BGO-9AA between 150 and 153 ft and in well HMD-1C at 125 ft. It consists of fine, subangular to angular, monocrystalline quartz ( $\bar{x}$  = 14.3 percent) and low-Mg calcite allochems ( $\bar{x}$  = 35.5 percent) "floating" in a light brown matrix of massive opal-CT ( $\bar{x}$  = 42.6 percent). Mg-calcite pelecypods are the dominant skeletal allochem, averaging 25 percent of whole-rock volume. Other Mg-calcite skeletal allochems include foraminifers, mollusc fragments, comminuted skeletal debris, and gastropods. Bryozoans and echinoderms are present in trace amounts. Minor constituents include micrite patches under pelecypod "umbrellas," micritized carbonate grains, carbonate intraclasts, glauconite pellets, heavy and opaque minerals, sponge spicules, organic debris, and collophane. Besides opal-CT, authigenic cements and replacements include pyrite, glauconite, chalcedony, and zeolite. Pyrite and glauconite fill or partially fill microborings in Mg-calcite pelecypod valves; pyrite also partially fills the internal chambers of some benthic foraminifers. Fibrous, length-fast chalcedony fills some molds formed by dissolution of sponge spicules and partially replaces low-Mg calcite pelecypod and gastropod shells. Tabular crystals of 10-30  $\mu$ m zeolite (clinoptilolite?) partially line micropores within the opal-CT matrix. Porosity of this unit is low, averaging 2.7 percent for the three samples. The main porosity types in the sandy, skeletal siliceous mudstone are intercrystal pores, moldic pores, and intraparticle pores; all are meso-sized.

#### 2.3.3.2 Interpretation

The siliceous mudstone microfacies is interpreted to be a diagenetic replacement of sandy, skeletal wackestone. The wackestone was deposited in clear, open-marine water of normal salinity on the inner to middle shelf as indicated by the presence of glauconite and a normal marine fauna, including foraminifers, pelecypods, gastropods, bryozoans, and echinoderms. Most of the opal-CT matrix was originally micrite, and its abundance indicates deposition in quiet water below normal marine wave base. The presence of abraded and well-worn skeletal grains along with considerable terrigenous sand and some quartz gravel indicates that bottom transport by currents or storm-generated waves alternated with quiet-water conditions in

which the lime mud could accumulate. The lack of laminations in this microfacies probably results from homogenization by burrowing organisms shortly after deposition. It is also possible that the diagenetic alteration of micritic carbonate to opal-CT destroyed the original laminations.

The diagenetic history of the siliceous mudstone microfacies includes changes in the marine and freshwater phreatic environments. Events occurring in the marine phreatic environment include micro-boring and micritization of some Mg-calcite bioclasts, as well as precipitation of pyrite and glauconite cements. Framboidal pyrite is associated with organic matter in the matrix and within microborings and foraminiferal tests, indicating that it formed under localized reducing conditions where sulfate-reducing bacteria were numerous. Glauconite precipitated within microborings, foraminiferal chambers, and bryozoan zooecia under slightly reducing conditions in water depths greater than 10 m; its presence indicates slow sedimentation rates for the original sediment (Nystrom and others, 1989, 1991).

The skeletal wackestone underwent post-depositional compaction starting within the first few hundred feet of burial. Effects of compaction included breakage of delicate skeletal allochems and formation of concavo-convex contacts (Appendix A-10) where durable quartz grains and softer Mg-calcite pelecypod valves were in contact. Following withdrawal of the sea, the sediment underwent the following changes in the subaerial freshwater phreatic environment:

- 1) High-Mg calcite allochems, mainly echinoderms, were converted to low-Mg calcite by leaching of  $Mg^{++}$  or solution-precipitation on a micro-scale (Bathurst, 1971; Thayer and Textoris, 1977);
- 2) Aragonitic skeletal allochems, chiefly pelecypods, dissolved to form molds, which in turn underwent solution-enlargement to create vugs. This was a minor process in this microfacies because aragonitic pelecypods were not abundant in the original sediment (Appendix B-4);
- 3) Some of the carbonate material from dissolution of aragonite precipitated within nearby molds and vugs as low-Mg calcite cement. This process was rare in this microfacies;
- 4) Biogenic opal-A as sponge spicules and diatom valves underwent dissolution;
- 5) Opal-CT lepispheres precipitated from silica-rich pore water and replaced micrite matrix and some skeletal allochems, and formed narrow linings within a few molds, vugs, and intra-foram pores. Lepisphere formation postdates solution of aragonitic allochems and micrite matrix because the lepispheres line the interiors of molds;
- 6) Chalcedony partially replaced Mg-calcite pelecypod shells, filled sponge spicule molds, and precipitated locally as rim cement on detrital quartz. Textural relationships indicate that the opal-CT precipitated prior to chalcedony. The opal-CT probably precipitated at the highest dissolved silica

concentrations whereas chalcedony formed at lower concentrations (Maliva and Siever, 1988); 7) Authigenic zeolite precipitated in micropores within the siliceous sediment. The zeolite postdates opal-CT formation because euhedral zeolite crystals have grown on top of the opal-CT lepispheres. The zeolite probably formed after chalcedony cementation because zeolite inclusions have not been found within chalcedony.

#### **2.3.4 *Sandy Terrigenous Mud***

##### **2.3.4.1 Description**

Three thin sections of this microfacies were studied (Appendix B-3 and B-6). The samples are from wells BGX-2B, HPC-1, and HSB-TB. All samples are poorly indurated, massively bedded, and light greenish-gray in color. The fabric of each sample was disrupted during preparation of the thin sections, hence information on sedimentary structures as well as pore type and abundance cannot be determined. This microfacies consists of quartz-rich terrigenous mud (Figure 17) containing minor heavy and opaque minerals, glauconite pellets, and trace quantities of feldspar, organic debris, and comminuted skeletal debris. Rare pelecypods and benthic foraminifers are present within this microfacies. The clay minerals that form much of the matrix consist of illite and smectite (Dennehy and others, 1989). The quartz is found as subangular and predominantly unstrained monocrystalline grains. The average grain size ranges from very fine to medium (Appendix B-6). Authigenic mineral phases include pyrite and glauconite cements, both of which are present within foraminiferal tests and other skeletal debris. Rare opal-CT lepispheres and tabular-shaped clinoptilolite crystals are present within foraminiferal tests. Laboratory analyses of horizontal and vertical permeability on representative undisturbed samples of the clay-rich parts of confining unit IIA-IIB range from  $3.8 \times 10^{-6}$  ft/day to  $2.7 \times 10^{-3}$  (Bledsoe and others, 1990).

##### **2.3.4.2 Interpretation**

Terrigenous mud and the presence of glauconite and foraminiferal and molluscan allochems indicates deposition in relatively quiet water within an open-marine environment. The abundance of terrigenous mud and sand indicates proximity to the shoreline and probable riverine input. Organic debris, normally abundant in close proximity to the shoreline, are sparse in this microfacies. This may be a result of current bypassing or consumption of the

organic material by bottom-dwelling organisms. The massive fabric observed in cores suggests considerable bioturbation at the depositional site. The presence of glauconite pellets indicates a slow rate of deposition in water depths greater than 10 m and temperatures 17 °C or cooler (Nystrom and others, 1989, 1991).

Diagenetic events affecting the terrigenous mud microfacies include minor micritization of skeletal allochems (primarily pelecypods) by boring algae and fungi while the sediment was exposed on the sea floor. The mud underwent slight post-depositional compaction within the first few hundred feet of burial. Pyrite formation probably occurred early on within the marine phreatic realm in areas containing putrefying tissue or organic material where sulfate-reducing bacteria were abundant (Scoffin, 1987). Timing of authigenic clinoptilolite and opal-CT formation cannot be determined for this microfacies because neither phase is associated with other cements.

### 2.3.5 *Terrigenous Sand and Sandstone*

#### 2.3.5.1 Description

Two thin sections from this microfacies were examined. One is an unconsolidated, muddy quartz sand from well HPC-1 and the other is a well-indurated, chalcedony-cemented quartzarenite from well FSB-115C. Examination of GSA core included in this microfacies indicates that most of it is massively bedded, unconsolidated, and light greenish gray, light gray, orange brown or tan in color. Textural analysis indicates that this microfacies consists of poorly sorted, slightly calcareous muddy sand with subordinate muddy sand, and calcareous sand (Appendix A-11).

Five unconsolidated samples were analyzed for carbonate from the terrigenous sand facies of confining unit IIA-IIB (Appendices B-8 and B-9; Figures 5 through 9). Average carbonate content for the five samples is 2.5 weight percent with a standard deviation of  $\pm 4.3$  percent. Carbonate ranges from zero to a maximum of 9.9 weight percent. Wet-sieve analysis of the insoluble terrigenous fraction shows that the average sand plus gravel content is 75.5 percent and the mud (silt + clay) content is 22 percent. The terrigenous sand fraction of all samples is subangular and all sands are all texturally immature. Grain size analysis of the sand plus gravel fraction shows that the mean grain size of the five samples is 1.33  $\phi$  (upper medium sand) with a standard deviation of  $\pm 0.92 \phi$ ; mean size of the samples ranges from lower very



coarse ( $0.13 \phi$ ) to lower fine ( $2.69 \phi$ ) sand (Appendix B-9). Sorting of the sand fraction averages  $1.27 \pm 0.85 \phi$  (poorly sorted) and ranges from  $0.13\phi$  (very well sorted) to  $2.69\phi$  (very poorly sorted). Inclusive graphic skewness averages  $-0.03 \pm 0.11$ , which is near symmetrical according to the Folk and Ward (1957) verbal scale. Skewness ranges from  $-0.15$  (coarse skewed) to  $+0.13$  (fine skewed). Graphic kurtosis of the sand plus gravel fraction averages  $0.90$ , which is mesokurtic on the Folk and Ward (1957) scale. Kurtosis ranges from  $0.54$  (very platykurtic) to  $1.38$  (leptokurtic).

Study of thin sections of unconsolidated muddy sand from well HPC-1 indicates that the sediment consists of subangular monocrystalline quartz "floating" in a hematite-stained matrix of clay and silt, which forms nearly 45 percent of the total sample (Figure 18). The sediment fabric was disrupted during preparation of the thin section, therefore type and abundance of pore space could not be determined. The sand contains trace amounts of glauconite, heavy minerals, opaque minerals, skeletal fragments, and authigenic chalcedony.

The chalcedony-cemented quartzarenite (Figure 19) is medium-grained, moderately sorted and texturally submature. It consists of subangular monocrystalline quartz with trace quantities of polycrystalline quartz, microcline, glauconite, collophane, and heavy and opaque minerals. Total porosity in thin section is 12.2 percent and is dominantly mesomoldic that formed by dissolution of aragonitic pelecypod valves. Minor interparticle and intercrystal pores are present. Chalcedony is the dominant authigenic phase with minor opal-CT and a 5-10  $\mu\text{m}$  tabular-shaped, weakly birefringent zeolite, probably clinoptilolite. The opal is light brown in plane light and is present chiefly as a botryoidal rim cement lining pelecypod molds and interparticle pores between framework quartz grains. Length-fast chalcedony is present as a rim cement that partially or completely fills interparticle pores between framework quartz grains or as cement within pelecypod mesomolds. Where they coexist, opal cement is found adjacent to framework grains, with chalcedony filling the central part of the pore.

#### 2.3.5.2 Interpretation

The presence of glauconite, collophane, and skeletal fragments, including disarticulated pelecypod molds indicates that this microfacies is a shallow-marine deposit that probably accumulated on the inner or middle shelf. The abundance of terrigenous mud and the poor sorting of the sand fraction suggest that wave and current velocities varied considerably. It is

also possible that the poor sorting and abundance of terrigenous mud resulted from the mixing of different mud and sand layers by burrowing organisms. The presence of medium- to coarse-grained sand suggests proximity to land and riverine input. Although porosity cannot be determined in thin section because of sample disruption, similar unconsolidated muddy sands typically have porosity in the range of 10-20 percent (Davis, 1969).

The main diagenetic events that affected the unconsolidated muddy sand included algal and fungal microborings of skeletal fragments while the sediment was on the sea floor. Upon burial the unconsolidated sediment underwent minor compaction. Following withdrawal of the sea, the sediment was flushed by fresh water leading to dissolution of aragonitic skeletal grains, feldspar, and some unstable heavy minerals.

Cementation of the sand by opal or chalcedony is uncommon and is restricted to localized areas within confining unit IIA-IIB. Pre-cement porosity of the chalcedony-cemented sample is 37 percent (Appendix B-2). If initial porosity of the sand is assumed to be 40-45 percent (Pettijohn and others, 1987), then between 2-8 percent of the original porosity was destroyed by compaction prior to cementation. The source of silica for opal and chalcedony cementation was most likely the dissolution of diatom and sponge spicule opal-A from fossil-rich units within confining unit IIA-IIB. Wise and Weaver (1973) and Carver (1980) also suggested a biogenic source for the opal- and chalcedony-bearing Tertiary sediments of the southeastern Atlantic Coastal Plain. As noted earlier, where opal-CT and chalcedony coexist, opal cement is present adjacent to detrital framework quartz, whereas chalcedony fills the central part of the pore. This indicates that the opal-CT formed prior to chalcedony cementation. The work of Maliva and Siever (1988) demonstrated that opal-CT formed at the highest dissolved silica concentrations whereas chalcedony precipitated at lower concentrations. The authigenic zeolite (clinoptilolite?) is found most frequently as small euhedral crystals that have grown on top of chalcedony, indicating that it postdates chalcedony cementation.

## 2.4 Aquifer Zone IIB<sub>1</sub>

### 2.4.1 General

Three hundred and forty-four samples from aquifer zone IIB<sub>1</sub> were analyzed for total carbonate content (Appendices B-8 and B-9). The average carbonate content of the sampled population is 30.7 percent with a large standard deviation of  $\pm 25.1$  percent. The carbonate content of the 344 samples ranges from zero to 86.7 percent.

Figure 20 is a ternary plot showing the weight percentage of carbonate material, terrigenous sand, and terrigenous mud for a subset of 148 samples from the calcareous interval within aquifer zone IIB<sub>1</sub> in the GSA. The data were derived from wet-sieve analyses of insoluble residues (Appendix B-9). Figure 20 indicates that most of the carbonate sediments and rocks in aquifer zone IIB<sub>1</sub> are mixtures of calcareous material and terrigenous sand end members with subordinate amounts of terrigenous mud (silt + clay). Terrigenous sand averages  $52.8 \pm 2.0$  weight percent and ranges from 2.7 to 93.4 weight percent; the standard deviation is high at 24.6 percent. Terrigenous mud ranges from 1.5 to 64.2 weight percent and averages  $15.2 \pm 0.9$  weight percent; the standard deviation is 10.9 percent. Soluble carbonate material of the 148 sample subset averages  $32.0 \pm 2.1$  weight percent and ranges from 0 to 85.8 percent; the standard deviation is 24.9 percent. Figure 20 shows that the preponderance of samples classify as sandy carbonate sediment, calcareous sand, slightly calcareous sand, slightly calcareous muddy sand, muddy sand, and sand according to Lindholm's (1987) modified classification. Minor muddy carbonate sediment, calcareous mud, and sandy mud are present (Figure 20).

Figure 21 is a triangular diagram showing the composition of 84 carbonate sediment and rock thin-section samples from aquifer zone IIB<sub>1</sub> according to Folk's (1962) classification scheme. Percentages of replacement microspar (low-Mg calcite with a crystal size smaller than  $30\mu\text{m}$ ) and pseudospar (low-Mg calcite with a crystal size larger than  $30\mu\text{m}$ ) were recast as microcrystalline calcite matrix (micrite) because the original sediment (rock) could have only contained carbonate allochemicals, micrite, and pore-filling sparry calcite cement (low-Mg calcite with a crystal size larger than  $30\mu\text{m}$ ). The figure indicates that these sediments are dominantly Type I microcrystalline (micritic) limestones containing variable percentages of allochemical grains. Figure 22 is a triangular diagram showing percentages of the most common skeletal allochemicals in calcareous sediments of aquifer zone IIB<sub>1</sub> in the GSA. Echinoderm, molluscan and foraminiferal skeletal grains are the dominant allochemicals in these calcareous sediments.

Data from binocular microscope and thin-section examination of 103 samples indicates that aquifer zone IIB<sub>1</sub> is divided into five carbonate, two terrigenous, and one siliceous microfacies (Figure 23). The eight microfacies include: 1) lime mud; 2) skeletal wackestone; 3) skeletal packstone; 4) skeletal grainstone; 5) microsparite; 6) terrigenous mud; 7) terrigenous sand and sandstone; and 8) siliceous mudstone. Figure 23 is a pie diagram showing the percentage of samples forming each microfacies. Appendix B-3 summarizes point count data for confining unit IIA-IIB and Appendix B-6 gives textural data for the same samples.

#### 2.4.2 *Lime Mud*

##### 2.4.2.1 Description

Three samples of poorly indurated, light gray, sandy lime mud (Figure 24) were studied. Two samples are from well BGO-14A between a depth of 126 and 133 ft and the other is from well YSC-5A (Appendices B-4 and B-7). In thin section, the samples lack laminations and appear homogeneous, possibly as the result of burrowing organisms. The sandy lime mud averages 37 percent fine-grained, subangular monocrystalline quartz, which is set in micrite matrix that has locally aggraded to microspar. Rounded and abraded skeletal allochems form about four percent of the total and include fragmented and micritized skeletal grains, foraminifers, molluscs, and echinoderms. The skeletal allochems are fine and medium calcarenite-sized although some molluscan grains attain lengths up to 4 mm long. Examination of smear slides of several samples indicates that the micrite matrix consists in part of low-Mg calcite coccoliths. Accessory constituents include potassium feldspar, detrital heavy minerals, glauconite, and authigenic pyrite and opal-CT. Authigenic framboidal pyrite formed within foraminiferal tests and grew displacively within the lime mud matrix. Authigenic opal-CT is present as 2-5  $\mu$ m lepispheres that replace micrite matrix and partially fill a few foraminiferal tests; many of the lepispheres have coalesced to form cauliflower-like aggregates. Visual porosity in thin section is very low and is dominantly interparticle between quartz grains. Moldic pores, vugs, and intraparticle pores within foraminifers are minor constituents. Most pores are not connected, hence permeability values are very low for this microfacies.

Wet-sieve analysis of the insoluble fraction of the three samples shows that terrigenous sand plus gravel forms 75.7 percent and mud (silt + clay) 24.3 percent. Grain-size analysis of the sand plus gravel fraction indicates that the mean grain size of the samples is 2.72 $\phi$  (lower fine

sand) with a standard deviation of  $\pm 0.15\phi$ ; mean size ranges from  $2.61\phi$  to  $2.82\phi$  (Appendix B-9). Sorting of the sand fraction averages  $0.67\phi \pm 0.14\phi$  (moderately well sorted) and ranges from  $0.58\phi$  (moderately well sorted) to  $0.77\phi$  (moderately sorted). Inclusive graphic skewness averages  $-0.16 \pm 0.06$ , which is coarse skewed according to the Folk and Ward (1957) verbal scale. Skewness ranges from  $-0.11$  to  $-0.20$  (coarse skewed). Graphic kurtosis of the sand plus gravel fraction averages 1.16, which is slightly leptokurtic on the Folk and Ward (1957) scale. Kurtosis ranges from 1.05 to 1.27 (very platykurtic).

#### 2.4.2.2 Interpretation

The presence of glauconite along with a normal marine fauna, including foraminifers, molluscs and echinoderms, indicates that the lime mud facies was deposited in clear, open-marine water of normal salinity on the inner or middle continental shelf. The abundance of micrite indicates deposition in quiet water below normal marine wave base. The presence of abraded and well-worn skeletal grains indicates that bottom transport by currents or storm-generated waves alternated with quiet-water conditions in which fine lime mud could accumulate. The abundance of fine quartz sand and terrigenous mud suggests closeness to riverine input. The lack of laminations in this microfacies most likely results from homogenization by burrowing organisms.

Post-depositional diagenetic events that have affected the lime mud microfacies occurred in the marine and freshwater phreatic environments. Events occurring in the marine phreatic environment included borings and partial micritization of bioclasts, mainly molluscs, by endolithic algae and fungi; and precipitation of several cements, including pyrite and glauconite. Framboidal pyrite is found within foraminiferal tests indicating that it formed under reducing conditions in areas containing putrefying tissue where sulfate-reducing bacteria were abundant (Scoffin, 1987).

The original unconsolidated sediment was dominated by low-Mg calcite molluscs and foraminifers and high-Mg echinoderms; aragonitic pelecypods were a minor constituent. After deposition, the lime mud underwent minor compaction within the first few hundred feet of burial. Following withdrawal of the sea, the sediment underwent the following changes in the subaerial, fresh-water phreatic environment: 1) High-Mg calcite allochems, mainly echinoderms, were converted to low-Mg calcite by leaching of  $Mg^{++}$  or solution-precipitation

on a micro-scale (Bathurst, 1971; Thayer and Textoris, 1977); 2) Some of the aragonitic skeletal allochems, mainly pelecypods, dissolved to create molds, which in turn underwent solution-enlargement to form vugs. This was not an important process in the lime mud microfacies because there were relatively few aragonitic pelecypods available for solution; 3) Opal-CT lepispheres precipitated within intraforam pores and micropores in the lime mud matrix. Formation of lepispheres postdates solution of aragonitic allochems and micrite matrix because the lepispheres line the interiors of molds.

### 2.4.3 *Skeletal Wackestone*

#### 2.4.3.1 Description

Skeletal wackestone, the dominant microfacies in aquifer zone IIB<sub>1</sub>, is present throughout the GSA, forming nearly 55 percent of the total sample suite (Figure 23). Petrographic data gathered from thin sections indicate that this microfacies is divided into two subtypes: skeletal wackestone (Table 2), which contains less than 10 percent terrigenous quartz (Figure 25); and quartz-rich skeletal wackestone (Table 3), containing greater than 10 percent detrital quartz (Figure 26). Acid-soluble carbonate material of a subset of 31 samples (Appendix B-9) from this microfacies averages  $52.7 \pm 14.1$  weight percent and ranges from 28.3 to 78.2 weight percent. Wet-sieve analysis of the acid-insoluble terrigenous fraction shows that sand plus gravel forms  $34.9 \pm 14.7$  weight percent, and terrigenous mud (silt + clay) averages  $12.4 \pm 5.9$  percent. Most samples plot as sandy carbonate on the Lindholm (1987) carbonate-terrigenous ternary diagram (Appendix A-11).

Grain-size analysis of the insoluble sand plus gravel fraction shows that mean size of the 31 samples is  $2.48\phi$  (upper fine sand) with a standard deviation of  $\pm 0.42\phi$ ; mean size ranges from  $1.11\phi$  (upper medium sand) to  $2.82\phi$  (lower fine sand) (Appendix B-9). Sorting of the sand fraction averages  $0.76\phi \pm 0.14\phi$  (moderately sorted) and ranges from  $0.35\phi$  (well sorted) to  $1.61\phi$  (poorly sorted). The poorly sorted sand fractions are typically bimodal. Inclusive graphic skewness averages  $-0.12 \pm 0.20$ , which is coarse skewed according to the Folk and Ward (1957) verbal scale. Skewness ranges from -0.54 (very coarse skewed) to +0.24 (fine skewed). Graphic kurtosis of the sand plus gravel fraction averages  $1.22 \pm 0.45$ , which is slightly leptokurtic on the Folk and Ward (1957) scale. Kurtosis ranges from 0.85 (platykurtic) to 3.19 (extremely leptokurtic).

Skeletal wackestone is present in wells BGO-9AA, BGO-10A, and HMD-1C (Appendices B-4 and B-7). It is unconsolidated to moderately well-indurated and typically light to medium gray in color. The microfacies consists of rounded and subrounded skeletal allochems set in a micrite matrix that has undergone localized aggrading coalescive neomorphism to form microspar and pseudospar (Appendix B-4). Echinoderms, molluscs, and foraminifers are the dominant allochems (Figure 22), with subordinate bryozoans, fragmented skeletal debris, micritized grains, pellets, and intraclasts. Serpulid worm tubes, barnacles, ostracodes, and sponge spicules are present in trace amounts. Fine, subangular monocrystalline quartz averages 5.2 percent and ranges from 1.7 to 8.0 percent. Glauconite pellets, heavy and opaque minerals, and traces of collophane and muscovite are present in minor amounts. Authigenic mineral phases include pyrite, glauconite cement, fibrous chalcedony, and rare opal-CT lepispheres. Framboidal pyrite partially fills foraminiferal tests and microborings in molluscan and other allochems. The pyrite is also associated with organic debris in the micrite matrix. Glauconite cement partially fills foraminiferal chambers, bryozoan zooecia, and microborings in molluscan and other skeletal allochems. Fibrous, length-fast spherulitic chalcedony is present as a partial replacement of Mg-calcite molluscan and echinoderm shell fragments. The chalcedony is generally found near the center of the skeletal fragment, and appears to have grown out toward the periphery. Ghosts of original shell microstructure are rarely preserved as inclusions of fine shell that appear brown in transmitted light. The chalcedony frequently reaches, but does not extend beyond the fossil-matrix contact. Rare opal-CT lepispheres are usually found within micropores and mesopores formed by dissolution of skeletal allochems. Porosity of the skeletal wackestone averages 10.9 percent and consists primarily of interparticle pores and moldic pores with lesser vugs, and intraparticle and intercrystal pores. Most of the pores in this subtype are meso-sized.

Forty-six of the thin sections examined for this study are sandy, skeletal wackestone (Appendices B-4 and B-7). This lithology is usually moderately to well-indurated but is friable to poorly indurated where terrigenous sand or mud content is high. Colors of this subtype are yellowish-gray and light and very light gray except near the contact with confining unit IIA-IIB, where grayish-green and greenish-gray colors are common.

The sandy, skeletal wackestone consists of sand-sized terrigenous quartz and sand-sized and gravel-sized skeletal allochems "floating" without preferred orientation in a micrite matrix that forms nearly 50 percent of the total sediment or rock. Subangular, fine-grained monocrystalline quartz forms slightly more than one-fourth of the total sediment or rock

(Appendix B-4). Rounded and subrounded skeletal allochems average almost 20 percent of the total sediment or rock (Appendix B-4) and are mainly pelecypods, other molluscs, echinoderms, and foraminifers. Additional skeletal grains include fragmented and micritized skeletal debris, bryozoans, gastropods, ostracodes, sponge spicules, bone and teeth (collophane), serpulid worm tubes, and barnacles. The abundant micrite matrix is usually structureless and has undergone localized aggrading neomorphism to microspar and pseudospar. Examination of smear slides prepared from the micrite matrix indicates that coccoliths are a common constituent in some samples but many have been recrystallized making recognition difficult. Minor accessory constituents include feldspar, glauconite pellets, carbonate intraclasts and pellets, and heavy and opaque minerals. Authigenic minerals include framboidal pyrite, glauconite cement, fibrous replacement chalcedony, clinoptilolite, and rare opal-CT lepispheres. The authigenic minerals have characteristics similar to those described for the skeletal wackestone above. In thin section, porosity of the sandy, skeletal wackestone averages 9.4 percent and comprises primary molds and interparticle pores with subordinate channels, vugs, intraparticle pores, and intercrystal pores. Most of the pores are meso-sized. Permeability in this microfacies is probably low because molds and other pores are isolated from each other by areas of microporous micrite or microspar, which have low permeability because pore-throat diameters are very small (Pittman, 1971). Porosity and permeability values have been significantly decreased in areas where pores have been reduced or closed by growth of secondary sparry calcite cement.

#### 2.4.3.2 Interpretation

The depositional environment envisioned for the skeletal wackestone is very similar to that proposed for the lime mud facies. The presence of glauconite along with diagnostic faunal elements, including foraminifers, molluscs, echinoderms, and others, indicates that this facies was deposited in clear, marine water of normal salinity on the inner or middle continental shelf. The abundance of micrite suggests deposition in quiet water below normal marine wave base. The presence of abraded and well-worn skeletal grains indicates that bottom transport by currents or storm-generated waves alternated with quiet-water conditions in which the lime mud accumulated. The abundance of fine, subangular quartz sand and terrigenous mud indicates proximity to riverine input. The scarcity of laminations in this microfacies probably results from homogenization by burrowing organisms.



Diagenetic events affecting the skeletal wackestone microfacies occurred in the marine and freshwater phreatic environments. Events occurring in the marine phreatic environment included: 1) borings and micritization of skeletal grains, mainly pelecypods, by endolithic algae and fungi; and 2) precipitation of subsea cements, including pyrite and glauconite. Framboidal pyrite is present within foraminiferal tests, microborings in molluscan shells, and is associated with organic matter within the micrite matrix, indicating that it formed under localized reducing conditions in areas where sulfate-reducing bacteria were abundant.

The skeletal wackestone underwent minor compaction during shallow burial, as shown by the presence of broken pelecypod and other shells. Also present are collapsed micrite envelopes about pelecypod molds, which formed by compaction following the dissolution of aragonitic allochems, as discussed below. Following a drop in sea level, the unconsolidated sediment underwent the following changes in the freshwater phreatic environment: 1) High-Mg calcite echinoderms were converted to low-Mg calcite by leaching of  $Mg^{++}$  or by solution-precipitation on a micro-scale (Bathurst, 1971); 2) Most of the aragonitic pelecypods, dissolved to create molds. The molds underwent solution-enlargement to form vugs and channels. This was an important porosity-creating process in the skeletal wackestone microfacies because aragonitic pelecypods formed up to 19 percent of the original unconsolidated sediment (Appendix B-4); 3) Some of the carbonate derived from aragonite dissolution in stage 2 above was precipitated nearby as low-Mg calcite overgrowths on echinoderm fragments and as pore-reducing or pore-filling equant spar cement. Most of the carbonate material released from dissolution of aragonitic allochems was exported out of the system as indicated by the small number of pores that are lined or filled with sparry calcite cement; 4) The micrite matrix underwent localized coalescive aggrading neomorphism to form microspar and pseudospar; 5) Biogenic opal-A in the form of sponge spicules and diatom valves dissolved to create silica-rich pore water. Some of the silica was precipitated as opal-CT lepispheres within intraforam pores and micropores in the lime mud matrix. This was a minor process in the skeletal wackestone microfacies. Lepisphere formation postdates solution of aragonitic allochems and micrite matrix because the lepispheres line the interiors of some molds; 6) Spherulitic chalcedony partially replaced Mg-calcite molluscan shells and filled some sponge-spicule molds. Cement stratigraphy indicates that chalcedony formed after precipitation of opal-CT.

#### 2.4.4 *Skeletal Packstone*

##### 2.4.4.1 Description

Quartz-rich skeletal packstone (Figure 27) is present in well BGO-9AA between 125 and 127 ft, and in wells BGX-4A and HSB-TB (Appendix B-4 and B-7). This microfacies is poorly to moderately indurated and light to medium gray in color. Analysis of petrographic data from seven thin sections indicates that this microfacies consists of broken and rounded skeletal allochems that are set in a micrite matrix (Table 4). In places the micrite matrix has undergone aggrading coalescive neomorphism to form microspar and minor pseudospar. The allochems are mainly pelecypods, echinoderms, foraminifers, undifferentiated molluscs, and fragmented and micritized skeletal debris. Barnacles, bryozoans, ostracodes, sponge spicules, and serpulid worm tubes are present in trace amounts. Average size of the skeletal grains ranges from 0.1 to 4.0 mm; most are fine and medium calcarenites. Fine-grained, subangular monocrystalline quartz averages 17 percent of whole rock volume. Quartz grains are disseminated evenly throughout the sediment. Minor accessory constituents include feldspar, muscovite, heavy minerals, opaque minerals, glauconite pellets, organic debris, and collophane (bone and teeth). In thin section, porosity of the seven samples averages 9.3 percent and ranges from near zero to a maximum of 22.1 percent. Mesomoldic pores and mesovugs are the dominant pore types with subordinate interparticle, intraparticle, and intercrystal pores. Permeability of this microfacies is estimated to be high because many of the molds and vugs are connected as a result of the close packing of original skeletal allochems. Authigenic cements and replacements include low-Mg sparry calcite, pyrite, glauconite, opal-CT, and chalcedony.

Minor sparry calcite cement partially fills molds formed by the dissolution of aragonitic pelecypods and is present as syntaxial rim cement on echinoderm fragments. Authigenic pyrite exists as framboids and cubes that are most often associated with organic matter in the lime mud matrix or within foraminiferal tests. Glauconite cement fills foraminiferal tests, bryozoan zooecia, and borings in Mg-calcite pelecypod valves. Authigenic opal-CT lepispheres are found within foraminiferal tests, axial canals of sponge spicules, and as linings within molds and vugs. Chalcedony partially replaces Mg-calcite pelecypod shells, fills sponge spicule molds, and is present as rim cement on detrital quartz.

#### 2.4.4.2 Interpretation

The presence of glauconite, pelecypods, bryozoans, echinoderms, foraminifers, and other skeletal allochems indicates a marine depositional environment. Faunal elements in this microfacies show that the water was relatively clear and of normal salinity. The sediment probably accumulated on the inner to middle shelf based on the fossil assemblage and presence of glauconite (Milliman, 1972). The large size and abraded and rounded shape of the bioclasts suggest bottom transport by strong currents or storm-generated waves. Micrite accumulated under quiet-water conditions or may have filtered into the coarse, grain-supported bioclastic sediment after deposition. Burrowing activities by bottom-dwelling organisms may have contributed to mixing the coarse, well-rounded skeletal bioclasts with fine micrite. The fine-grained, subangular terrigenous quartz suggests proximity to deltaic or riverine input. However, it could also represent relict or palimpsest sediment that was incorporated into the packstone during transgression of the sea.

Diagenetic events affected this microfacies in the marine and freshwater phreatic environments. Events occurring in the marine phreatic environment included microborings and micritization of bioclasts, and precipitation of pyrite and glauconite cements. Framboidal pyrite is associated with organic matter in the matrix and is present within foraminiferal tests, indicating that it formed under reducing conditions where sulfate-reducing bacteria were abundant.

The skeletal lime packstone underwent minor post-depositional compaction within the first few hundred feet of burial. Following withdrawal of the sea, the sediment underwent the following changes in the subaerial freshwater phreatic environment: 1) High-Mg calcite allochems, mainly echinoderms, were converted to low-Mg calcite by leaching of  $Mg^{++}$  or solution-precipitation on a micro-scale (Bathurst, 1971; Thayer and Textoris, 1977); 2) Aragonitic skeletal allochems, chiefly pelecypods, dissolved to form molds, which in turn underwent solution-enlargement to create vugs. This was an important porosity-creating process in this microfacies because aragonitic pelecypods formed up to 20 percent of the original sediment volume (Appendix B-4); 3) Some of the carbonate material from the dissolution of aragonite precipitated nearby as low-Mg calcite cement within molds and vugs, and as syntaxial rim overgrowths on echinoderm fragments. This process was minor in the packstone microfacies. The original sediment had high permeability; allowing the dissolved calcium and bicarbonate ions to be rapidly transported out of the system, having little

opportunity to precipitate as low-Mg calcite (Moore, 1979); 4) Micrite matrix underwent localized aggrading recrystallization to form microspar and pseudospar; 5) Biogenic opal-A sponge spicules and diatom valves underwent dissolution; 6) Opal-CT lepispheres precipitated from silica-rich pore water created by dissolution of biogenic opal-A. The 2-5  $\mu\text{m}$  lepispheres precipitated within intraforam pores, axial canals of sponge spicules and as linings within molds and vugs. Formation of lepispheres postdates solution of aragonitic allochems and micrite matrix because the lepispheres commonly line the interiors of molds; 7) Chalcedony partially replaced Mg-calcite pelecypod shells, filled sponge spicule molds, and precipitated locally as rim cement on detrital quartz grains. Textural relationships indicate that opal-CT precipitated prior to chalcedony. Maliva and Siever (1988) demonstrated that opal-CT precipitated at the highest dissolved silica concentrations whereas chalcedony formed at lower concentrations.

#### 2.4.5 *Skeletal Grainstone*

##### 2.4.5.1 Description

Quartz-rich skeletal grainstone (Figure 28) is a minor microfacies of aquifer zone IIB<sub>1</sub> in the GSA and is only found in well BGO-10A (Appendix B-4). The grainstone is moderately indurated and light gray in color. It consists of well-rounded and well-sorted skeletal allochems mixed with subangular, fine-grained quartz sand which is partially cemented by sparry calcite cement. Echinoderms are the dominant skeletal allochem with subordinate foraminifers, molluscs, comminuted skeletal fragments, and micritized skeletal grains. Minor to trace constituents include glauconite, heavy and opaque minerals, and collophane. Several types of sparry calcite cement are present in this microfacies. A very finely crystalline equant calcite cement coats some skeletal grains and lines internal cavities of a few foraminifers. Medium to coarsely crystalline calcite overgrowths are present on some echinoderm fragments. Finely to medium crystalline sparry calcite cement partially fills some molds and vugs. The spar shows crystal enlargement towards the pore center, indicating that it is a cement rather than a product of grain recrystallization. Porosity is 16.7 percent and is mainly interparticle pores and intercrystal pores with minor moldic and intraparticle pores.

#### 2.4.5.2 Interpretation

The quartz-rich skeletal grainstone accumulated in an open-marine environment on the inner continental shelf. The presence of well-rounded and well-sorted skeletal allochems along with the presence of fine, well-sorted quartz sand indicates constant and relatively high energy conditions at the depositional site. This facies probably formed as a shallow marine bank in water less than 50 feet deep.

The grainstone went through the following sequence of diagenetic changes in the marine phreatic environment. Grain micritization either produced micrite envelopes on skeletal grains, or totally obliterated skeletal microstructure forming amorphous grains of micrite that resemble fecal pellets. Following burial, minor compaction occurred as indicated by some broken foraminifer and pelecypod grains. Collapsed micrite envelopes about pelecypod molds are present. These formed by compaction following dissolution of aragonitic allochems as discussed below. The very finely crystalline, equant calcite cement that coats exterior and interior walls of foraminifers as well as exterior margins of other allochems probably formed early on within the saturated meteoric phreatic zone (Longman, 1980). Syntaxial rim overgrowth on echinoderms, inversion of high-Mg skeletal allochems to low-Mg calcite, and minor recrystallization of molluscan allochems to anhedral calcite also occurred in the meteoric phreatic realm. Dissolution of aragonite and possibly some high-Mg calcite allochems followed early cementation by equant calcite and created molds and vugs. Absence of finely crystalline calcite cement lining molds and vugs indicates that the dissolution phase post-dated early calcite cementation. Dissolution probably occurred in the undersaturated part of the freshwater phreatic zone (Longman, 1980). The last diagenetic event was the growth of finely to medium crystalline low-Mg calcite cement in some molds, vugs and intraparticle pores. This cementation probably occurred in the saturated part of the meteoric phreatic environment as suggested by Longman (1980).

#### 2.4.6 *Microsparite*

##### 2.4.6.1 Description

Microsparite includes fine-grained recrystallized carbonate sediment or rock that consists predominantly of subhedral to euhedral low-Mg calcite crystals smaller than 60  $\mu\text{m}$  (Folk, 1959; Flügel, 1982). Crystal size and shape is typically uniform and homogeneous within an

individual sample, and terrigenous clay or organic matter is often present between crystals. According to Folk (1959), microsparite originates from recrystallization of micrite calcite, which is possible only after the removal of  $Mg^{++}$  ions. The removal of Mg was caused by freshwater input into the carbonate beds following a drop in sea level.

Microsparite is present throughout aquifer zone IIB<sub>1</sub> in the GSA, forming nearly 14 percent of the samples studied (Figure 23). It is massive, moderately to very well-indurated, and usually light gray, light greenish gray, or tan colored. Sedimentary structures are not present in any of the samples examined. Acid-soluble carbonate of a subset of 15 samples (Appendix B-9) from this microfacies averages  $54.1 \pm 21.8$  weight percent and ranges from 21.6 to 85.8 weight percent. Wet-sieve analysis of the acid-insoluble terrigenous fraction shows that sand plus gravel forms  $35.1 \pm 15.9$  weight percent, and terrigenous mud (silt + clay) averages  $10.8 \pm 8.1$  percent. The majority of samples plot as sandy carbonate sediment on the Lindholm (1987) carbonate-terrigenous ternary diagram (Figure 20, Appendix A-11).

Grain-size analysis of the insoluble sand plus gravel fraction shows that mean size of the 15 samples is  $2.31\phi$  (upper fine sand) with a standard deviation of  $\pm 0.61\phi$ ; mean size ranges from  $0.90\phi$  (lower coarse sand) to  $2.93\phi$  (lower fine sand) (Appendix B-9). Sorting of the sand fraction averages  $0.84\phi \pm 0.27\phi$  (moderately sorted) and ranges from  $0.46\phi$  (well sorted) to  $1.45\phi$  (poorly sorted). Inclusive graphic skewness averages  $-0.15 \pm 0.34$ , which is coarse skewed according to the Folk and Ward (1957) verbal scale. Skewness ranges from  $-0.59$  (very coarse skewed) to  $+0.88$  (very fine skewed). Graphic kurtosis of the sand plus gravel fraction averages  $1.23 \pm 0.74$ , which is leptokurtic on the Folk and Ward (1957) scale. Kurtosis ranges from 0.35 (very platykurtic) to 3.44 (extremely leptokurtic).

Table 5 gives the average composition of 19 microsparite samples from aquifer zone IIB<sub>1</sub>. The microsparite consists of fine-grained subangular quartz along with rounded skeletal allochems "floating" without preferred orientation in a fine-grained carbonate matrix consisting predominantly of microspar and pseudospar (Figure 29). Skeletal allochems are fine and medium calcarenite-sized and consist of pelecypods, foraminifers, echinoderms, bryozoans, gastropods, and fragmented and micritized skeletal debris. Many of the skeletal allochems show evidence of partial replacement by microspar or pseudospar as indicated by truncation of grains against calcite spar. Other constituents include feldspar, muscovite, terrigenous mud, glauconite pellets, colophonane, carbonate intraclasts and pellets, organic debris, and heavy and opaque minerals. Trace quantities of authigenic phases include pyrite,

glauconite cement, opal-CT lepispheres, and chalcedony. Pyrite and glauconite commonly fill or partly fill foraminifer tests, bryozoan zooecia, and microborings in molluscan and other allochems. Rare opal-CT lepispheres are found within foraminiferal tests and as linings within small mesomolds and mesovugs. Spherulitic chalcedony partially replaces Mg-calcite pelecypod shells and echinoderm fragments. Porosity of this microfacies averages 5 percent and is dominantly moldic pores, vugs and intercrystal pores with minor interparticle and intraparticle pores. Most of the pores are small meso-sized.

#### 2.4.6.2 Interpretation

Textural analysis of thin sections and the presence of relict skeletal allochems indicates that the microsparite is a product of the recrystallization of lime mud, skeletal wackestone and possibly skeletal packstone. Evidence indicating recrystallization includes uniform grain size of the microspar and pseudospar, relict patches of micrite and allochems 'floating' within the spar, and spar transgression of skeletal allochems and original micrite matrix more or less indiscriminately (Folk, 1980). Most of the precursor sediment types were quartz-rich as indicated by the comparatively high quartz content of the microsparite microfacies. Insoluble-residue study of the microsparite shows that it contains about 10 percent terrigenous mud, indicating that the original sediment also contained terrigenous silt-sized and clay-sized particles. The inferred depositional environments have been discussed previously.

Recrystallization of the original micrite matrix occurred by gradual crystal enlargement, which maintained a uniform crystal size throughout the process. Folk (1980) has termed this type of recrystallization coalescive neomorphism. Continued growth of the neomorphic spar destroyed most of the original depositional and diagenetic textures. Microsparites that truncate micrite and grains alike are a late diagenetic feature that formed in the freshwater phreatic environment (Folk, 1980; Longman, 1980; and Scoffin, 1987). The diagenetic sequence of the microsparite followed that of the parent lithology until the formation of neomorphic spar. Thus, the formation of pyrite and glauconite cements, as well as the dissolution of aragonitic allochems and matrix to form moldic and vug pores occurred prior to growth of neomorphic spar. Critical textural evidence is lacking to determine whether opal-CT and chalcedony formed before, during, or after growth of neomorphic spar.

#### 2.4.7 *Siliceous Mudstone*

##### 2.4.7.1 Description

Nine thin sections of quartz-rich siliceous mudstone from aquifer zone IIB<sub>1</sub> were examined (Table 6; Appendices B-4 and B-7). All samples are massive, moderately well-indurated and tan, very light gray, light yellowish gray, or light greenish-gray in color.

Quartz-rich siliceous mudstone (Figure 30) consists of fine and medium-grained, subangular monocrystalline quartz, other terrigenous grains, and skeletal allochems "floating" without preferred orientation in a light brown, felted matrix of coalesced opal-CT lepispheres (Table 6; Figure 30). The opal matrix averages 38.5 percent of whole-rock volume and is structureless in transmitted light. Rounded and sub-rounded skeletal allochems constitute 9.1 percent of whole-rock volume and include foraminifers, molluscs, echinoderms, bryozoans, sponge spicules, and fragmented and micritized skeletal grains. Minor accessory constituents include polycrystalline quartz, feldspar, muscovite, glauconite pellets, heavy and opaque minerals, organic debris, and collophane. Relict patches of micrite and microspar display corroded margins where they are in contact with secondary opal-CT cement.

In addition to opal-CT, authigenic cements and replacement minerals include framboidal pyrite, glauconite, chalcedony, and zeolite. Pyrite and glauconite fill or partially fill microborings in Mg-calcite skeletal grains, chiefly pelecypod valves; both also are found within some foraminiferal chambers and bryozoan zooecia. Spherulitic, length-fast chalcedony fills molds formed by dissolution of sponge spicules and partially replaces low-Mg calcite pelecypod shells. Tabular crystals of 5-40  $\mu\text{m}$  euhedral zeolite (clinoptilolite?) partially fill micropores within the opal-CT matrix and line some foraminiferal chambers.

Porosity averages 10.4 percent and is dominated by small mesomolds and mesovugs (Table 6). Many of the molds were originally aragonitic pelecypod valves that were leached prior to silicification; others formed by sponge spicule dissolution. The vugs most likely formed by solution enlargement of pelecypod molds prior to silicification. Other pore types include interparticle pores, intraparticle pores within foraminifers and bryozoans, and intercrystal pores. All pores are small meso-sized.



#### 2.4.7.2 Interpretation

The siliceous mudstone microfacies is interpreted to be a diagenetic replacement of sandy, skeletal wackestone. The wackestone was deposited in clear, open-marine water of normal salinity on the inner to middle shelf as indicated by the presence of glauconite and a normal marine fauna, including foraminifers, pelecypods, gastropods, bryozoans, and echinoderms. Most of the opal-CT matrix was originally micrite, and its abundance indicates deposition in quiet water below normal marine wave base. The presence of abraded and well-worn skeletal grains along with considerable terrigenous sand and some quartz gravel indicate that bottom transport by currents or storm-generated waves alternated with quiet-water conditions in which lime mud could accumulate. The absence of laminations or other primary sedimentary structures in this microfacies may result from homogenization by burrowing organisms. Alternatively, the diagenetic alteration of micritic carbonate material to opal-CT may have destroyed all original texture and structure.

The diagenetic history of the siliceous mudstone microfacies includes changes in the marine and freshwater phreatic environments. Events occurring in the marine phreatic environment include microborings and micritization of some Mg-calcite bioclasts, as well as precipitation of pyrite and glauconite cements. Framboidal pyrite is associated with organic matter in the matrix and within microborings and foraminiferal tests, indicating that it formed under localized reducing conditions where sulfate-reducing bacteria were numerous. Glauconite precipitated in microborings, foraminiferal chambers, and bryozoan zooecia under slightly reducing conditions in water depths greater than 10 m; its presence indicates slow sedimentation rates (Nystrom and others, 1989, 1991).

The skeletal wackestone underwent post-depositional compaction. Following regression of the sea, the sediment underwent the following changes in the subaerial freshwater phreatic environment: 1) High-Mg calcite allochems, mainly echinoderms, were converted to low-Mg calcite by leaching of  $Mg^{++}$  or solution-precipitation on a micro-scale (Bathurst, 1971); 2) Aragonitic skeletal allochems, chiefly pelecypods, dissolved to form molds, which in turn underwent solution-enlargement to create vugs; 3) Some of the carbonate from aragonite dissolution precipitated within nearby molds and vugs as low-Mg calcite cement. This process was rare in this microfacies; 4) Biogenic opal-A as sponge spicules and diatom valves underwent dissolution; 5) Opal-CT lepispheres precipitated from silica-rich pore water and replaced micrite matrix, some skeletal allochems, and formed linings within a few molds, vugs,

and intraforam pores. Lepisphere formation post-dates solution of aragonitic allochems and micrite matrix because the lepispheres line the interiors of molds and vugs; 6) Chalcedony partially replaced Mg-calcite pelecypod shells, filled sponge spicule molds, and precipitated locally as rim cement on detrital quartz. Textural relationships indicate that the opal-CT precipitated prior to chalcedony. The opal-CT probably precipitated at the highest dissolved silica concentrations whereas chalcedony formed at lower concentrations (Maliva and Siever, 1988); 7) Authigenic zeolite precipitated in micropores within the siliceous sediment. The zeolite postdates opal-CT formation because euhedral zeolite crystals have grown on top of the opal. The zeolite probably formed after chalcedony cementation because zeolite inclusions have not been found within chalcedony.

#### **2.4.8 *Terrigenous Mud***

##### **2.4.8.1 Description**

Five thin sections of quartz-rich terrigenous mud from this microfacies were examined (Table 7; Appendix B-4 and B-7). The samples are from wells BGX-2B, HPC-1, and HSB-TB. All are poorly indurated, massively bedded, and light gray or light greenish-gray in color. The fabric of each sample was disrupted during preparation of the thin section. Because of this, information on sedimentary structures as well as pore type and abundance could not be determined. This microfacies consists of quartz-rich terrigenous mud (Figure 31) that contains subordinate micrite, heavy and opaque minerals, glauconite pellets, and trace quantities of feldspar, organic debris, and fragmented and micritized skeletal debris. One sample (HSB-TB-152B) contains almost 30 percent coarse calcarenite-sized skeletal allochems, chiefly pelecypods with minor foraminifers, echinoderms, and comminuted skeletal debris. The quartz in this microfacies is subangular and predominantly unstrained monocrystalline; average grain size ranges from lower very fine to upper medium (Appendix B-7). Authigenic constituents include pyrite and glauconite cements, both of which are found within foraminiferal tests and other skeletal debris. The pyrite is also associated with organic fragments within the matrix.

#### 2.4.8.2 Interpretation

The abundance of terrigenous mud and the presence of glauconite and foraminiferal, pelecypod, and echinoderm allochems indicates deposition in quiet water within an open-marine environment of normal salinity. The abundance of terrigenous mud and sand indicates close proximity to coastal riverine input. The massive fabric observed in cores suggests bioturbation at the depositional site. The presence of glauconite indicates a slow rate of deposition in water depths greater than 10 m and temperatures 17 °C or cooler (Nystrom and others, 1991).

Chief diagenetic events affecting the terrigenous mud microfacies include: 1) Minor micritization of skeletal allochems (primarily pelecypods) by boring algae and fungi while the sediment was exposed on the sea floor, 2) Slight compaction of the mud within the first few feet of burial, and 3) Formation of pyrite early on within the marine phreatic realm in areas containing putrefying tissue or organic debris where sulfate-reducing bacteria were abundant.

#### 2.4.9 *Terrigenous Sand and Sandstone*

##### 2.4.9.1 Description

This microfacies consists of friable to poorly consolidated muddy sand and calcareous muddy sand, along with well-indurated silica-cemented quartzarenite. The muddy sand is tan, yellowish orange, and greenish gray in color, and frequently contains thin pebbly zones. The sandstone is tan or light gray. The unconsolidated muddy sand is medium grained, poorly sorted and texturally immature (Appendix B-7). The silica-cemented sandstone is medium grained, moderately sorted and texturally submature.

Examination of four thin sections from samples of muddy sand indicates that the unit consists primarily of subangular, unstrained monocrystalline quartz ( $\bar{x}$  = 57.4 percent) with considerable silty clay matrix ( $\bar{x}$  = 37.7 percent) (Figure 32). Minor accessory constituents include polycrystalline quartz, feldspar, glauconite pellets, and opaque and heavy minerals. The calcareous muddy sand contains well-rounded echinoderm and comminuted skeletal debris (Appendix B-4). Porosity measured in undisturbed thin sections from two samples averages  $17.7 \pm 4.7$  percent and is nearly all small mesointerparticle between terrigenous quartz grains.

Two samples of silica-cemented sandstone were examined from this microfacies. One sample is a chalcedony-cemented sandstone from well YSC-2A and the other is an opal-cemented sandstone from well BGO-29A (Appendix B-4 and B-7). Both samples consist predominantly of unstrained monocrystalline quartz and are cemented by botryoidal opal-CT or spherulitic chalcedony (Figure 33.) The opal and chalcedony are present as rim cements on detrital quartz grains and partially occlude intergranular pore space as well as pore throats. The opal-cemented sandstone has 1 percent porosity whereas the chalcedony-cemented sandstone has 15.6 percent. Small mesovugs are the dominant pore type in both samples. The silica-cemented sandstone contains trace amounts of feldspar, rounded echinoderm fragments, collophane, and heavy and opaque minerals.

#### 2.4.9.2 Interpretation

The presence of glauconite, collophane, and rounded echinoderm and other skeletal debris indicates that this microfacies is a shallow marine shelf deposit. The presence of substantial mud in the unconsolidated sand suggests that energy conditions at the depositional site fluctuated considerably. Alternatively, the mud may have been introduced into the sand from adjacent beds by burrowing organisms shortly after deposition. The scarcity of labile constituents, such as feldspar and rock fragments, suggests intense chemical weathering in the source terrane, or could have resulted from post-depositional subsurface leaching by groundwater in the freshwater vadose or freshwater phreatic environment.

Post-depositional diagenetic changes in this microfacies are minor, but include leaching of aragonitic skeletal grains, feldspar and unstable heavy minerals, such as garnet. Cementation by opal or chalcedony is uncommon and is restricted to small areas within the aquifer zone IIB<sub>1</sub>, particularly near its basal contact with confining unit IIA-IIB. The most likely source of dissolved silica for opal-CT and chalcedony cementation is the dissolution of diatom and sponge spicule opal-A from other microfacies within aquifer zone IIB<sub>1</sub>, or from confining unit IIA-IIB. The opal-CT probably precipitated at the highest dissolved silica concentrations whereas chalcedony formed at lower concentrations (Maliva and Siever, 1988).

### 3.0 SUMMARY AND CONCLUSIONS

1. Layers of calcareous sediment beneath the General Separations Area are laterally and vertically discontinuous. They are present within aquifer unit IIA, confining unit IIA-IIB, and aquifer zone IIB<sub>1</sub>. Most of the calcareous sediment beneath the GSA is included in aquifer zone IIB<sub>1</sub>.
2. Aquifer unit IIA is divisible into two microfacies: terrigenous mud and terrigenous sand and sandstone. Average carbonate content for 20 samples from aquifer unit IIA is 3.1 weight percent with a standard deviation of 10.1 weight percent. Terrigenous sand forms the bulk of aquifer unit IIA and consists of thick beds of unconsolidated quartz sand that contains thin, discontinuous layers of mud and minor zones of opal- and chalcedony-cemented sandstone.
3. Confining unit IIA-IIB is divisible into four microfacies: lime mud; siliceous mudstone, including sandy, siliceous mudstone, and sandy, skeletal siliceous mudstone; sandy, terrigenous mud; and terrigenous sand. Average carbonate content for 32 representative samples is 14.3 weight percent with a standard deviation of  $\pm 16.9$  percent. Carbonate ranges from zero to a maximum of 79.6 weight percent. Quartz-rich terrigenous mud is the dominant microfacies within confining unit IIA-IIB.
4. Aquifer zone IIB<sub>1</sub> is divisible into five carbonate, two terrigenous, and one siliceous microfacies. The eight microfacies include 1) lime mud; 2) skeletal wackestone; 3) skeletal packstone; 4) skeletal grainstone; 5) microsparite; 6) terrigenous mud; 7) terrigenous sand and sandstone; and 8) siliceous mudstone. The average carbonate content of 344 samples from aquifer zone IIB<sub>1</sub> is 30.7 percent with a standard deviation of  $\pm 25.1$  percent; the range is from zero to 86.7 percent.
5. Skeletal wackestone is the dominant microfacies in aquifer zone IIB<sub>1</sub>, and is found throughout the "calcareous zone" beneath GSA, forming nearly 55 percent of the sampled population. This microfacies is divisible into two subtypes: skeletal wackestone, which contains less than 10 percent terrigenous quartz; and quartz-rich skeletal wackestone, containing greater than 10 percent terrigenous quartz.

6. Diagenetic pathways for the carbonate sediments typically included: (1) marine phreatic — skeletal micritization and rare fibrous cementation within foraminiferal tests; (2) meteoric vadose — minor leaching of aragonitic skeletal grains; and (3) meteoric phreatic — neomorphism of micrite to microspar and pseudospar, wholesale dissolution of opal-A and aragonitic skeletal grains, formation of equant low-Mg calcite spar, and development of syntaxial calcite overgrowths on echinoderm fragments. Minor opal-CT and fibrous chalcedony cements are ubiquitous in all microfacies. The source of the silica was dissolution of biogenic opal-A from sponge spicules and diatom valves.

7. The dominant porosity types in the carbonate microfacies are secondary moldic and vug, with subordinate channel, interparticle, intraparticle, and intercrystal. Interparticle is the dominant pore type in the sand and sandstone microfacies. Moldic pores formed chiefly from dissolution of aragonitic pelecypods and gastropods. Solution-enlargement of molds produced vug and channel pores. Minor cementation by low-Mg calcite spar has locally reduced moldic, vug, and interparticle pores. Permeability of the carbonate microfacies is controlled by allochem composition and packing, volume of micrite and terrigenous mud, and amount of secondary dissolution and cementation.

## REFERENCES

---

- AADLAND, R. K., 1990, Classification of hydrostratigraphic units at Savannah River Site, South Carolina: U.S. Department of Energy Report WSRC-RP-90-987: Aiken, S.C., Westinghouse Savannah River Company, 22 p.
- AADLAND, R. K., HARRIS, M. K., LEWIS, C. M., GAUGHAN, T. F., and WESTBROOK, T. M., 1991, Hydrostratigraphy of the General Separations Area, Savannah River Site (SRS): U.S. Department of Energy Report WSRC-RP-91-13, Aiken, S.C., Westinghouse Savannah River Company, 114 p.
- AADLAND, R. K., THAYER, P. A., AND SMITS, A. D., 1992a, Hydrogeologic atlas of west-central South Carolina: U.S. Department of Energy Report WSRC-RP-92-632, Aiken, S.C., Westinghouse Savannah River Company, 126 p.
- AADLAND, R. K., THAYER, P. A., AND SMITS, A. D., 1992b, Hydrostratigraphy of the Savannah River Site Region, South Carolina and Georgia: *in* Fallaw, W.C., and Price, V., eds., Geological Investigations of the Central Savannah River Area, South Carolina and Georgia: Carolina Geological Society Field Trip Guidebook 1992, p. BX1-BX6.
- AUCOTT, W. R., 1988, The pre-development groundwater flow system and hydrologic characteristics of coastal plain aquifers of South Carolina: U.S. Geological Survey, Water-Resources Investigations Report 86-4347, 66 p.
- AUCOTT, W. R., DAVIS, M. E., and SPEIRAN, G. K., 1987, Geohydrologic framework of the Coastal Plain aquifers of South Carolina: U.S. Geological Survey Water-Resources Investigations Report 85-4271, 7 sheets.
- BATHURST, R. G. C., 1971, Carbonate sediments and their diagenesis: Amsterdam, Elsevier, 620 p.
- BAUM, G. R., COLLINS, J. S., JONES, R. J., MADINGER, B. A., and POWELL, R. J., 1979, Correlation of the Eocene strata of the Carolinas: South Carolina Geological Notes, v. 24, p. 19-27.
- BEARD, D.C., and WEYL, P. K., 1973, Influence of texture on porosity and permeability of unconsolidated sand: American Association of Petroleum Geologists Bulletin 57, p. 349-369.
- BLEDSE, H. W., AADLAND, R. K., and SARGENT, K. A., 1990, Baseline hydrogeologic investigation – summary report: U.S. Department of Energy Report WSRC-RP-90-1010, Aiken, S. C., Westinghouse Savannah River Company, 200 p.
- BROOKS, R., CLARKE, J. S., and FAYE, R. E., 1985, Hydrogeology of the Gordon aquifer system of east-central Georgia: Georgia Geological Survey Information Circular 75, 41 p.

## **REFERENCES (Continued)**

---

- CARVER, R. E., 1980, Petrology of Paleocene-Eocene and Miocene opaline sediments, southeastern Atlantic Coastal Plain: *Journal of Sedimentary Petrology*, v. 50, p. 569-582.
- CHOQUETTE, P. W., and PRAY, L. C., 1970, Geologic nomenclature and classification of porosity in sedimentary carbonates: *American Association of Petroleum Geologists Bulletin*, v. 54, p. 207-250.
- CLARKE, J. S., BROOKS, R., AND FAYE, R. E., 1985, Hydrogeology of the Gordon aquifer system of east-central Georgia: *Georgia Geological Survey Information Circular* 75, 41 p.
- CLARKE, J. S., HACKE, C. M., AND PECK, M. F., 1990, Geology and groundwater resources of the coastal area of Georgia: *Georgia Geological Survey Bulletin* 113, 106 p.
- COLQUHOUN, D. J., and JOHNSON, H. S., Jr., 1968, Tertiary sea-level fluctuation in South Carolina: *Palaeogeography, Palaeoclimatology, Palaeoecology*, v. 5, p. 105-126.
- COLQUHOUN, D. J., OLDHAM, R. W., BISHOP, J. W., AND HOWELL, P. D., 1982, Updip delineation of the Tertiary limestone aquifer, South Carolina: Final Completion Report to the Office of Water Policy, U.S. Department of the Interior, Washington, D.C., Water Resources Research Institute, Clemson University, Clemson, South Carolina, 93 p.
- COLQUHOUN, D.J., WOOLEN, I. D., VAN NIEUWENHUISE, D. S., PADGETT, G. G., OLDHAM, R. W., BOYLAN, D. C., BISHOP, J. W., and HOWELL, P. D., 1983, Surface and subsurface stratigraphy, structure and aquifers of the South Carolina Coastal Plain: Columbia, South Carolina, Department of Geology, University of South Carolina, Report to the Department of Health and Environmental Control, Ground Water Protection Division, published through the Office of the Governor, State of South Carolina, 78 p. (folio).
- COOKE, C. W., 1936, Geology of the Coastal Plain of South Carolina: U.S. Geological Survey Bulletin 867, 196 p.
- COOKE, C. W., and MACNEIL, F. S., 1952, Tertiary stratigraphy of South Carolina: U.S. Geological Survey Professional Paper 243-B, p. 19-29.
- DAVIS, S. N., 1969, Porosity and permeability of natural materials, in DeWiest, R. J. M., ed., *Flow Through Porous Media*: New York, Academic Press, p. 53-89.
- DENNEHY, K. F., PROWELL, D. C., and McMAHON, P. B., 1989, Reconnaissance hydrogeologic investigation of the defense waste processing facility and vicinity, Savannah River Plant, South Carolina: U.S. Geological Survey Water-Resources Investigations Report 88-4221, 74 p.



## REFERENCES (Continued)

---

- DENNISON, J. M., and SHEA, J. H., 1966, Reliability of visual estimates of grain abundance: *Journal of Sedimentary Petrology*, v. 36, p. 81-89.
- DRYDEN, A. L., 1931, Accuracy in percentage representation of heavy mineral frequencies: *Proceedings of the National Academy of Sciences*, v. 17, p. 233-238.
- DUNHAM, R. J., 1962, Classification of carbonate rocks according to depositional texture, *in* Ham, W. E., ed., *Classification of Carbonate Rocks: American Association of Petroleum Geologists Memoir 1*, p. 108-121.
- FALLAW, W. C., and PRICE, V., 1992, Outline of stratigraphy at the Savannah River Site: *in* Fallaw, W. C., and Price, V., Jr., eds., *Geological Investigations of the Central Savannah River Area, South Carolina and Georgia: Carolina Geological Society Field Trip Guidebook 1992*, p. B-II-1 - B-II-33.
- FALLAW, W. C., PRICE, V., AND THAYER, P. A., 1992, Stratigraphy of the Savannah River Site, South Carolina, *in* Zullo, V. A., Harris, W. B., and Price, V., Jr., eds., *Savannah River Region: Transition Between the Gulf and Atlantic Coastal Plains — Proceedings of the Second Bald Head Island Conference on Coastal Plains Geology: Wilmington, North Carolina, The University of North Carolina at Wilmington*, p. 29-32.
- FLÖRKE, O. W., HOLLMANN, R., VON RAD, U., AND RÖSCH, H., 1976, Intergrowth and twinning in opal-CT lepispheres: *Contributions to Mineralogy and Petrology*, v. 58, p. 235-242.
- FLÜGEL, E., 1982, *Microfacies Analysis of Limestones*: New York, Springer-Verlag, 633 p.
- FOLK, R. L., 1951, Stages of textural maturity in sedimentary rocks: *Journal of Sedimentary Petrology*, v. 21, p. 127-130.
- FOLK, R. L., 1959, Practical petrographic classification of limestones: *American Association of Petroleum Geologists Bulletin*, v. 43, p. 1-38.
- FOLK, R. L., 1965, Some aspects of recrystallization in ancient limestones, *in* Pray, L. C., and Murray, R. C., eds., *Dolomitization and Limestone Diagenesis: SEPM Special Publication 13*, p. 14-48.
- FOLK, R. L., 1980, *Petrology of sedimentary rocks*: Austin, Hemphill Publishing Co., 182 p.
- FOLK, R. L., and PITTMAN, J. S., 1971, Length-slow chalcedony: a new testament for vanished evaporites: *Journal of Sedimentary Petrology*, v. 41, p. 1045-1058.
- FOLK, R. L., and WARD, W. C., 1957, Brazos River Bar — a study in the significance of grain-size parameters: *Journal of Sedimentary Petrology*, v. 27, p. 3-26.

## REFERENCES (Continued)

---

- FRIEDMAN, G. M., 1971, Staining, *in* Carver, R. E., ed., *Procedures in Sedimentary Petrology*: New York, Wiley-Interscience, p. 511-530.
- FRIEDMAN, G. M., 1965, Terminology of crystallization textures and fabrics in sedimentary rocks: *Journal of Sedimentary Petrology*, v. 35, p. 643-655.
- GALEHOUSE, J.S., 1971, Point Counting, *in* Carver, R. E., ed., *Procedures in Sedimentary Petrology*: New York, Wiley-Interscience, p. 385-407.
- GODDARD, B. N., Chairman, 1948, Rock-color chart: Boulder, Colorado, Geological Society of America, 11 p.
- GOHN, G. S., 1988, Late Mesozoic and early Cenozoic geology of the Atlantic Coastal Plain: North Carolina to Florida, *in* Sheridan, R. E., and Grow, J. A., eds., *The Geology of North America*, v. 1-2, *The Atlantic Continental Margin, U.S.*: Geological Society of America, p. 107-130.
- GORDAY, L. L., 1985, The hydrogeology of the Coastal Plain strata of Richmond and northern Burke counties, Georgia: Georgia Geological Survey Information Circular 61, 43 p.
- HARRELL, J. A., 1984, A visual comparator for degree of sorting in thin and plane sections: *Journal of Sedimentary Petrology*, v. 54, p. 648-650.
- HARRELL, J. A., and ERIKSSON, K. A., 1979, Empirical conversion equations for thin section and sieve derived size distribution parameters: *Journal of Sedimentary Petrology*, v. 49, p. 273-280.
- HARRIS, M. K., AADLAND, R. K., AND WESTBROOK, T. M., 1992, Lithological and hydrogeological characteristics of Tertiary hydrostratigraphic systems of the General Separations Area, Savannah River Site, South Carolina, *in* Zullo, V. A., Harris, W. B., and Price, V., eds., *Savannah River Region: Transition Between the Gulf and Atlantic Coastal Plains — Proceedings of the Second Bald Head Island Conference on Coastal Plains Geology*: Wilmington, North Carolina, The University of North Carolina at Wilmington, p. 68-73.
- HARRIS, W. B., and ZULLO, V. A., 1992, Sequence stratigraphy of Paleocene and Eocene deposits in the Savannah River region: *in* Zullo, V. A., Harris, W. B., and Price, V., eds., *Savannah River Region: Transition Between the Gulf and Atlantic Coastal Plains — Proceedings of the Second Bald Head Island Conference on Coastal Plains Geology*: Wilmington, North Carolina, The University of North Carolina at Wilmington, p. 134-142.

## **REFERENCES (Continued)**

---

- HAQ, B. U., HARDENBOL, J., and VAIL, P. R., 1987, Chronology of fluctuating sea levels since the Triassic: *Science*, v. 235, p. 1156-1167.
- HUDDLESTUN, P. F., and HETRICK, J. H., 1979, The stratigraphy of the Barnwell Group in Georgia: Georgia Geological Society Guidebook, 14th Annual Field Trip, Georgia Geological Survey Open-File Report. 80-1, 89 p.
- HUDDLESTUN, P. F., and HETRICK, J. H., 1986, Upper Eocene stratigraphy of central and eastern Georgia: Georgia Geological Survey Bulletin 95, 78 p.
- INGRAM, R. L., 1971, Sieve Analysis, *in* Carver, R. E., ed., *Procedures in Sedimentary Petrology*: New York, Wiley-Interscience, p. 49-67.
- IRELAND, H. A., 1971, Insoluble residues, *in* Carver, R. E., ed., *Procedures in Sedimentary Petrology*: New York, Wiley-Interscience, p. 479-498.
- JONES, J. B., and SEGNI, E. R., 1971, The nature of opal. I. Nomenclature and constituent phases: *Journal of the Geological Society of Australia*, v. 18, p. 57-68.
- KRAUSE, R. E., and RANDOLPH, R. B., 1989, Hydrology of the Floridan aquifer system in southeast Georgia and adjacent parts of Florida and South Carolina: U.S. Geological Survey Professional Paper 1403-D, 65 p.
- LINDHOLM, R. C., 1987, *A Practical Approach to Sedimentology*: London, Allen & Unwin, 276 p.
- LOGAN, W. R., and EULER, G. M., 1989, Geology and ground-water resources of Allendale, Bamberg, and Barnwell counties and part of Aiken county, South Carolina: South Carolina Water Resources Commission Report 155, 113 p.
- LONGIARU, S. L., 1986, Visual comparators for estimating the degree of sorting from plane and thin section: *Journal of Sedimentary Petrology*, v. 57, p. 791-794.
- LONGMAN, M. W., 1980, Carbonate diagenetic textures from near-surface diagenetic environments: *American Association of Petroleum Geologists Bulletin*, v. 64, p. 461-487.
- MALIVA, R. G., AND SIEVER, R., 1988, Mechanisms and controls of silicification of fossils in limestones: *Journal of Geology*, v. 96, p. 387-398.
- MILLER, J. A., 1986, Hydrogeologic framework of the Floridan aquifer system in Florida and in parts of Georgia, Alabama, and South Carolina: U.S. Geological Survey Professional Paper 1403-B, 91 p.
- MILLIMAN, J. D., 1972, Atlantic continental shelf and slope of the United States—Petrology of the sand fraction of sediments, northern New Jersey to southern Florida: U.S. Geological Survey Professional Paper 529-J, p. J1-J40.

## REFERENCES (Continued)

---

- MOORE, C. H., Jr., 1979, Porosity in carbonate rock sequences: American Association of Petroleum Geologists Short Course Notes, Series 11, p. A1-A124.
- NEWCOME, R., JR., 1993, Pumping tests of the Coastal Plain aquifers in South Carolina: S.C. Water Resources Commission Report 174, 52 p.
- NYSTROM, P. G., Jr., WILLOUGHBY, R. H., and PRICE, L. E., 1989, The Cretaceous and Tertiary stratigraphy of the upper Coastal Plain of South Carolina, *in* Harris, W. B., Vernon, J. H., Nystrom, P. G., Jr., and Ward, L. W., eds., Upper Cretaceous and Cenozoic Geology of the Southeastern Atlantic Coastal Plain: 28th International Geological Congress, Field Trip Guidebook T172, p. 23-42.
- NYSTROM, P. G., Jr., WILLOUGHBY, R. H., and PRICE, L. E., 1991, Cretaceous and Tertiary stratigraphy of the upper Coastal Plain, South Carolina, *in* Horton, J. W., Jr., and Zullo, V. A., eds., The Geology of the Carolinas: Knoxville, Tennessee, The University of Tennessee Press, p. 221-240.
- PETTIJOHN, F. J., POTTER, P. E., and SIEVER, R., 1987, Sand and Sandstone, 2nd ed: New York, Springer-Verlag, 553 p.
- PILKEY, O. H., MORTON, R. W., and LUTENAUER, J., 1967, The carbonate fraction of beach and dune sands: Sedimentology, v. 8, p. 311-327.
- PITTMAN, E. D., 1971, Microporosity in carbonate rocks: American Association of Petroleum Geologists Bulletin, v. 55, p. 1873-1878.
- POWELL, R. J., 1984, Lithostratigraphy, depositional environment, and sequence framework of the middle Eocene Santee Limestone, South Carolina Coastal Plain: Southeastern Geology, v. 25, p. 79-100.
- POWELL, R. J., and BAUM, G. R., 1981, Porosity controls of the Black Mingo and Santee carbonate aquifers, Georgetown County, South Carolina: South Carolina Geology, v. 25, p. 53-68.
- POWELL, R. J., and BAUM, G. R., 1982, Eocene biostratigraphy of South Carolina and its relationship to Gulf Coast zonations and global changes in coastal onlap: Geological Society of America Bulletin, v. 93, p. 1099-1108.
- PROWELL, D. C., CHRISTOPHER, R. A., EDWARDS, L. E., BYBELL, L. M., AND GILL, H. E., 1985, Geologic section of the updip Coastal Plain from central Georgia to western South Carolina: U.S. Geological Survey Miscellaneous Field Studies Map, MF-1737, 10 p.

## **REFERENCES (Continued)**

---

- POWERS, M. C., 1953, A new roundness scale for sedimentary particles: *Journal of Sedimentary Petrology*, v. 23, p. 117-119.
- PRICE, V., JR., FALLAW, W. C., AND THAYER, P. A., 1992, Lower Eocene strata at the Savannah River Site, South Carolina, *in* Zullo, V. A., Harris, W. B., and Price, V., eds., *Savannah River Region: Transition Between the Gulf and Atlantic Coastal Plains — Proceedings of the Second Bald Head Island Conference on Coastal Plains Geology: Wilmington, North Carolina, The University of North Carolina at Wilmington*, p. 134-142.
- ROBERTSON, C. G., 1990, A textural, petrographic, and hydrogeological study of the Congaree Formation at the Savannah River Site, South Carolina: M.S. Thesis, University of North Carolina at Wilmington, Wilmington, N.C., 65 p.
- ROBERTSON, C. G., and THAYER, P. A., 1992, Petrology and reservoir characteristics of the Congaree Formation at the Savannah River Site, South Carolina, *in* Zullo, V. A., Harris, W. B., and Price, V., eds., *Savannah River Region: Transition Between the Gulf and Atlantic Coastal Plains — Proceedings of the Second Bald Head Island Conference on Coastal Plains Geology: Wilmington, North Carolina, The University of North Carolina at Wilmington*, p. 54-55.
- SCOFFIN, T. P., 1987, *An introduction to carbonate sediments and rocks*: New York, Chapman & Hall, 274 p.
- SELLWOOD, B. W., 1986, Shallow-marine carbonate environments, *in* Reading, H. G., ed., *Sedimentary Environments and Facies*, (2nd ed.): Boston, Blackwell Scientific Publications, p. 283-342.
- SIPLE, G. E., 1967, Geology and ground water of the Savannah River Plant and vicinity, South Carolina: U.S. Geological Survey Water-Supply Paper 1841, 113 p.
- SNIPES, D. S., FALLAW, W. C., PRICE, V., JR., and CUMBEST, R. J., 1993, The Pen Branch fault: documentation of Late Cretaceous-Tertiary faulting in the Coastal Plain of South Carolina: *Southeastern Geology*, v. 33, p. 195-218.
- STEELE, K. B., 1985, Lithostratigraphic correlation of Cretaceous and younger strata of the Atlantic Coastal Plain province within Aiken, Allendale and Barnwell Counties, South Carolina: M.S. Thesis, University of South Carolina, Columbia, South Carolina, 174 p.
- STROM, R. N., AND KABACK, D. S., 1992, SRP baseline hydrogeologic investigation: aquifer characterization, groundwater geochemistry of the Savannah River Site and vicinity: U.S. Department of Energy Report WSRC-RP-92-450, Aiken, S.C., Westinghouse Savannah River Company, 96 p.

## **REFERENCES (Continued)**

---

- TAYLOR, J. M., 1950, Pore space reduction in sandstones: American Association of Petroleum Geologists Bulletin, v. 34, p. 701-716.
- TEXTORIS, D. A., 1967, Preliminary investigation of the petrology of the Castle Hayne Limestone: Proceedings of the Symposium on Hydrology of the Coastal Waters of North Carolina, Water Resources Research Institute, University of North Carolina, Report 5, p. 3-23.
- TEXTORIS, D. A., RANDAZZO, A. F., and THAYER, P. A., 1972, Diagenesis of carbonate sediments as important non-cavern porosity controls: Montreal, 24th International Geological Congress Proceedings, Section 6, p. 190-197.
- THAYER, P. A., and TEXTORIS, D. A., 1972, Petrology and diagenesis of Tertiary aquifer carbonates, North Carolina: Transactions Gulf Coast Association of Geological Societies, v. 22, p. 257-266.
- THAYER, P. A., and TEXTORIS, D. A., 1977, Faunal and diagenetic controls of porosity and permeability in Tertiary aquifer carbonates, North Carolina: North Carolina Department of Natural and Economic Resources, Division of Earth Resources Special Publication 7, 35 p.
- THAYER, P. A., FALLAW, W. C., AND PRICE, V., 1988, Petrology and diagenesis of Eocene carbonate sediments, Savannah River Plant, S.C. (abs.): Geological Society of America Abstracts with Programs, v. 20, p. 319-320.
- THAYER, P. A., and HARRIS, M. K., 1992, Petrology and reservoir characteristics of middle and late Eocene carbonate strata in downdip wells at the Savannah River Site, S.C., *in* Fallaw, W.C., and Price, V., eds., Geological Investigations of the Central Savannah River Area, South Carolina and Georgia: Carolina Geological Society Field Trip Guidebook 1992, p. BV1-BV7.
- THAYER, P. A., AND MILLER, J. A., 1988, Petrology of Eocene rocks, southeast Georgia coastal plain: Transactions Gulf Coast Association of Geological Societies, v. 38, p. 595.
- THAYER, P. A., SMITS, A. D., AND AADLAND, R. K., 1992, Petrology and porosity-permeability characteristics of Tertiary aquifer sands, Savannah River Site Region, South Carolina: *in* Fallaw, W.C., and Price, V., eds., Geological Investigations of the Central Savannah River Area, South Carolina and Georgia: Carolina Geological Society Field Trip Guidebook 1992, p. BXI1-BXI6.
- THAYER, P. A., SMITS, A. D., HARRIS, M. K., LEWIS, C. M., and AMIDON, M. B., 1993, Stratigraphic maps of the General Separations Area (GSA), Savannah River Site

## **REFERENCES (Continued)**

---

- (SRS), Aiken, South Carolina: U.S. Department of Energy Report WSRC-RP-93-287, Aiken, S.C., Westinghouse Savannah River Company, 103 p.
- THAYER, P. A., and TEXTORIS, D. A., 1972, Petrology and diagenesis of Tertiary aquifer carbonates, North Carolina: Transactions Gulf Coast Association of Geological Societies, v. 22, p. 257-266.
- THAYER, P. A., and TEXTORIS, D. A., 1977, Faunal and diagenetic controls of porosity and permeability in Tertiary aquifer carbonates, North Carolina: N.C. Department of Natural and Economic Resources, Geology and Mineral Resources Section, Special Publication 7, 35 p.
- U.S. ARMY CORPS OF ENGINEERS, 1952, Foundation grouting operations, Savannah River Site: Vicksburg, Waterways Experiment Station, 26 p.
- U.S. DEPARTMENT OF ENERGY, 1990, Application for a hazardous waste part B post-closure care permit, H-Area hazardous waste management facility, in v. 5, Book 2, Lithostratigraphic Sequence of the Hydrogeology Units at the GSA, Rev. No. 2 (December 1990): Aiken, South Carolina, Savannah River Plant, p. 154.
- VAN DER PLAS, L., and TOBI, A. C., 1965, A chart for judging the reliability of point counting results: American Journal of Science, v. 263, p. 87-90.
- WELTON, J. E., 1984, SEM Petrology Atlas: Tulsa, American Association of Petroleum Geologists, 237 p.
- WILSON, J. L., 1975, Carbonate Facies in Geologic History: New York, Springer-Verlag, 471 p.
- WISE, S. W., and WEAVER, F. M., 1973, Origin of cristobalite-rich Tertiary sediments in the Atlantic and Gulf Coastal Plain: Transactions Gulf Coast Association of Geological Sciences, v. 23, p. 305-323.

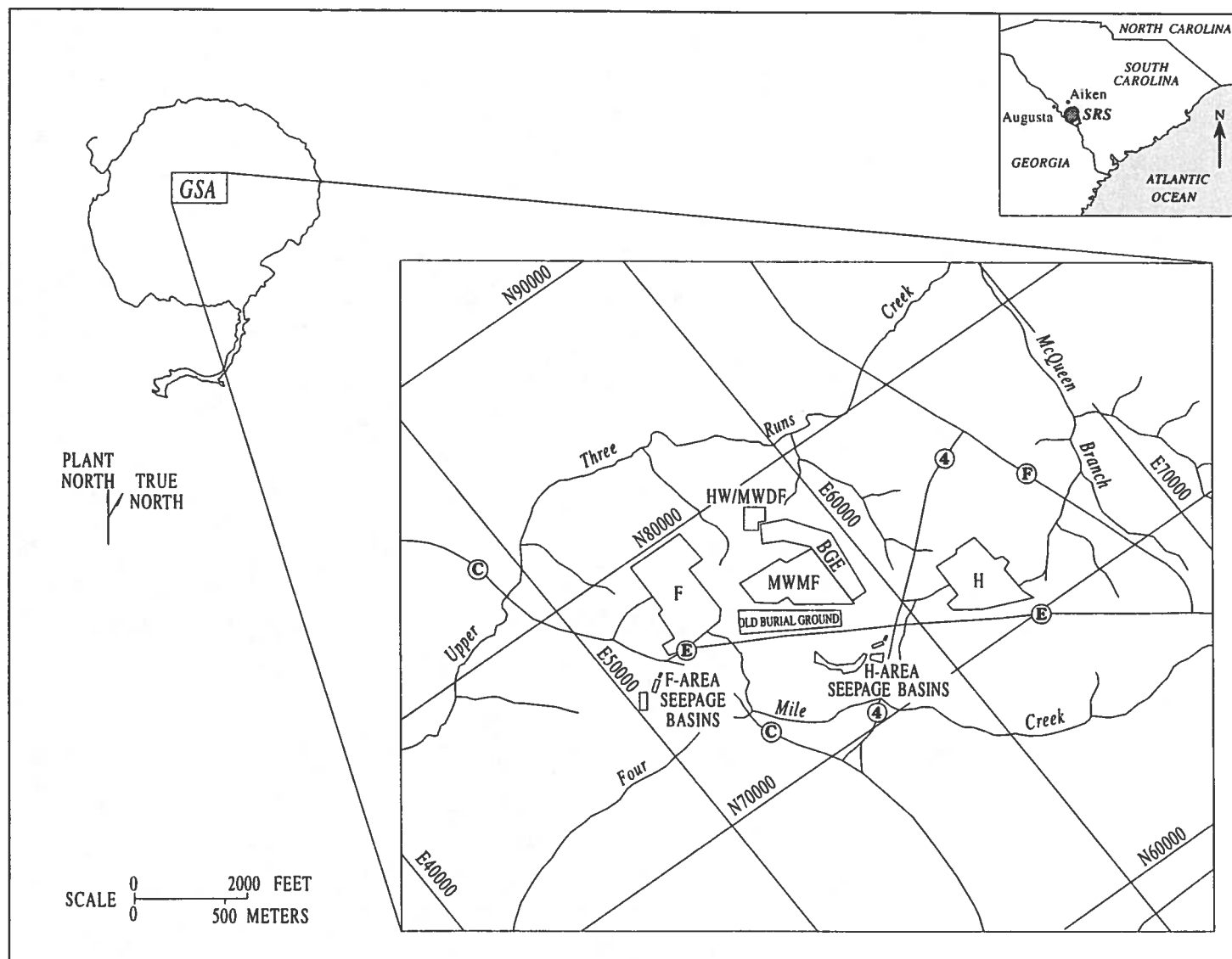


Figure 1. Location of the General Separations Area, Savannah River Site, South Carolina



AGE	LITHOSTRATIGRAPHY			HYDROSTRATIGRAPHY			
?	"Upland" Unit			Aquifer Unit IIB	Aquifer Zone IIB <sub>2</sub>	Aquifer System II	
Eocene	Barnwell Grp.	Tobacco Road Sand					C. Zone IIB <sub>1</sub> -IIB <sub>2</sub>
		Dry Branch Fm.	Irwinton Sand Mb.		Aquifer Zone IIB <sub>1</sub>		
			Twiggs Clay Mb.				
			Griffins Landing Mb.				
	McBean Formation				Confining Unit IIA-IIB		
	Warley Hill Formation						
Congaree Formation			Aquifer Unit IIA				
Paleocene	Williamsburg Formation			Confining System I-II			
	Ellenton Formation						

Figure 2. Lithostratigraphic and Hydrostratigraphic Nomenclature for the General Separations Area, SRS

55

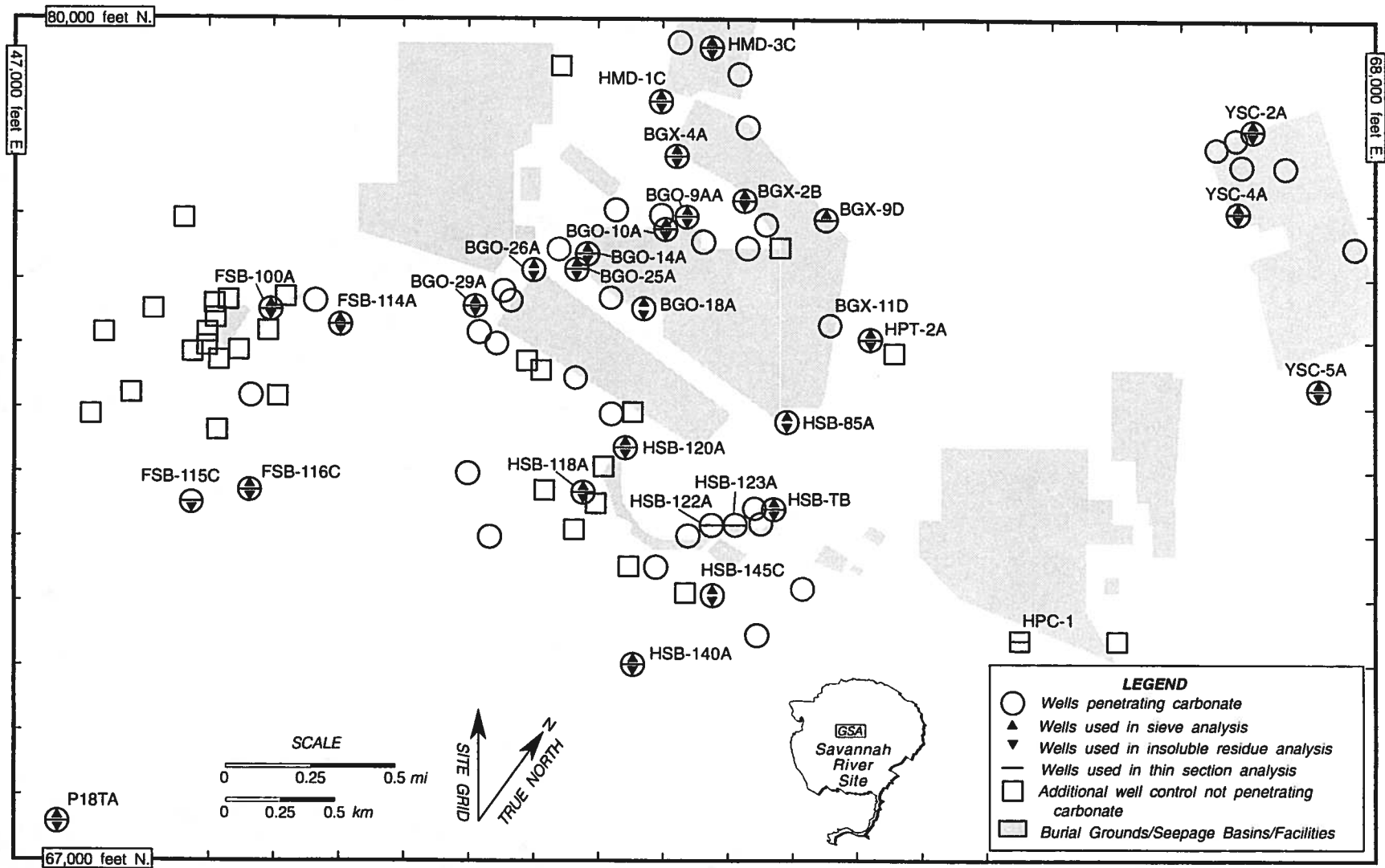


Figure 3. Wells and Boreholes in the General Separations Area that Penetrate Carbonate Sediment or Rock

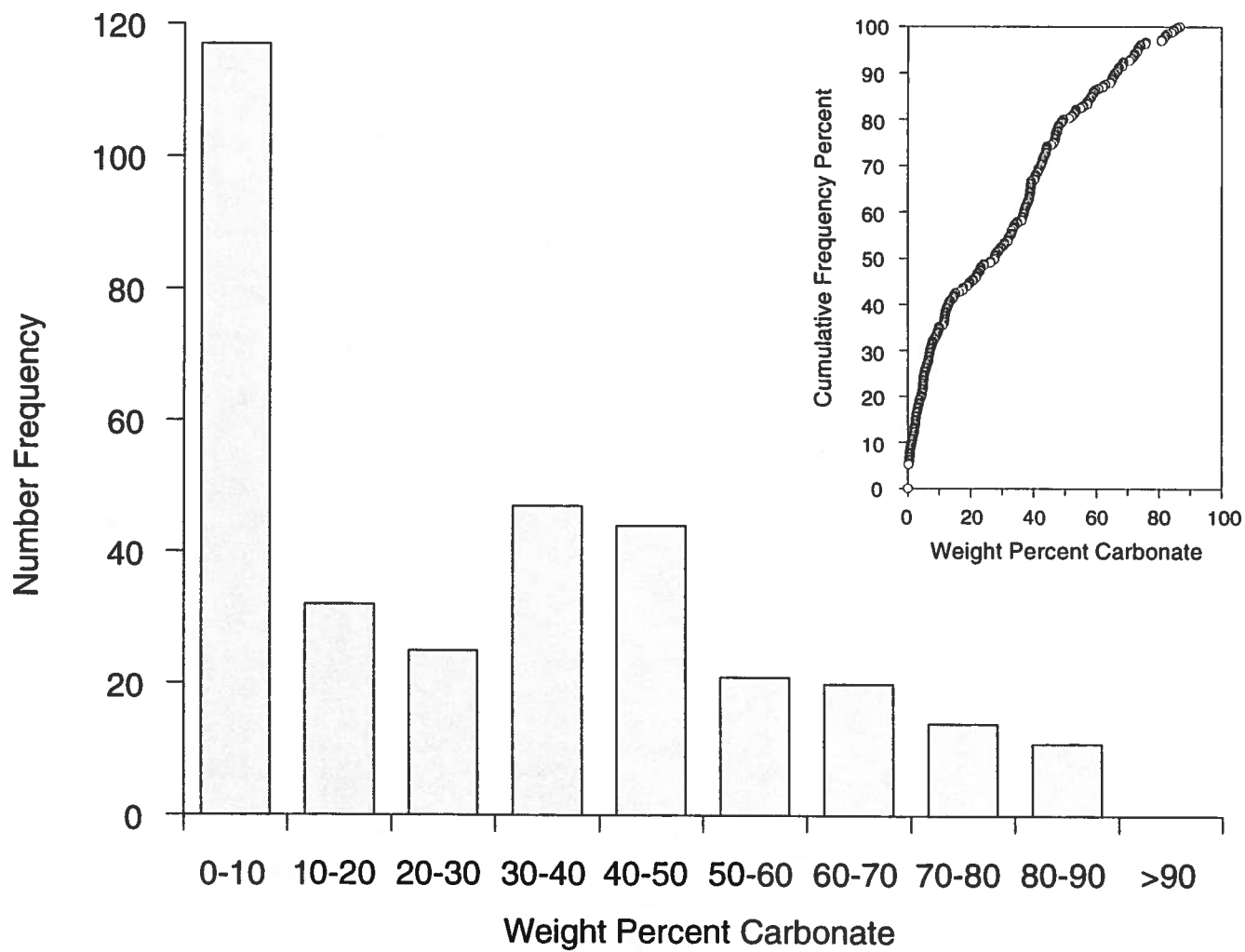
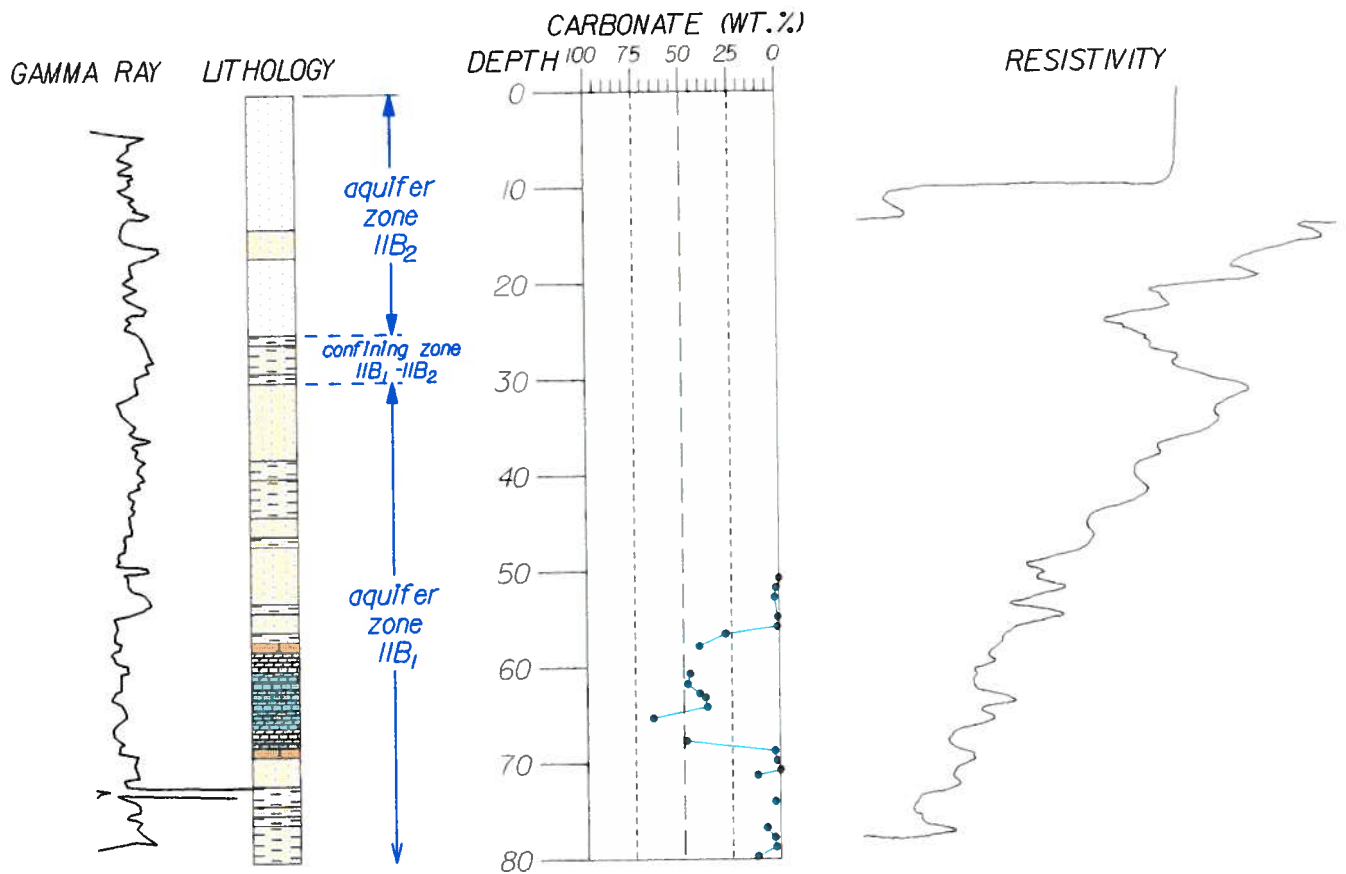


Figure 4. Computed Percentage of Carbonate for 396 "Calcareous Zone" Samples in the General Separations Area, SRS






Figure 5. Summary of Insoluble Residue Data for Well BGO-9AA, General Separations Area, SRS

Figure 6. Summary of Insoluble Residue Data for Well FSB-116C, General Separations Area, SRS


FSB-116C  
GROUND ELEVATION 200 FEET



LEGEND:

-  SAND
-  CLAYEY SAND
-  CALCAREOUS SAND
-  LIMESTONE
-  SANDY LIMESTONE

BLACK AND WHITE SYMBOLS INDICATE  
INFERRED LITHOLOGY IN ZONES OF NO RECOVERY.

-  RESULTS OF INSOLUBLE-RESIDUE ANALYSIS.  
CONNECTING LINES INDICATE CONTINUOUS  
SAMPLING AT ONE-FOOT INTERVALS.

PETROGRAPHIC ANALYSIS - HYDROSTRATIGRAPHIC UNITS, GSA  
WSRC-RP-94-54

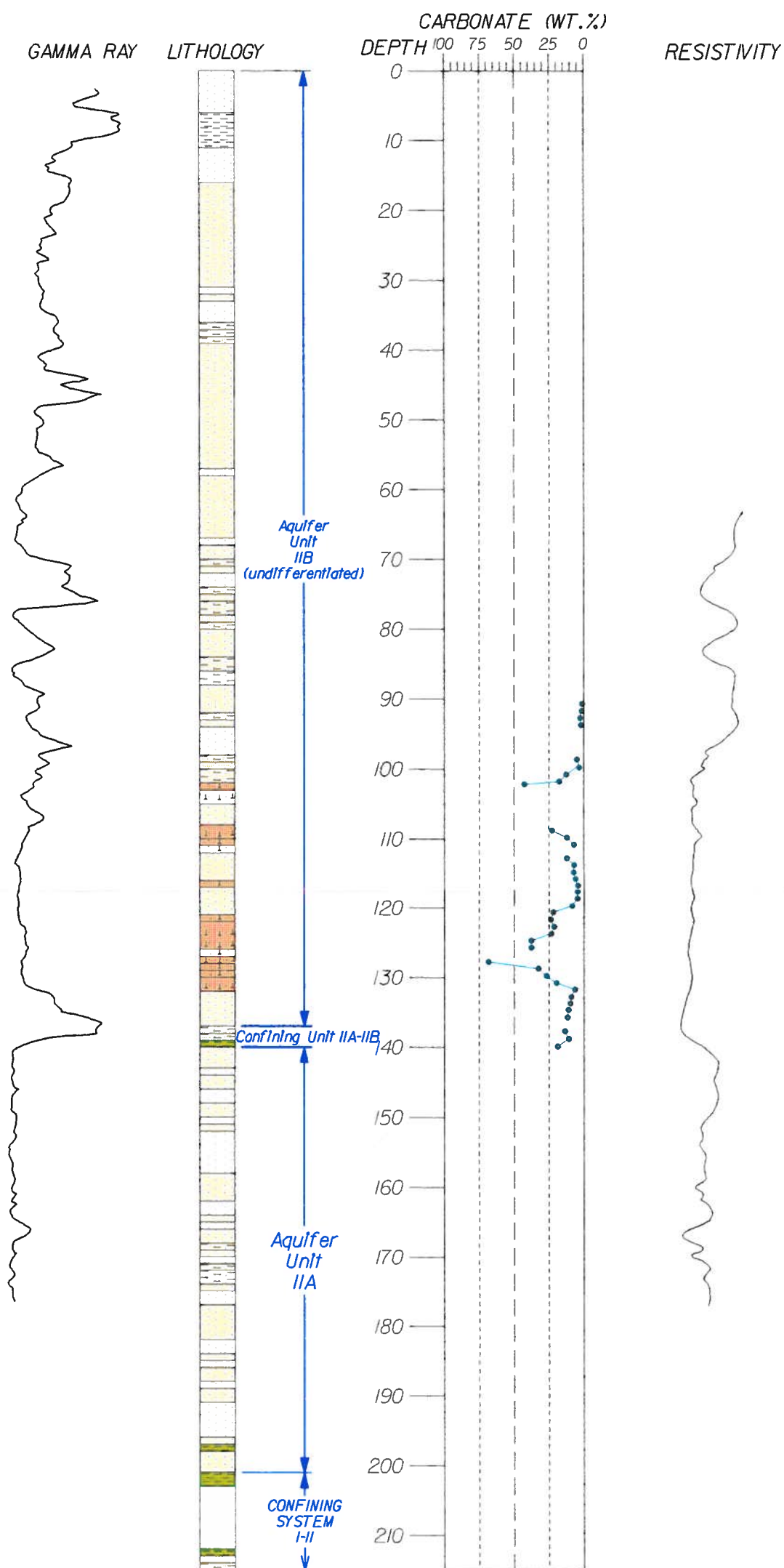
DRAWING NUMBER  
G00823

FIGURE 6.





SUMMARY OF INSOLUBLE-RESIDUE DATA  
FOR WELL FSB-116C,  
GENERAL SEPARATIONS AREA,  
SAVANNAH RIVER SITE

Figure 7. Summary of Insoluble Residue Data for Well HPT-2A, General Separations Area, SRS


HPT-2A  
GROUND ELEVATION 258 FEET



LEGEND:

-  SAND
-  CLAYEY SAND
-  CLAY
-  CALCAREOUS SAND

BLACK AND WHITE SYMBOLS INDICATE  
INFERRED LITHOLOGY IN ZONES OF NO RECOVERY.

-  RESULTS OF INSOLUBLE-RESIDUE ANALYSIS.  
CONNECTING LINES INDICATE CONTINUOUS  
SAMPLING AT ONE-FOOT INTERVALS.

PETROGRAPHIC ANALYSIS - HYDROSTRATIGRAPHIC UNITS, GSA  
WSRC-RP-94-54

DRAWING NUMBER  
G00823

FIGURE 7.

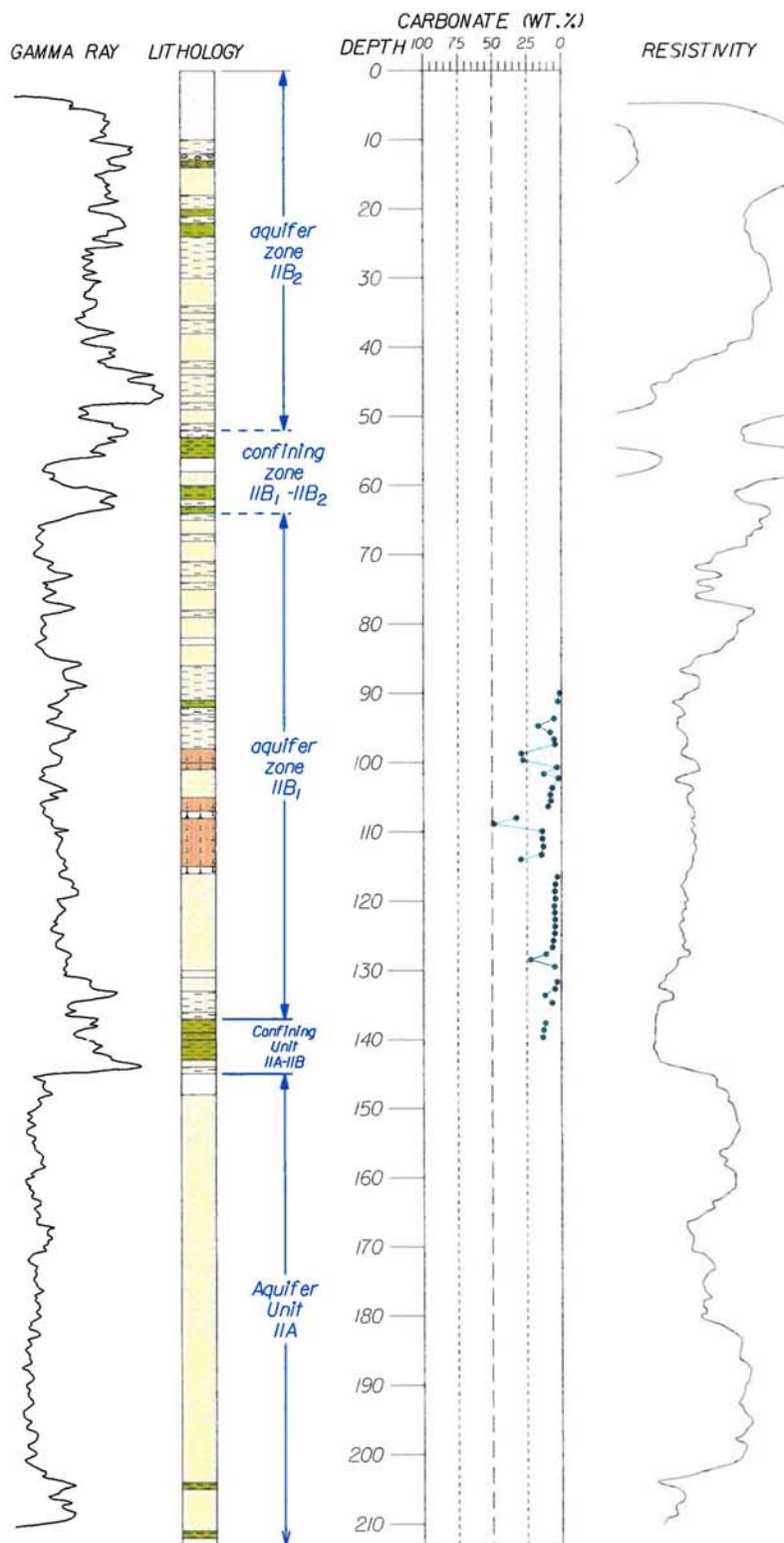
SUMMARY OF INSOLUBLE-RESIDUE DATA  
FOR WELL HPT-2A.



Figure 8. Summary of Insoluble Residue Data for Well HSB TB, General Separations Area, SRS

Figure 9. Summary of Insoluble Residue Data for Well YSC-5A, General Separations Area, SRS

YSC-5A  
GROUND ELEVATION 273 FEET



LEGEND:

- SAND
- CLAYEY SAND
- CLAYEY, PEBBLY SAND
- CLAY
- SANDY CLAY
- SANDY, PEBBLY CLAY
- CALCAREOUS SAND

BLACK AND WHITE SYMBOLS INDICATE  
INFERRED LITHOLOGY IN ZONES OF NO RECOVERY.

- RESULTS OF INSOLUBLE-RESIDUE ANALYSIS.
- CONNECTING LINES INDICATE CONTINUOUS  
SAMPLING AT ONE-FOOT INTERVALS.

PETROGRAPHIC ANALYSIS - HYDROSTRATIGRAPHIC UNITS, GSA  
WSRC-RP-94-54

DRAWING NUMBER  
G00823

FIGURE 9.

SUMMARY OF INSOLUBLE-RESIDUE DATA  
FOR WELL YSC-5A,  
GENERAL SEPARATIONS AREA,  
SAVANNAH RIVER SITE

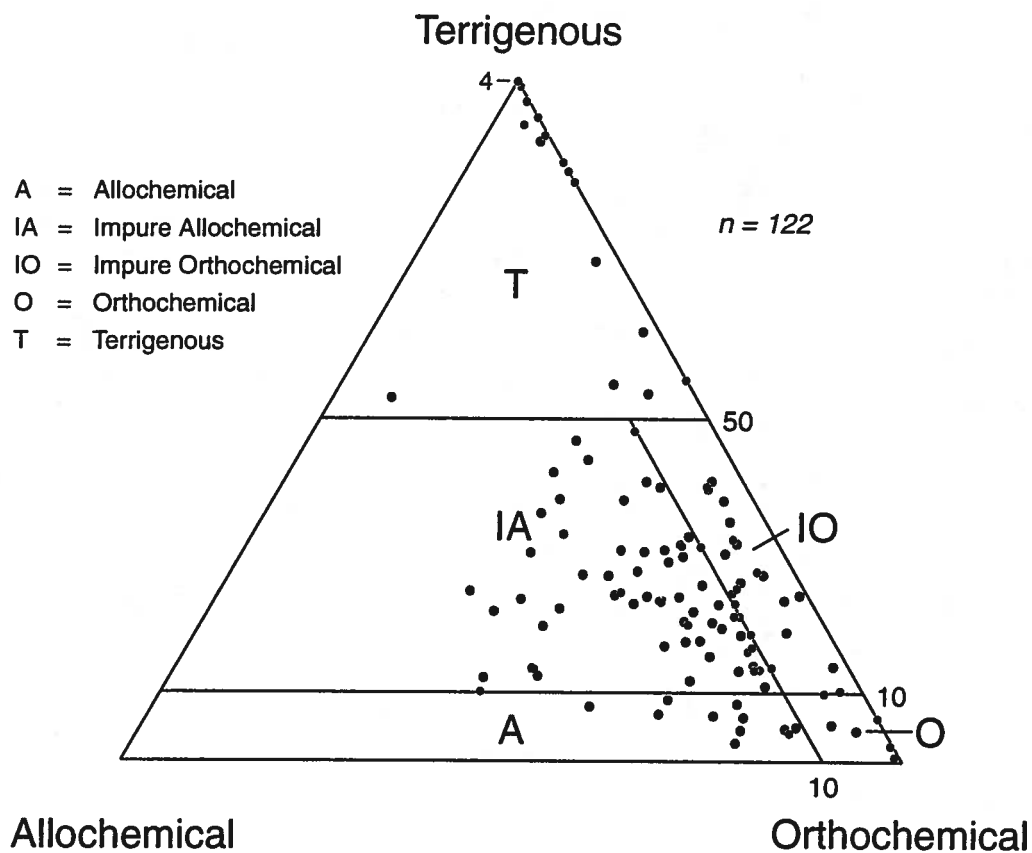


Figure 10. Classification of "Calcareous Zone" Sediments and Sedimentary Rocks according to Folk's (1980) Classification

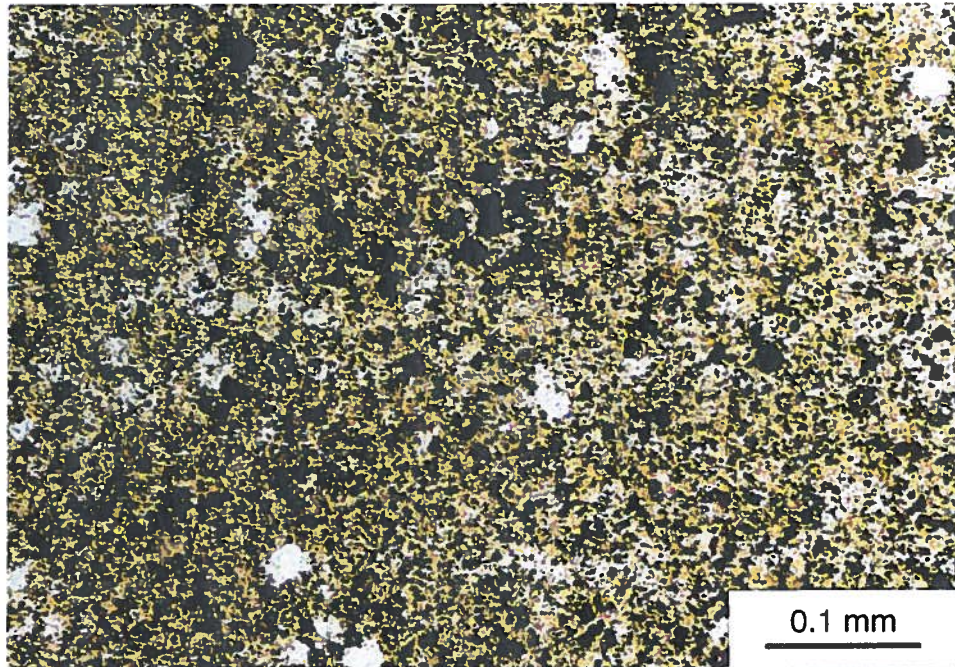


Figure 11. Photomicrograph of Unconsolidated Mud from the Terrigenous Mud Microfacies, Aquifer Unit IIA. Well BGX-2B, 176 ft., General Separations Area, SRS. Plane-polarized Light.

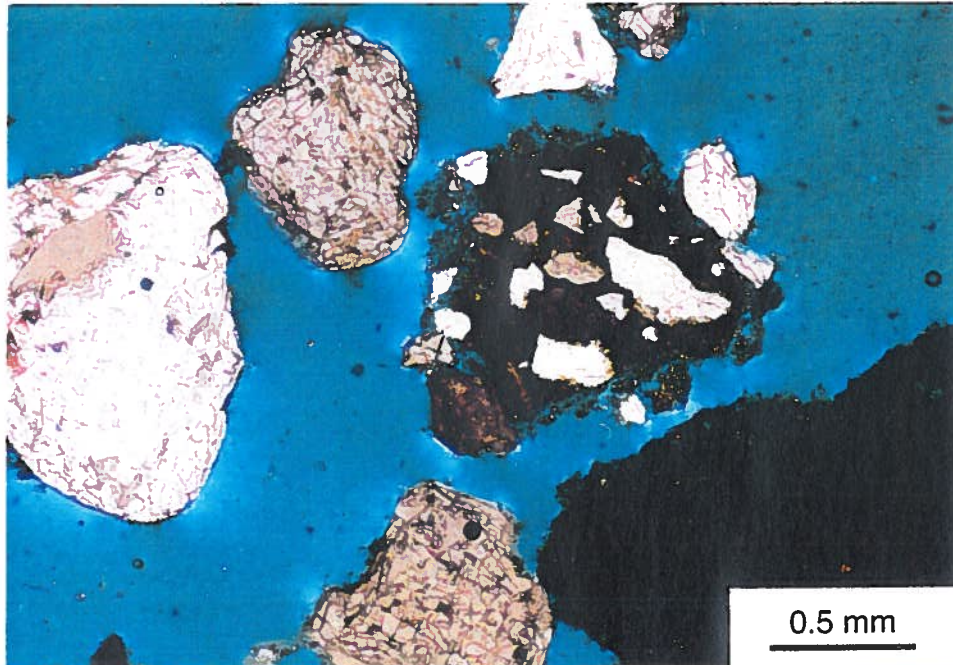


Figure 12. Photomicrograph of Unconsolidated, Muddy Sand from the Terrigenous Sand Microfacies, Aquifer Unit IIA, General Separations Area, SRS. Well HSB-120, 167 ft. Sample disrupted during thin-section preparation. Plane-polarized light.



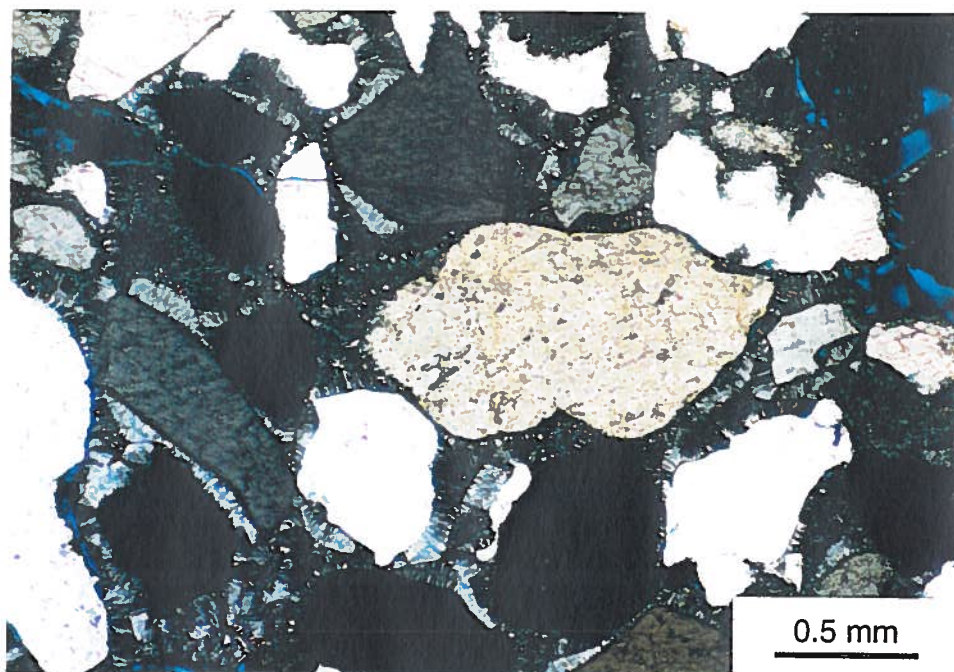


Figure 13. Photomicrograph of Chalcedony-Cemented Quartzarenite from the Terrigenous Sand and Sandstone Microfacies, Aquifer Unit IIA, General Separations Area, SRS. Well HSB-140A, 156 ft. Crossed nicols.

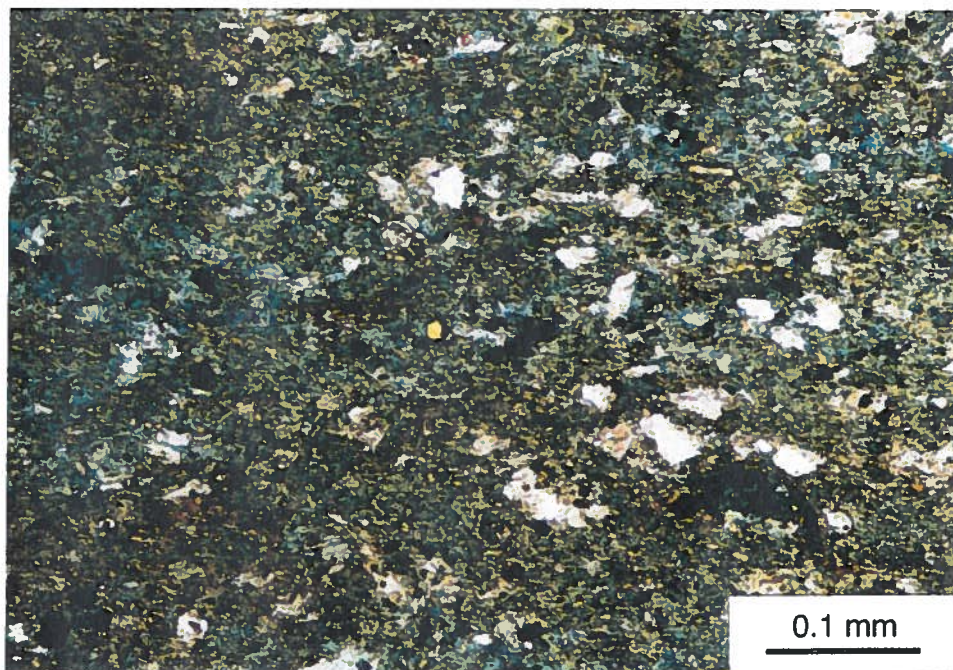


Figure 14. Photomicrograph of Unconsolidated Lime Mud, Lime Mud Microfacies, Confining Unit IIA-IIB, General Separations Area, SRS. Well BGO-9AA, 150 ft. (thin section BGO-9AA-150A). Partially crossed nicols.



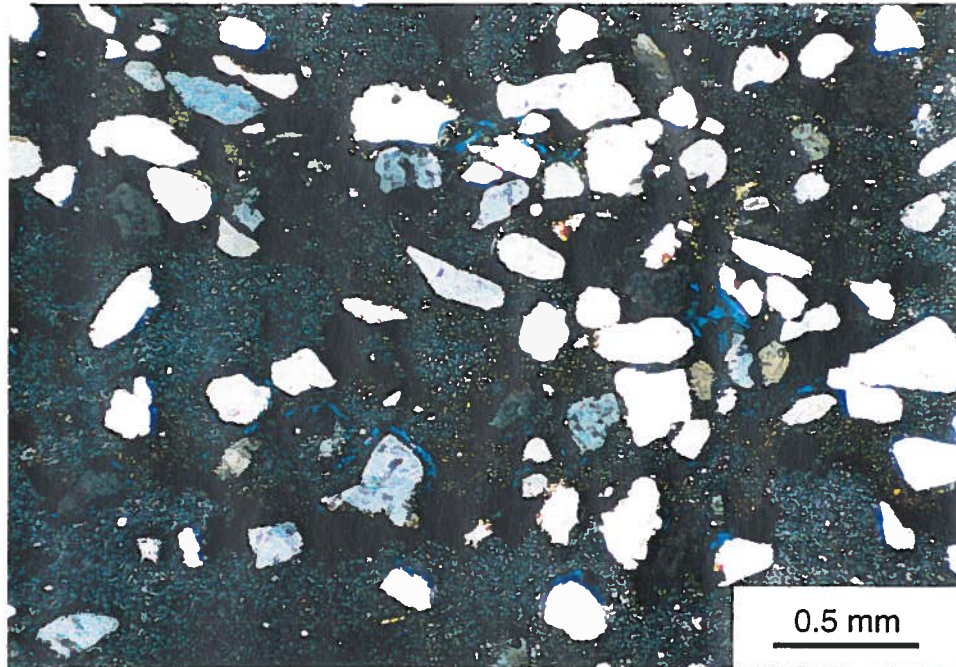


Figure 15. Photomicrograph of Sandy Siliceous Mudstone, Siliceous Mudstone Microfacies, Confining Unit IIA-IIB, General Separations Area, SRS. Well BGX-2B, 151.2 ft (thin section BGX-2B-152A). Crossed nicols.



Figure 16. Photomicrograph of Sandy, Skeletal Siliceous Mudstone, Siliceous Mudstone Microfacies, Confining Unit IIA-IIB, General Separations Area, SRS. Opal cement is light brown. Well BGO-9AA, 150 ft. (thin section BGO-9AA-150B). Plane-polarized light.



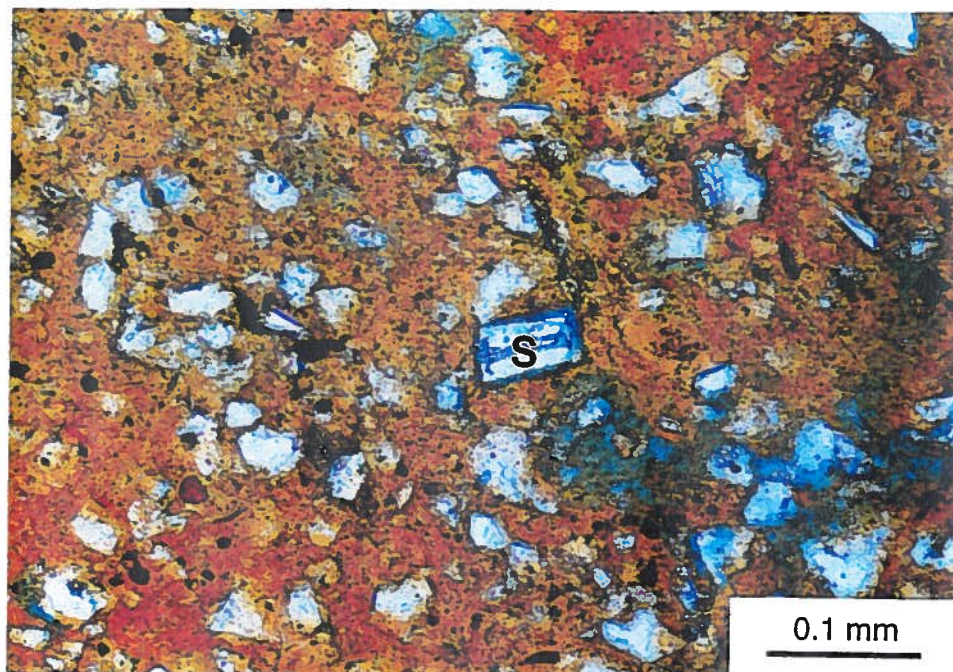


Figure 17. Photomicrograph of Quartz-Rich Mud, Terrigenous Mud Microfacies, Confining Unit IIA-IIB, General Separations Area, SRS. Well HPC-1, 182 ft. Note sponge spicule fragment (S) in center. Plane-polarized light.

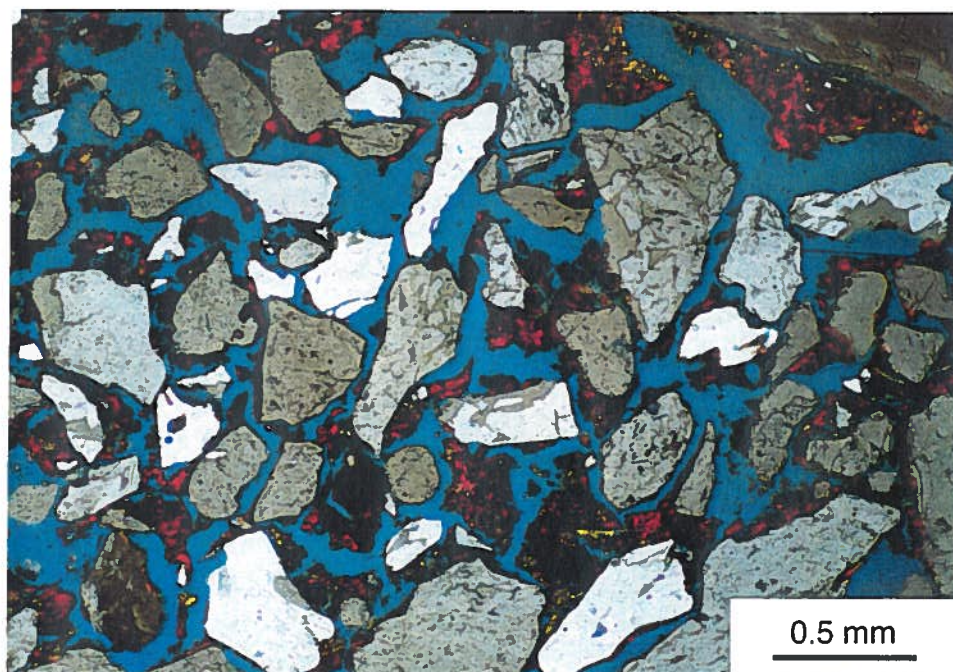


Figure 18. Photomicrograph of Unconsolidated Muddy Sand, Terrigenous Sand and Sandstone Microfacies, Confining Unit IIA-IIB, General Separations Area, SRS. Well HPC-1, 186 ft. Sample disrupted during thin section preparation. Partially crossed nicols.



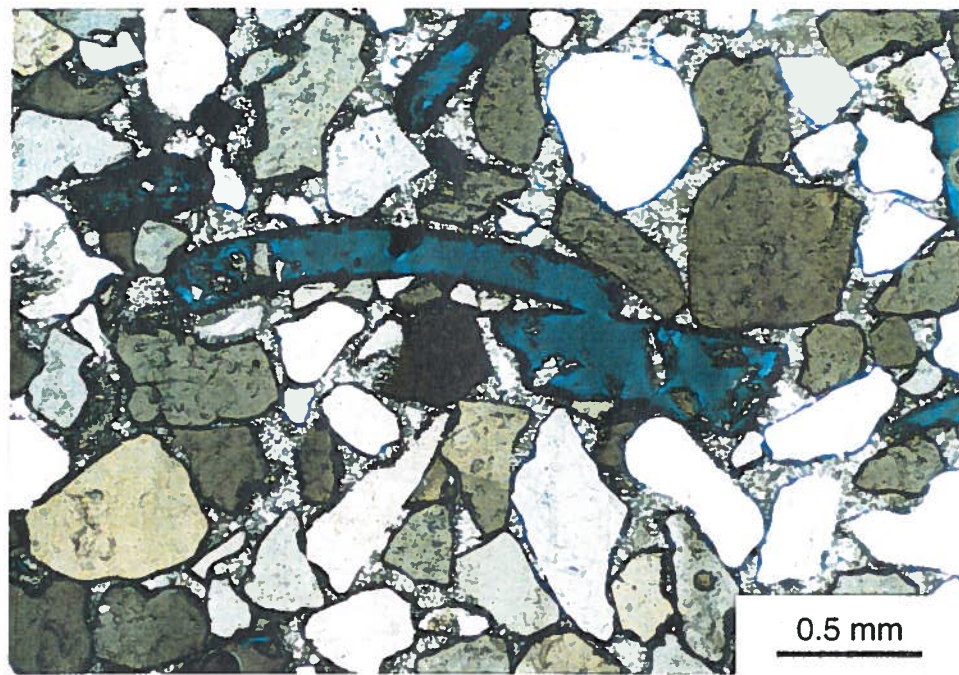


Figure 19. Photomicrograph of Chalcedony-Cemented Quartzarenite from the Terrigenous Sand and Sandstone Microfacies, Confining Unit IIA-IIB, General Separations Area, SRS. Note large pelecypod molds (blue) in center. Well FSB-115C, 118 ft. Partially crossed nicols.

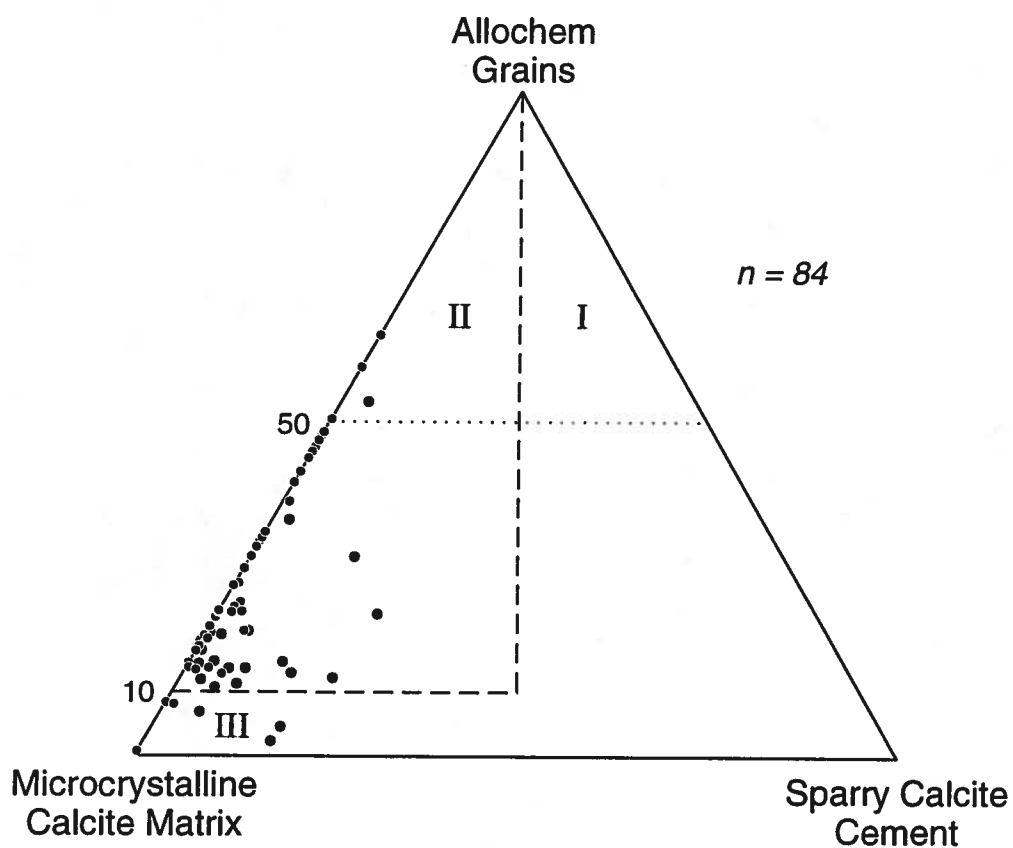


Figure 21. Ternary Diagram after Folk (1962) Showing Composition of Carbonate Sediment Samples from Aquifer Zone IIB<sub>1</sub>, General Separations Area, SRS

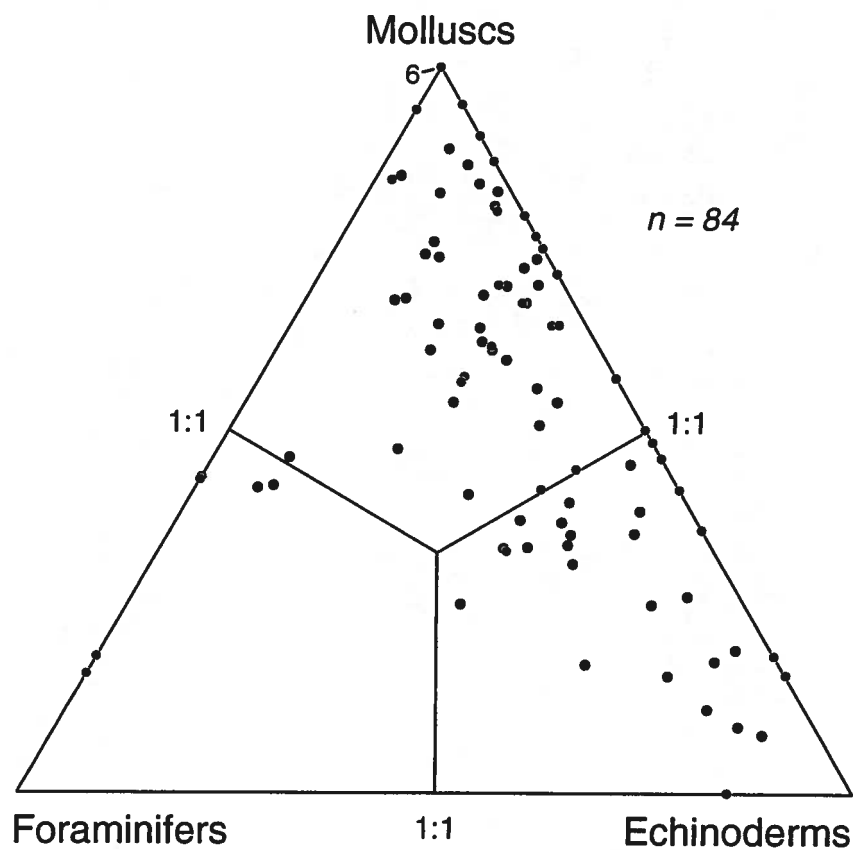


Figure 22. Ternary Diagram Showing Proportion of Skeletal Allochems in Carbonate Sediment Samples from Aquifer Zone IIB<sub>1</sub>, General Separations Area, SRS

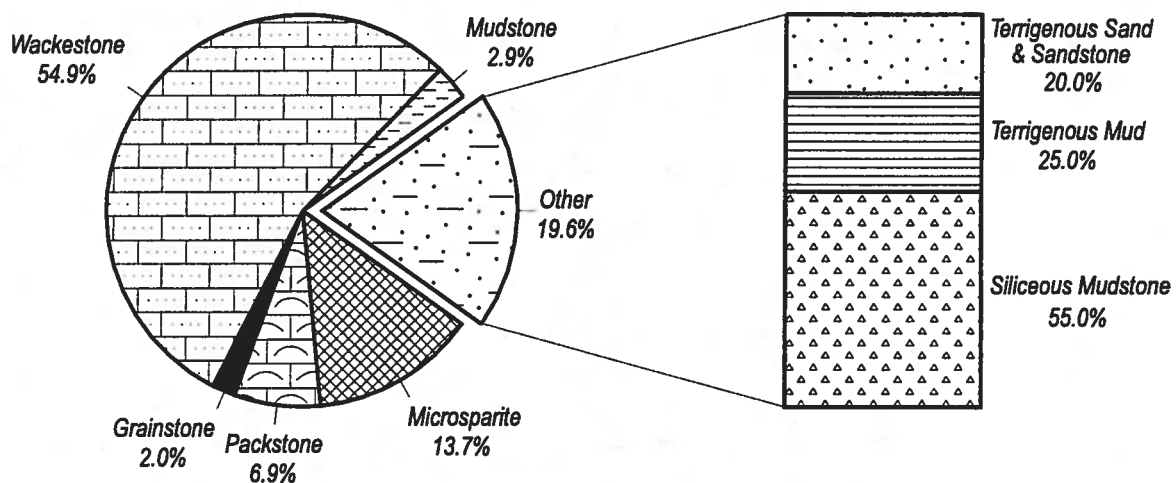


Figure 23. Composition of 103 Thin-Section Samples Collected from Aquifer Zone IIB<sub>1</sub>,  
General Separations Area, SRS

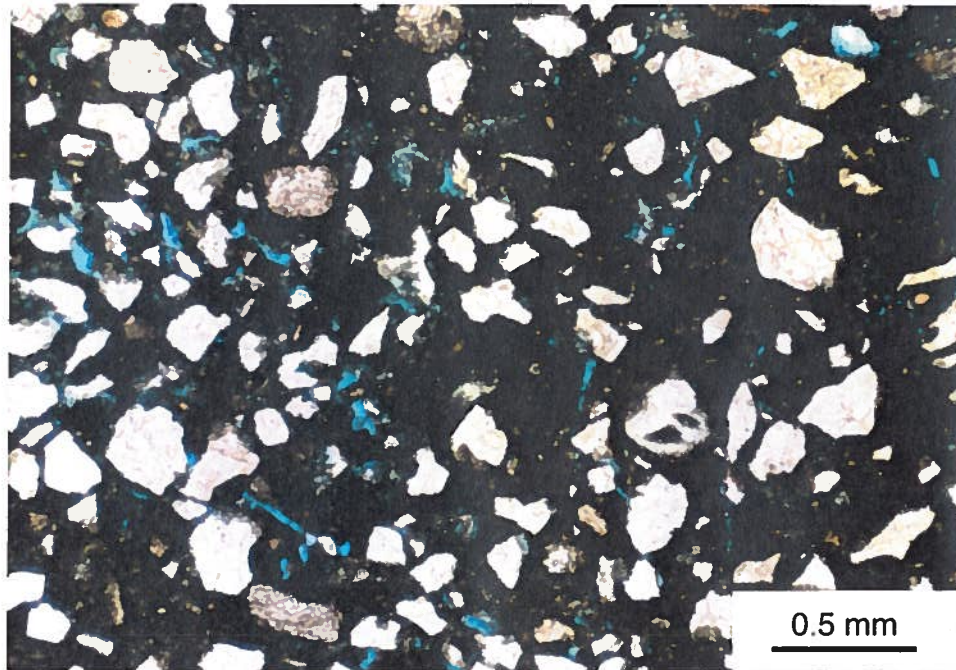


Figure 24. Photomicrograph of Quartz-Rich Lime Mud, Lime Mud Microfacies, Aquifer Unit IIB<sub>1</sub>, General Separations Area, SRS. Well BGO-14A, 126 ft. Note moldic and vug porosity (blue). Plane-polarized light.

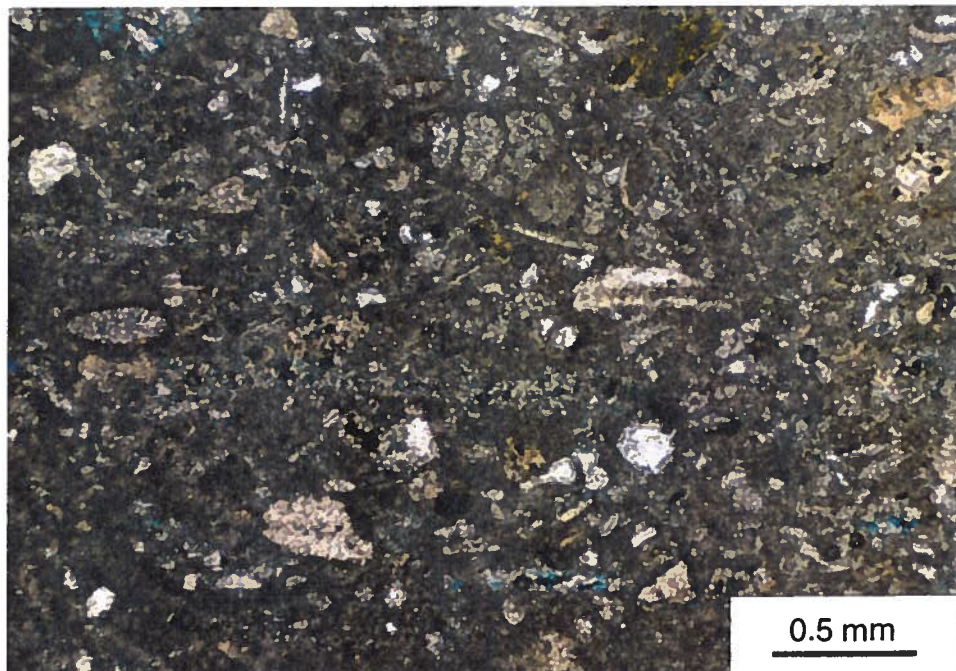


Figure 25. Photomicrograph of Skeletal Wackestone from Skeletal Wackestone Microfacies, Aquifer Unit IIB<sub>1</sub>, General Separations Area, SRS. Well BGO-9AA, 140.6 ft. (thin section BGO-9AA-141A). Plane-polarized light.



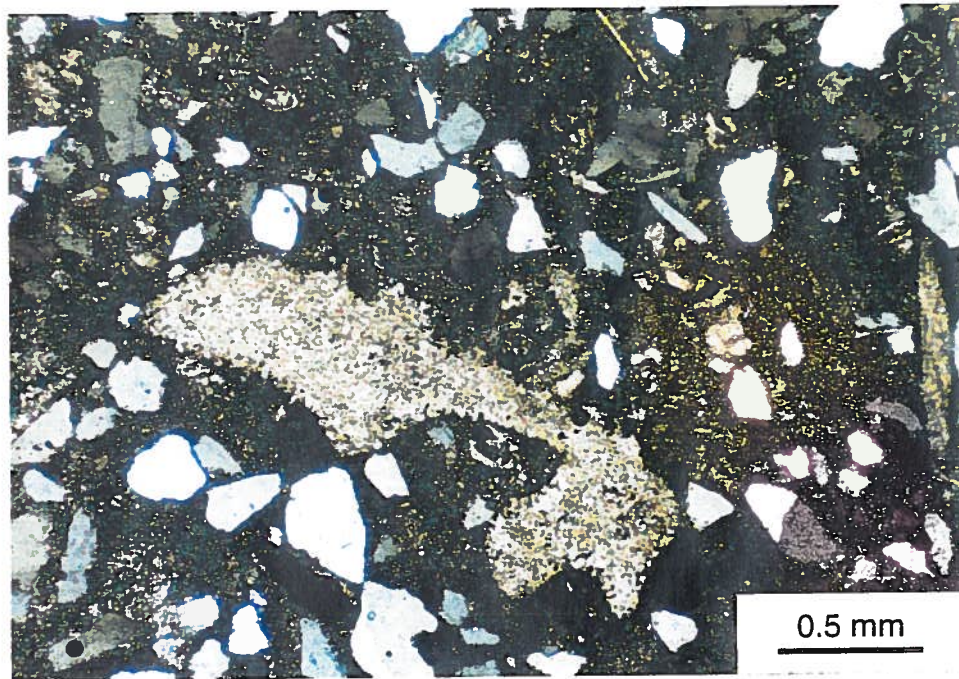


Figure 26. Photomicrograph of Quartz-Rich Skeletal Wackestone, Skeletal Wackestone Microfacies, Aquifer Unit IIB<sub>1</sub>, General Separations Area, SRS. Well BGO-9AA-127.3 ft. (Thin Section BGO-9AA-128A). Crossed nicols.

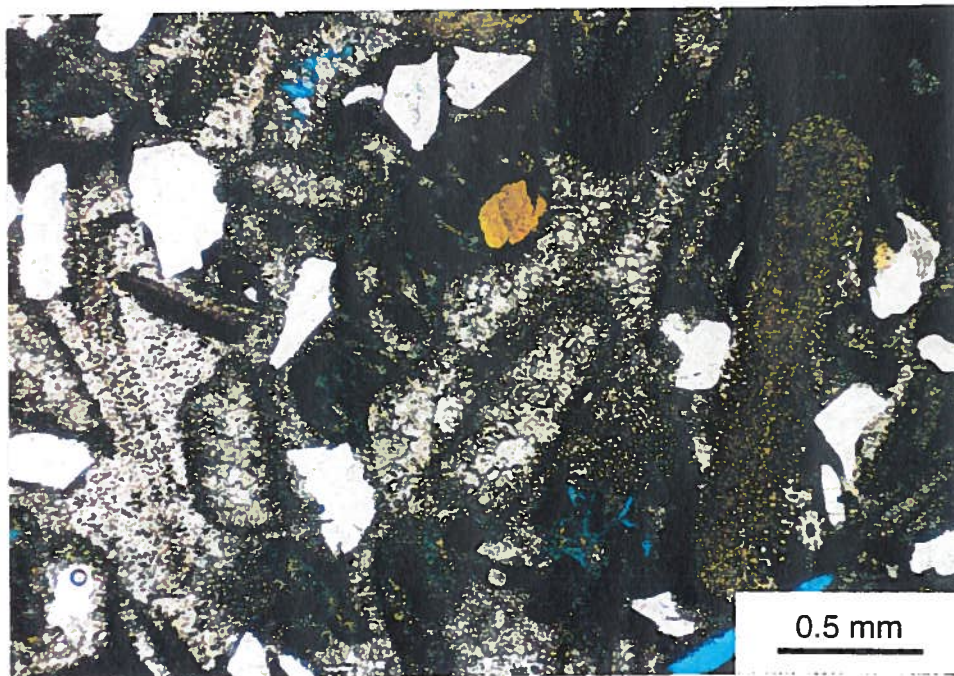


Figure 27. Photomicrograph of Quartz-Rich Skeletal Packstone that has been Diagenetically Altered to Sandy, Molluscan-Mold Microsparite. Aquifer unit IIB<sub>1</sub>, General Separations Area, SRS. Well BGO-14A, 122 ft. Crossed nicols.



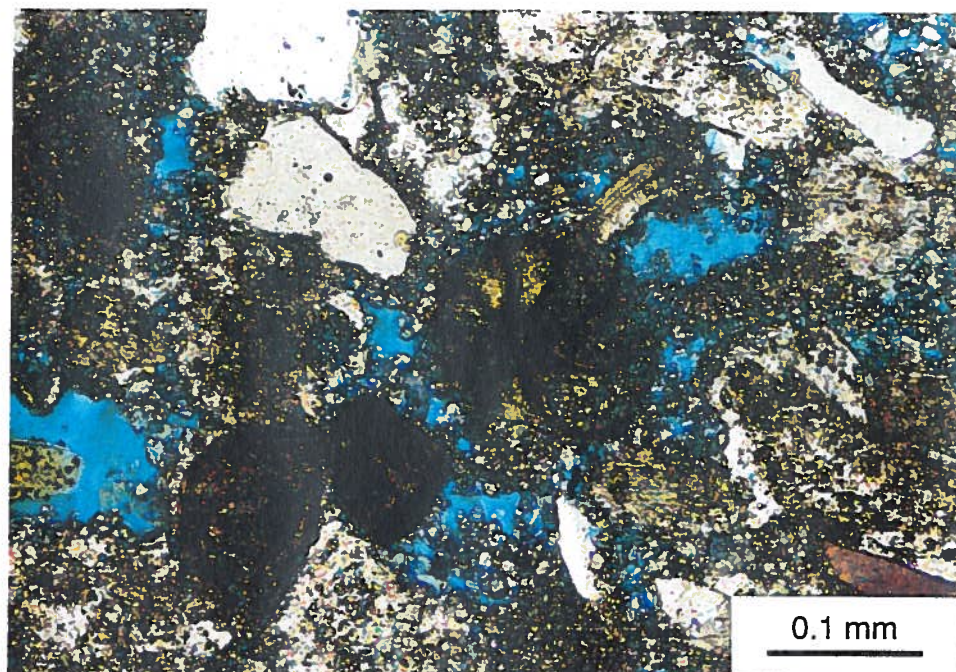


Figure 28. Photomicrograph of Quartz-Rich Skeletal Grainstone, Skeletal Grainstone Microfacies, Aquifer Unit IIB<sub>1</sub>, General Separations Area, SRS. Well BGO-10A, 147 ft. Partially crossed nicols.

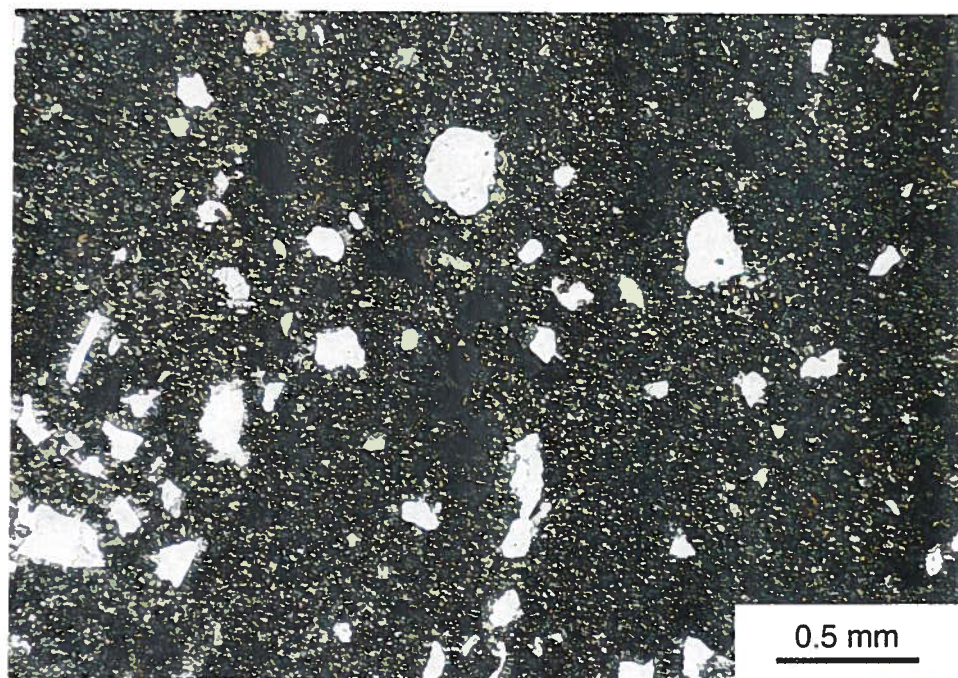


Figure 29. Photomicrograph of Quartz-Rich Microsparite, Microsparite Microfacies, Aquifer Unit IIB<sub>1</sub>, General Separations Area, SRS. Well HPT-2A, 105 ft. Plane-polarized light.



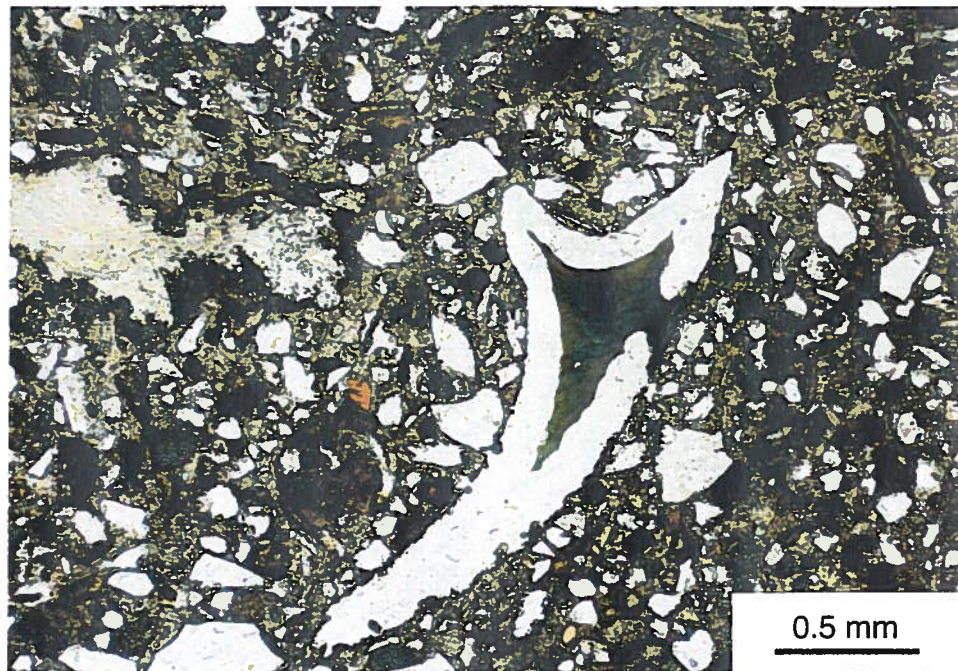


Figure 30. Photomicrograph of Quartz-Rich Siliceous Mudstone, Siliceous Mudstone Microfacies, Aquifer Unit IIB<sub>1</sub>, General Separations Area, SRS. Well BGX-4A, 146 ft. Plane-polarized light.



Figure 31. Photomicrograph of Quartz-Rich Terrigenous Mud, Terrigenous Mud Microfacies, Aquifer Unit IIB<sub>1</sub>, General Separations Area, SRS. Well HPC-1, 144 ft. Sample disrupted during thin-section preparation. Plane-polarized light.



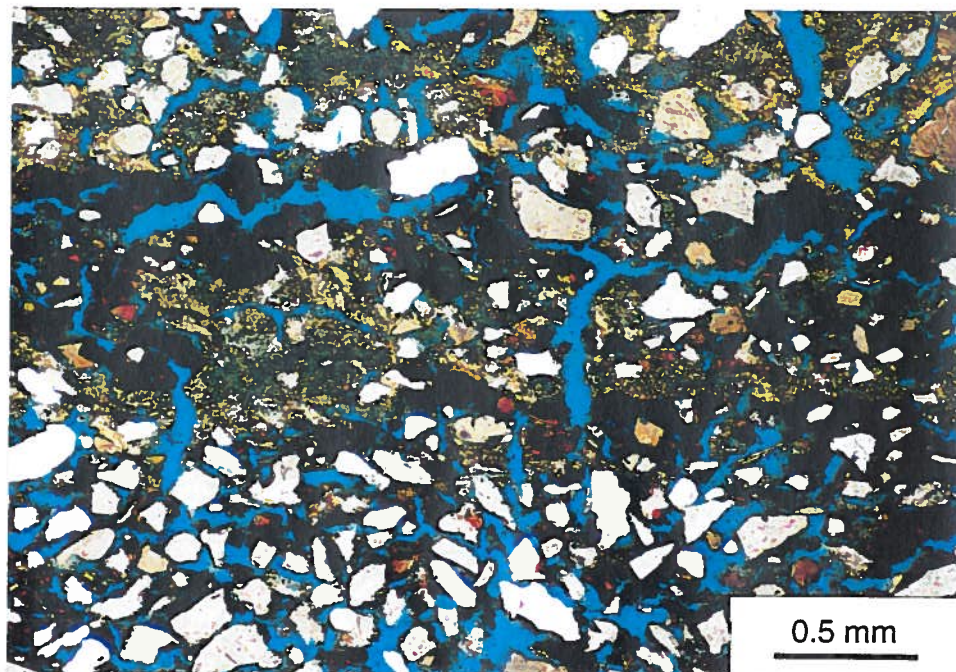


Figure 32. Photomicrograph of Muddy Sand from Terrigenous Sand and Sandstone Microfacies, Aquifer Unit IIB<sub>1</sub>, General Separations Area, SRS. Well HPC-1, 167 ft. Sample disrupted during thin-section preparation. Plane-polarized light.

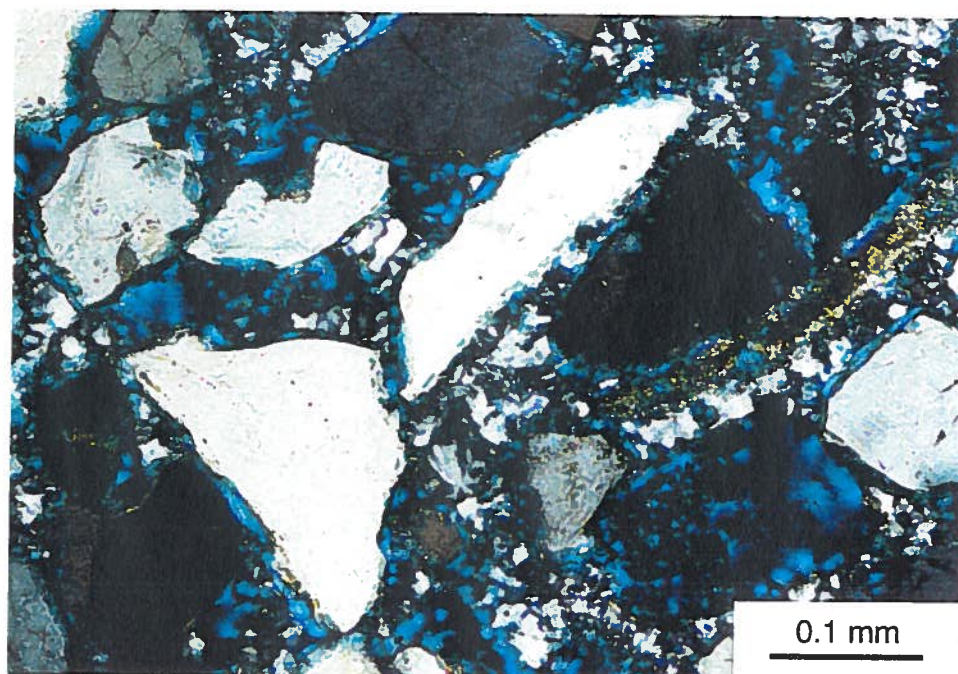


Figure 33. Photomicrograph of Chalcedony-Cemented Quartzarenite, Terrigenous Sand and Sandstone Microfacies, Aquifer Unit IIB<sub>1</sub>, General Separations Area, SRS. Well YSC-2A, 109 ft. Crossed nicols.

Table 1. Classifications and Terminology Used in this Report

---

Carbonate-Terrigenous Classification	Lindholm (1987) (Appendix A11)
Carbonate Classification	Dunham (1962) (Appendix A12)
Sand and Sandstone Classification	Folk (1980) (Appendix A13)
Terrigenous Grain Size Terminology	Wentworth (1922 in Folk, 1980) (Appendix A1)
Carbonate Grain Size Terminology	Folk (1959) (Appendix A14)
Grain Size Statistical Parameters	Folk and Ward (1957) (Appendix A2)
Terrigenous Textural Terminology	Folk (1954) (Appendix A16)
Textural Maturity	Folk (1951) (Appendix A17)
Carbonate Textural Terminology	Folk (1959, 1965, 1980), Friedman (1965)
Carbonate Diagenetic Terminology	Folk (1959, 1965, 1980), Bathurst (1971) Longman (1980), Flügel (1982), Scoffin (1987)
Pore Size and Type Classification	Choquette and Pray (1970), Pittman (1971) (Appendices A18 and A19)

---

Table 2. Composition of Skeletal Wackestone, Aquifer Zone IIB1

Constituent	Average	Standard Deviation	Maximum	Minimum	Number
Monocrystalline quartz	5.2	1.7	8.0	2.6	8
Polycrystalline quartz	Tr	0.0	0.0	0.0	8
Microcline	Tr	0.0	0.0	0.0	8
Untwinned potassium feldspar	Tr	0.0	0.0	0.0	8
Plagioclase	Tr	0.0	0.0	0.0	8
Rock fragment	0.0	0.0	0.0	0.0	8
Interparticle pore	2.6	3.2	10.3	0.3	8
Moldic pore	2.2	2.2	5.3	0.3	8
Intraparticle pore	0.3	0.4	1.0	0.0	8
Vug pore	0.8	1.3	4.0	0.0	8
Intercrystal pore	0.4	0.8	2.3	0.0	8
Terrigenous mud matrix	Tr	0.0	0.0	0.0	8
Micrite	42.7	12.1	60.3	23.7	8
Microspar	18.3	10.1	37.3	2.7	8
Sparry calcite cement & replacement	10.1	9.8	29.7	1.7	8
Muscovite	Tr	0.0	0.0	0.0	8
Authigenic pyrite	0.5	0.7	1.7	0.0	8
Authigenic glauconite cement	1.0	0.8	2.0	0.0	8
Chalcedony / chert cement & replacem	0.1	0.2	0.7	0.0	8
Opal cement & replacement	Tr	0.0	0.0	0.0	8
Foraminifer	1.6	0.5	2.0	0.7	8
Mollusk	2.2	2.4	7.3	0.0	8
Fragmented skeletal debris	3.2	2.5	7.3	0.0	8
Echinoderm	3.2	1.3	5.0	1.3	8
Bryozoan	0.3	0.6	1.7	0.0	8
Pelecypod	3.0	2.0	6.7	1.3	8
Gastropod	0.2	0.3	0.7	0.0	8
Sparry calcite-filled pelecypod mold	0.1	0.4	1.0	0.0	8
Micritized carbonate grain	0.7	1.2	3.0	0.0	8
Glauconite grain	0.8	1.0	2.3	0.0	8
Heavy mineral grain	Tr	0.0	0.0	0.0	8
Detrital opaque mineral grain	0.1	0.1	0.3	0.0	8
Collophane	0.0	0.0	0.0	0.0	8
Sponge spicule	0.1	0.4	1.0	0.0	8
Carbonate intraclast	0.3	0.4	1.0	0.0	8
Carbonate pellet	0.2	0.4	1.0	0.0	8
Total	100.0				

Table 3. Composition of Quartz-Rich Skeletal Wackestone, Aquifer Zone IIB1

Constituent	Average	Standard Deviation	Maximum	Minimum	Number
Monocrystalline quartz	25.1	9.2	42.7	11.0	46
Polycrystalline quartz	0.1	0.1	0.6	0.0	46
Microcline	0.1	0.2	1.0	0.0	46
Untwinned potassium feldspar	0.0	0.1	0.3	0.0	46
Plagioclase	Tr	0.1	0.3	0.0	46
Rock fragment	Tr	0.0	0.3	0.0	46
Interparticle pore	2.7	3.0	12.7	0.0	44
Moldic pore	4.0	5.2	19.7	0.0	44
Intraparticle pore	0.2	0.4	1.7	0.0	44
Vug pore	1.7	3.6	15.0	0.0	44
Intercrystal pore	0.8	1.7	6.7	0.0	44
Terrigenous mud matrix	Tr	0.1	0.3	0.0	46
Micrite	38.0	15.4	67.0	1.7	46
Microspar	9.9	12.4	38.0	0.0	46
Sparry calcite cement & replacement	1.7	5.4	34.7	0.0	46
Muscovite	Tr	0.1	0.3	0.0	46
Authigenic pyrite	0.4	0.8	4.3	0.0	46
Authigenic glauconite cement	1.2	2.3	14.4	0.0	46
Chalcedony / chert cement & replacement	Tr	0.1	0.3	0.0	46
Opal cement & replacement	Tr	0.0	0.0	0.0	46
Foraminifer	1.6	2.4	11.7	0.0	46
Mollusk	1.7	1.9	7.0	0.0	46
Fragmented skeletal debris	3.8	3.0	13.3	0.0	46
Echinoderm	3.1	2.1	10.0	0.0	46
Bryozoan	0.2	1.0	5.0	0.0	46
Pelecypod	2.4	3.3	15.0	0.0	46
Gastropod	Tr	0.1	1.0	0.0	46
Sparry calcite-filled pelecypod mold	Tr	0.0	0.3	0.0	46
Micritized carbonate grain	1.0	1.3	5.8	0.0	46
Glauconite grain	0.4	0.6	2.7	0.0	46
Heavy mineral grain	Tr	0.1	0.7	0.0	46
Detrital opaque mineral grain	0.1	0.1	0.3	0.0	46
Collophane	Tr	0.1	0.3	0.0	46
Sponge spicule	Tr	0.1	0.3	0.0	46
Carbonate intraclast	Tr	0.2	0.7	0.0	46
Carbonate pellet	Tr	0.1	0.3	0.0	46
Total	100.0				

Table 4. Composition of Quartz-Rich Skeletal Packstone, Aquifer Zone IIB1

Constituent	Average	Standard Deviation	Maximum	Minimum	Number
Monocrystalline quartz	17.1	3.8	22.6	10.3	7
Polycrystalline quartz	0.1	0.1	0.3	0.0	7
Microcline	0.1	0.3	0.7	0.0	7
Untwinned potassium feldspar	Tr	0.1	0.3	0.0	7
Plagioclase	Tr	0.0	0.0	0.0	7
Rock fragment	0.0	0.0	0.0	0.0	7
Interparticle pore	1.2	2.8	7.5	0.0	7
Moldic pore	3.2	5.3	14.6	0.0	7
Intraparticle pore	0.3	0.5	1.0	0.0	7
Vug pore	4.6	7.5	15.9	0.0	7
Intercrystal pore	Tr	0.1	0.3	0.0	7
Terrigenous mud matrix	Tr	0.0	0.0	0.0	7
Micrite	43.2	21.1	61.0	3.0	7
Microspar	3.7	9.4	25.1	0.0	7
Sparry calcite cement & replacement	0.1	0.1	0.3	0.0	7
Muscovite	0.1	0.2	0.5	0.0	7
Authigenic pyrite	0.9	1.9	5.3	0.0	7
Authigenic glauconite cement	1.0	2.5	6.7	0.0	7
Chalcedony / chert cement & replacement	4.1	5.8	12.3	0.0	7
Opal cement & replacement	0.5	0.9	2.3	0.0	7
Foraminifer	2.1	1.0	3.5	0.7	7
Mollusk	4.8	7.2	20.7	0.0	7
Fragmented skeletal debris	5.1	3.7	12.6	1.7	7
Echinoderm	3.1	2.9	7.7	0.0	7
Bryozoan	Tr	0.0	0.0	0.0	7
Pelecypod	2.0	4.1	11.0	0.0	7
Gastropod	Tr	0.0	0.0	0.0	7
Sparry calcite-filled pelecypod mold	0.0	0.0	0.0	0.0	7
Micritized carbonate grain	0.8	1.5	4.0	0.0	7
Glauconite grain	0.8	1.6	4.3	0.0	7
Heavy mineral grain	0.1	0.2	0.4	0.0	7
Detrital opaque mineral grain	0.2	0.4	1.0	0.0	7
Collophane	Tr	0.1	0.3	0.0	7
Sponge spicule	0.7	1.6	4.3	0.0	7
Carbonate intraclast	Tr	0.0	0.0	0.0	7
Carbonate pellet	Tr	0.0	0.0	0.0	7
Total	99.8				

Table 5. Composition of Quartz-Rich Microsparite, Aquifer Zone IIB 1

Constituent	Average	Standard Deviation	Maximum	Minimum	Number
Monocrystalline quartz	14.5	8.9	39.6	0.6	19
Polycrystalline quartz	0.0	0.1	0.5	0.0	19
Microcline	0.0	0.1	0.3	0.0	19
Untwinned potassium feldspar	0.0	0.1	0.3	0.0	19
Plagioclase	0.0	0.1	0.3	0.0	19
Rock fragment	0.0	0.1	0.3	0.0	19
Interparticle pore	0.4	0.8	2.7	0.0	18
Moldic pore	2.4	3.7	15.0	0.0	18
Intraparticle pore	0.1	0.2	0.7	0.0	18
Vug pore	0.9	2.8	11.7	0.0	18
Intercrystal pore	1.2	2.0	7.3	0.0	18
Terrigenous mud matrix	0.1	0.3	1.1	0.0	19
Micrite	6.2	6.9	20.0	0.0	19
Microspar	44.3	28.7	97.6	1.3	19
Sparry calcite cement & replacement	20.9	24.8	70.7	0.0	19
Muscovite	0.0	0.2	0.7	0.0	19
Authigenic pyrite	0.2	0.4	1.3	0.0	19
Authigenic glauconite cement	0.4	0.9	3.0	0.0	19
Chalcedony / chert cement & replacement	0.9	4.1	18.0	0.0	19
Opal cement & replacement	0.1	0.5	2.0	0.0	19
Foraminifer	0.4	0.5	1.7	0.0	19
Mollusk	0.7	0.9	3.7	0.0	19
Fragmented skeletal debris	1.5	2.1	7.7	0.0	19
Echinoderm	1.4	1.4	4.3	0.0	19
Bryozoan	0.0	0.1	0.3	0.0	19
Pelecypod	2.3	3.2	11.0	0.0	19
Gastropod	0.0	0.1	0.3	0.0	19
Sparry calcite-filled pelecypod mold	0.0	0.0	0.0	0.0	19
Micritized carbonate grain	0.9	1.3	4.0	0.0	19
Glauconite grain	0.1	0.2	1.0	0.0	19
Heavy mineral grain	0.1	0.2	0.7	0.0	19
Detrital opaque mineral grain	0.1	0.2	1.0	0.0	19
Collophane	0.0	0.1	0.3	0.0	19
Sponge spicule	0.0	0.0	0.0	0.0	19
Carbonate intraclast	0.1	0.5	2.3	0.0	19
Carbonate pellet	0.0	0.1	0.3	0.0	19
Total	100.2				

Table 6. Composition of Quartz-Rich Siliceous Mudstone, Aquifer Zone IIB1

Constituent	Average	Standard Deviation	Maximum	Minimum	Number
Monocrystalline quartz	23.8	9.4	35.3	6.0	9
Polycrystalline quartz	0.1	0.1	0.3	0.0	9
Microcline	0.4	0.7	2.0	0.0	9
Untwinned potassium feldspar	0.0	0.1	0.3	0.0	9
Plagioclase	Tr	0.1	0.3	0.0	9
Rock fragment	0.0	0.0	0.0	0.0	9
Interparticle pore	0.1	0.1	0.3	0.0	9
Moldic pore	2.6	2.5	6.7	0.0	9
Intraparticle pore	0.3	0.7	2.0	0.0	9
Vug pore	7.4	7.5	20.0	0.0	9
Intercrystal pore	Tr	0.1	0.3	0.0	9
Terrigenous mud matrix	7.4	14.9	39.5	0.0	9
Micrite	4.7	7.7	21.0	0.0	9
Microspar	0.2	0.3	1.0	0.0	9
Sparry calcite cement & replacement	0.1	0.2	0.3	0.0	9
Muscovite	0.1	0.1	0.3	0.0	9
Authigenic pyrite	0.7	1.5	4.0	0.0	9
Authigenic glauconite cement	0.1	0.2	0.7	0.0	9
Chalcedony / chert cement & replacement	3.8	6.1	17.3	0.0	9
Opal cement & replacement	38.5	17.4	68.3	18.0	9
Foraminifer	1.1	1.6	4.0	0.0	9
Mollusk	1.5	2.3	5.7	0.0	9
Fragmented skeletal debris	2.9	3.6	9.7	0.0	9
Echinoderm	1.2	1.0	2.0	0.0	9
Bryozoan	Tr	0.1	0.3	0.0	9
Pelecypod	1.4	2.6	7.0	0.0	9
Gastropod	Tr	0.0	0.0	0.0	9
Sparry calcite-filled pelecypod mold	0.0	0.0	0.0	0.0	9
Micritized carbonate grain	0.7	1.4	4.0	0.0	9
Glauconite grain	0.2	0.4	1.0	0.0	9
Heavy mineral grain	0.1	0.2	0.7	0.0	9
Detrital opaque mineral grain	0.2	0.3	1.0	0.0	9
Collophane	Tr	0.1	0.3	0.0	9
Sponge spicule	0.3	0.6	1.7	0.0	9
Carbonate intraclast	0.0	0.0	0.0	0.0	9
Carbonate pellet	0.0	0.0	0.0	0.0	9
Total	99.9				

Table 7. Composition of Quartz-Rich Terrigenous Mud, Aquifer Zone IIB1

Constituent	Average	Standard Deviation	Maximum	Minimum	Number
Monocrystalline quartz	34.7	15.3	48.7	10.0	5
Polycrystalline quartz	0.1	0.1	0.3	0.0	5
Microcline	0.2	0.3	0.7	0.0	5
Untwinned potassium feldspar	0.1	0.1	0.3	0.0	5
Plagioclase	0.0	0.0	0.0	0.0	5
Rock fragment	0.0	0.0	0.0	0.0	5
Interparticle pore	n/a	n/a	n/a	n/a	n/a
Moldic pore	n/a	n/a	n/a	n/a	n/a
Intraparticle pore	n/a	n/a	n/a	n/a	n/a
Vug pore	n/a	n/a	n/a	n/a	n/a
Intercrystal pore	n/a	n/a	n/a	n/a	n/a
Terrigenous mud matrix	51.1	12.5	65.0	36.7	5
Micrite	1.1	2.2	5.0	0.0	5
Microspar	0.1	0.1	0.3	0.0	5
Sparry calcite cement & replacement	0.0	0.0	0.0	0.0	5
Muscovite	0.0	0.0	0.0	0.0	5
Authigenic pyrite	0.1	0.3	0.7	0.0	5
Authigenic glauconite cement	1.7	2.6	6.0	0.0	5
Chalcedony / chert cement & replacement	0.0	0.0	0.0	0.0	5
Opal cement & replacement	0.0	0.0	0.0	0.0	5
Foraminifer	0.3	0.8	1.7	0.0	5
Mollusk	0.7	1.5	3.3	0.0	5
Fragmented skeletal debris	0.9	1.7	4.0	0.0	5
Echinoderm	0.1	0.1	0.3	0.0	5
Bryozoan	0.0	0.0	0.0	0.0	5
Pelecypod	4.2	9.4	21.0	0.0	5
Gastropod	0.0	0.0	0.0	0.0	5
Sparry calcite-filled pelecypod mold	0.0	0.0	0.0	0.0	5
Micritized carbonate grain	0.4	0.6	1.3	0.0	5
Glauconite grain	1.1	1.5	3.0	0.0	5
Heavy mineral grain	0.6	0.3	0.7	0.0	5
Detrital opaque mineral grain	0.3	0.5	1.0	0.0	5
Collophane	0.0	0.0	0.0	0.0	5
Sponge spicule	0.0	0.0	0.0	0.0	5
Carbonate intraclast	0.0	0.0	0.0	0.0	5
Carbonate pellet	0.0	0.0	0.0	0.0	5



## **APPENDIX A**

Table A1. Grain Size Terminology and Class Intervals for Grade Scales (from Folk, 1980)

	U.S. Standard sieve mesh	Millimeters	Phi ( $\phi$ ) units	Wentworth size class
GRAVEL	Use wire squares	4096	- 12	
		1024	- 10	Boulder
		256	256 - 8	
		64	64 - 6	Cobble
		16	- 4	Pebble
	5	4	4 - 2	
	6	3.36	- 1.75	
	7	2.83	- 1.5	Granule
	8	2.38	- 1.25	
	10	2.00	2 - 1.0	
SAND		12	- 0.75	
		14	- 0.5	Very coarse sand
		16	- 0.25	
		18	1 - 0.0	
		20	0.25	
		25	0.5	Coarse sand
		30	0.75	
		35	1/2 - 1.0	
		40	1.25	
		45	1.5	Medium sand
		50	1.75	
		60	1/4 - 2.0	
		70	2.25	
		80	2.5	Fine sand
		100	2.75	
		120	1/8 - 3.0	
		140	3.25	
		170	3.5	Very fine sand
		200	3.75	
		230	1/16 - 4.0	
SILT		270	4.25	
		325	4.5	Coarse silt
		0.037	4.75	
		0.031	1/32 - 5.0	
		0.0156	1/64 - 6.0	Medium silt
MUD	Use pipette or hydrometer	0.0078	1/128 - 7.0	Fine silt
		0.0039	1/256 - 8.0	Very fine silt
		0.0020	9.0	
		0.00098	10.0	Clay
		0.00049	11.0	
		0.00024	12.0	
		0.00012	13.0	
		0.00006	14.0	

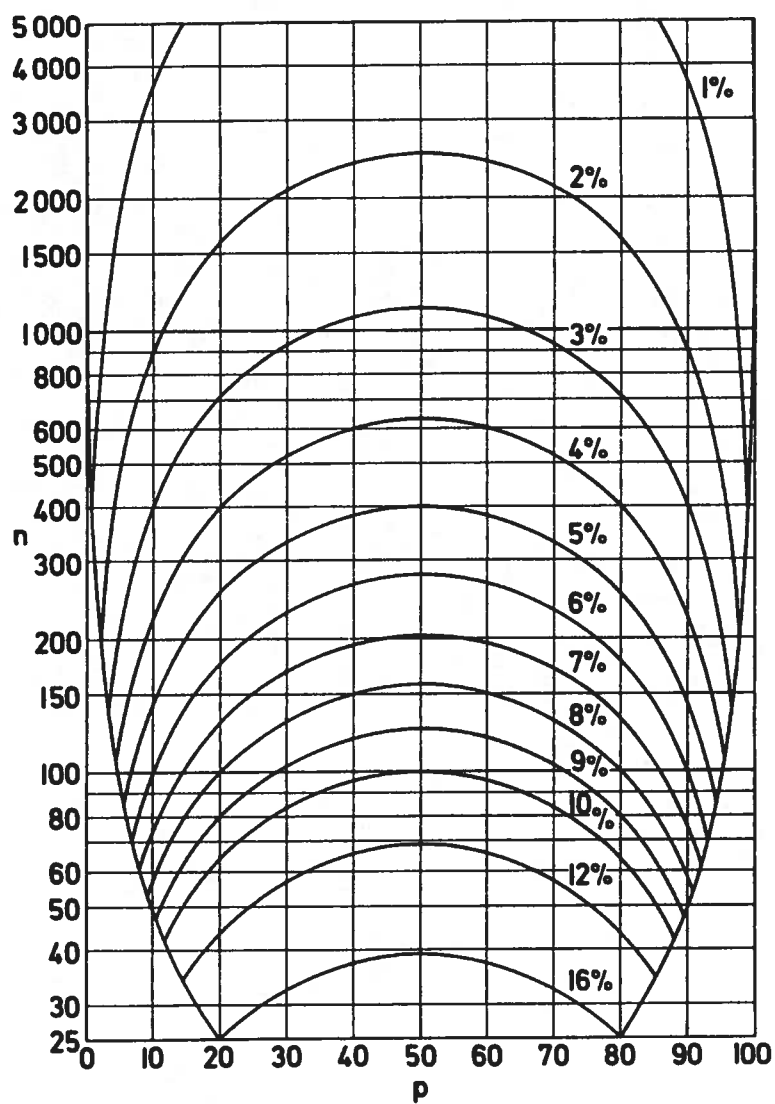
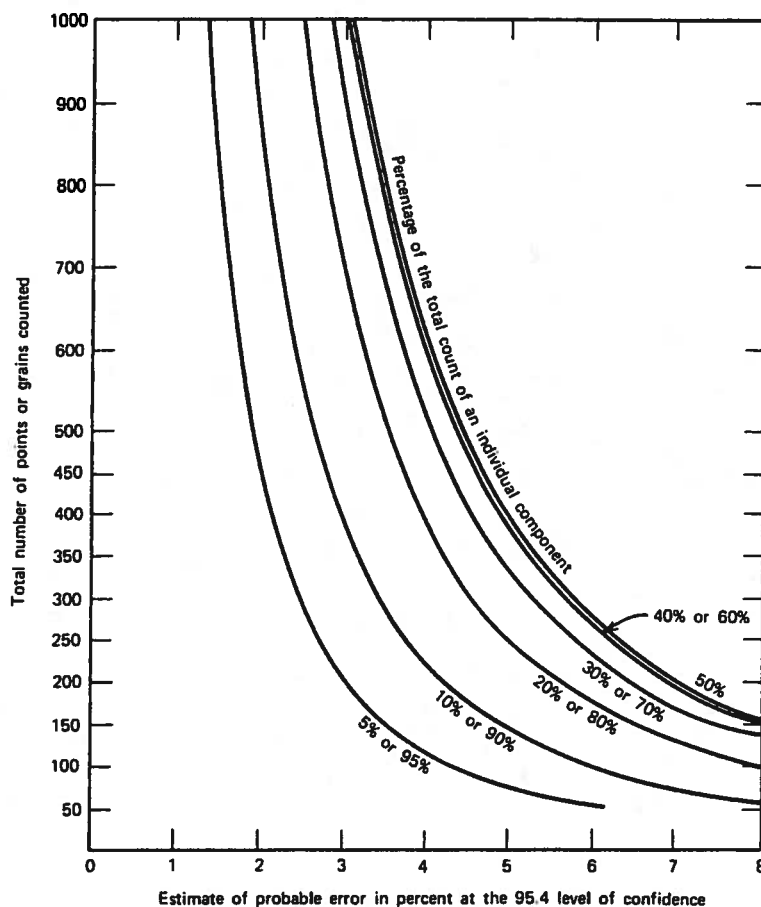


Figure A3. Ninety-five Percent Confidence Limits for Constituent Proportions, where  $n$  is the Total Number of Points Counted, and  $p$  is the Estimated Proportion of a Particular Constituent (from van der Plas and Tobi, 1965)



$$E_{95.4} = 2 \sqrt{\frac{P(100 \cdot P)}{N}}$$

where  $E$  = probable error in percent,  
 $N$  = total number of points or grains counted,  
 $P$  = percentage of  $N$  of an individual component.

Figure A4. Formula and Nomogram for Calculating Dryden's (1931) Probable Error at 95.4% for Number Percentages Obtained from the Line Method of Point Counting (modified from Galehouse, 1971)

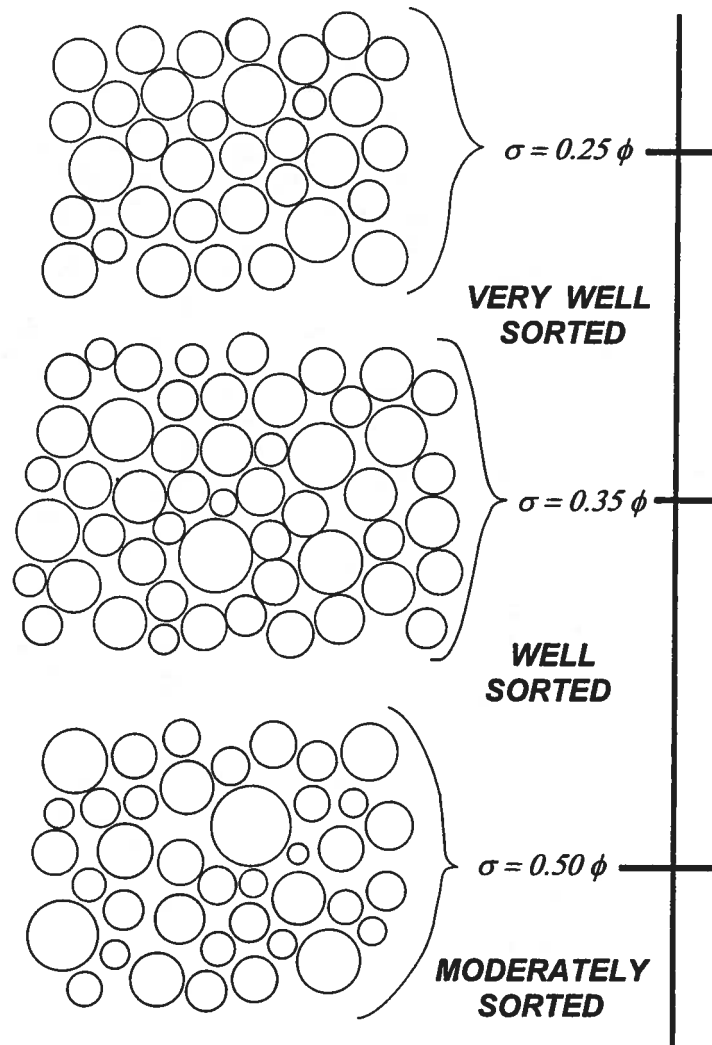


Figure A5. Sorting Images of Folk (1980)

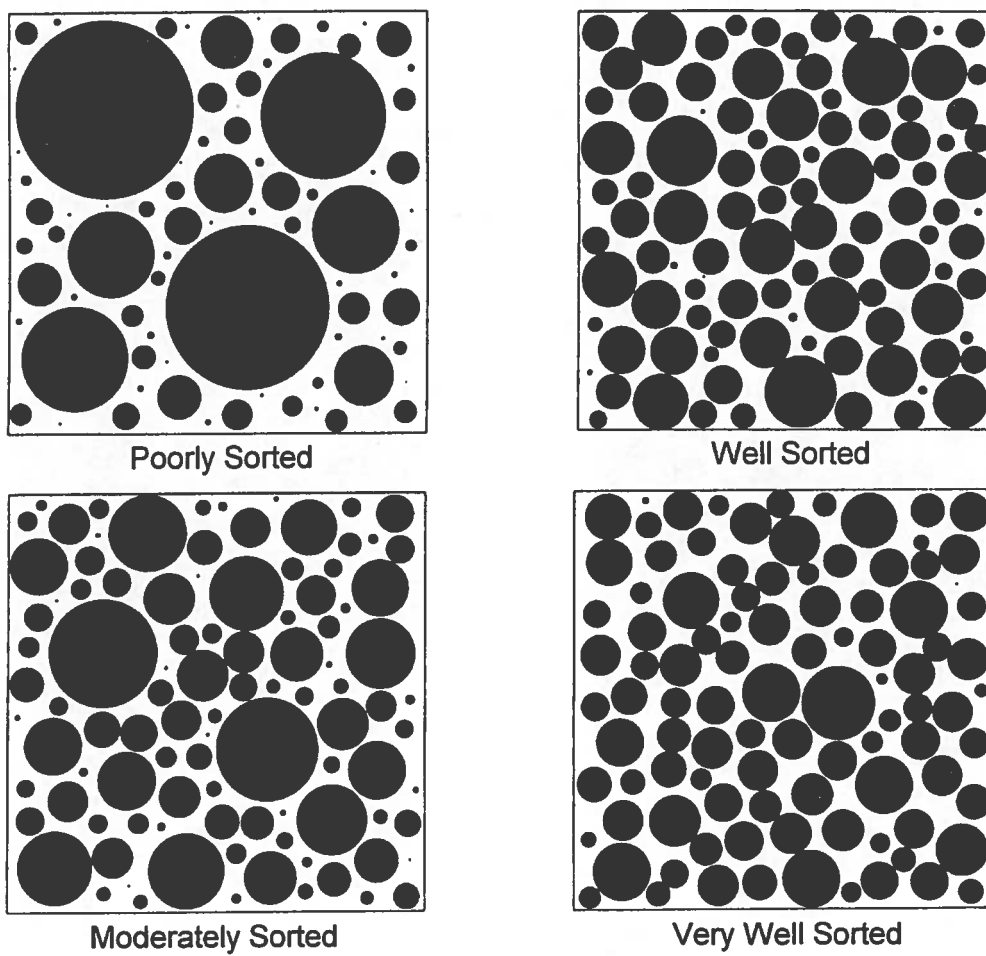


Figure A6. Sorting Images of Harrell (1984)

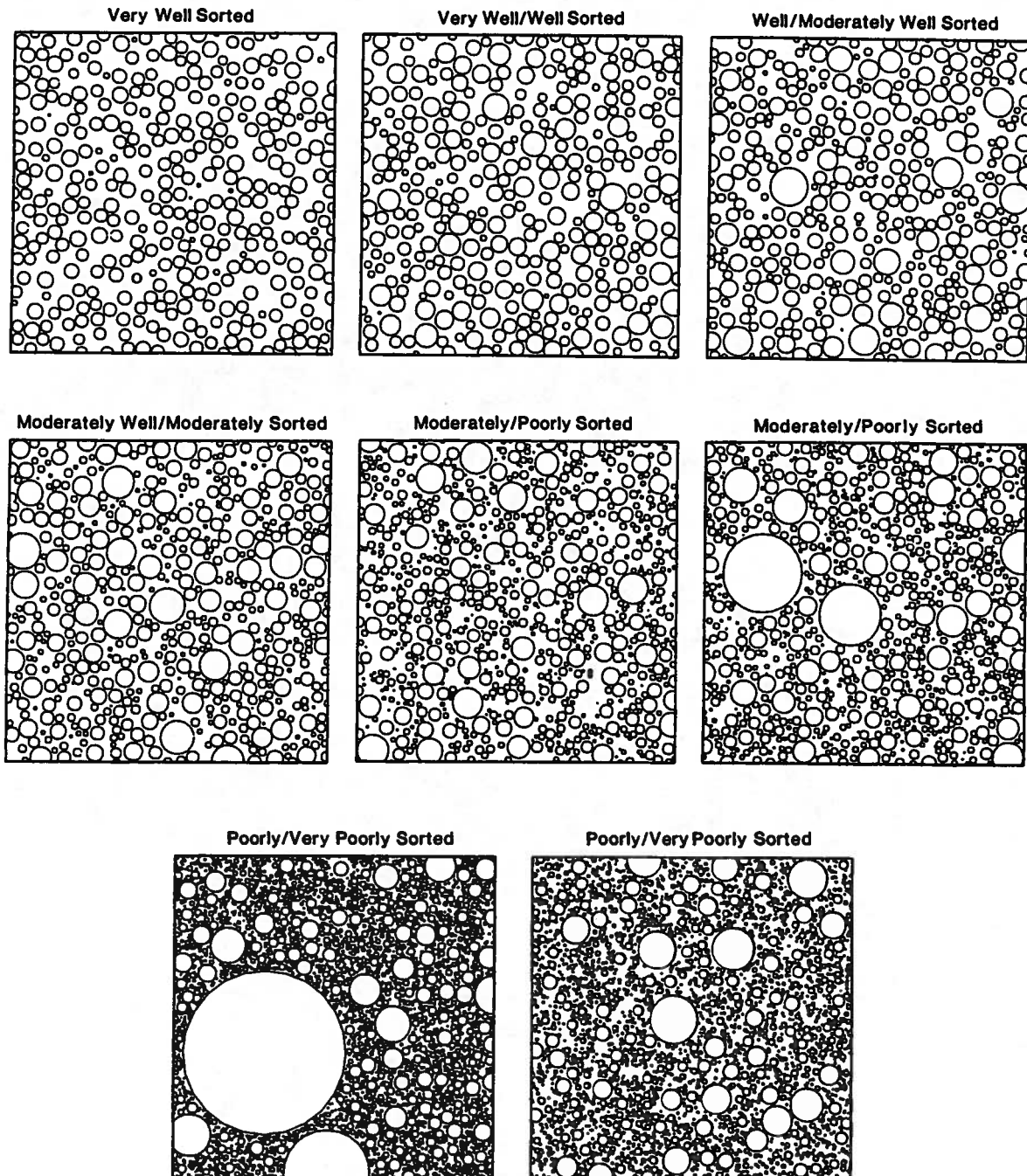


Figure A7. Sorting Images of Longiaru (1986)

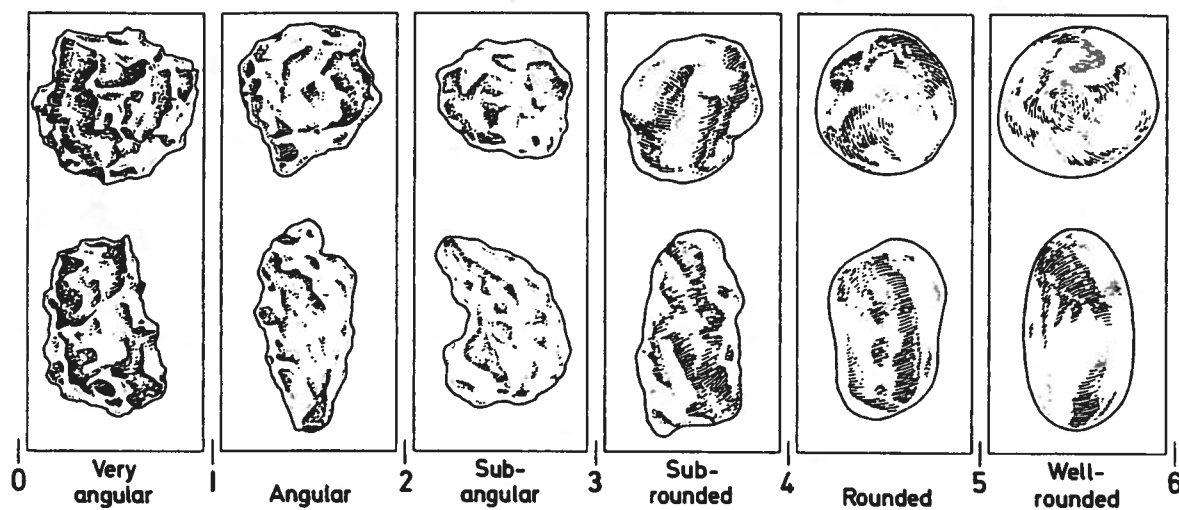


Figure A8. Roundness Images and Classes. Columns Show Grains of Similar Roundness but Different Sphericity (modified from Powers, 1953)



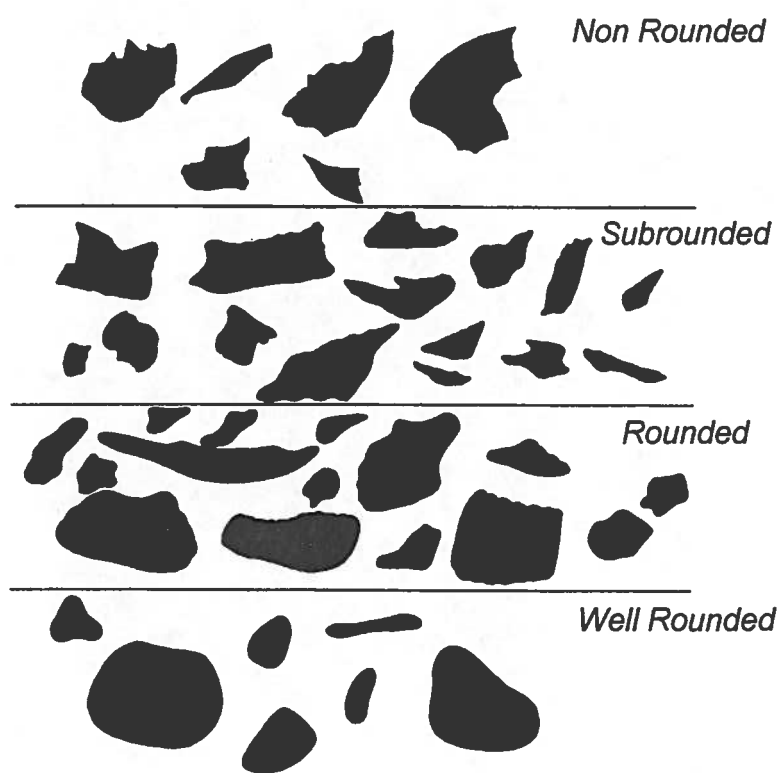


Figure A9. Comparison Chart for Describing the Roundness of Carbonate Bioclasts (modified from Pilkey and others, 1967)

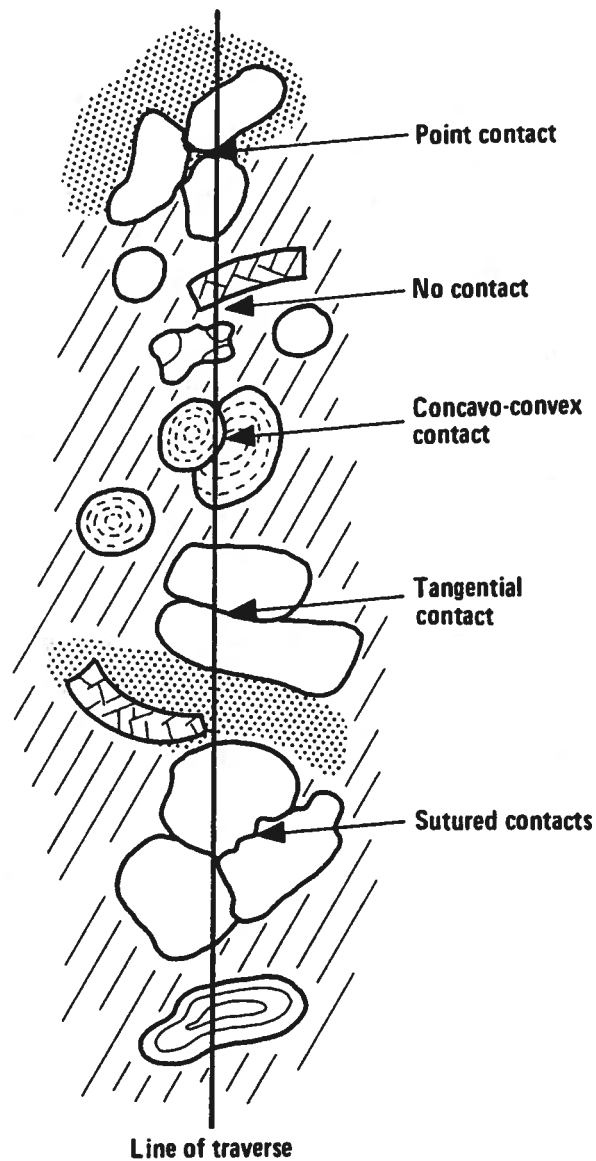


Figure A10. Description of Particle Contacts. When Expressed as Percentages, the Frequency of Contact Types Along Lines on Traverse Indicate the Amount of Packing (modified from Taylor, 1950; Flügel, 1982)



**Figure A11. Classification of Carbonate-Terrigenous Sediment Mixtures (modified from Lindholm, 1987)**

Table A12. Classification of Carbonate Sediments and Rocks According to Depositional Texture (from Dunham, 1962)

Depositional Texture Recognizable					Depositional Texture Not Recognizable
Original Components Not Bound Together During Deposition				Original Components Bound Together During Deposition	
Contains mud (particles of clay and fine silt size)		Lacks mud			
Mud-supported		Grain-supported			
< 10% grains	> 10% grains				
Mudstone	Wackestone	Packstone	Grainstone	Boundstone	Crystalline Carbonate

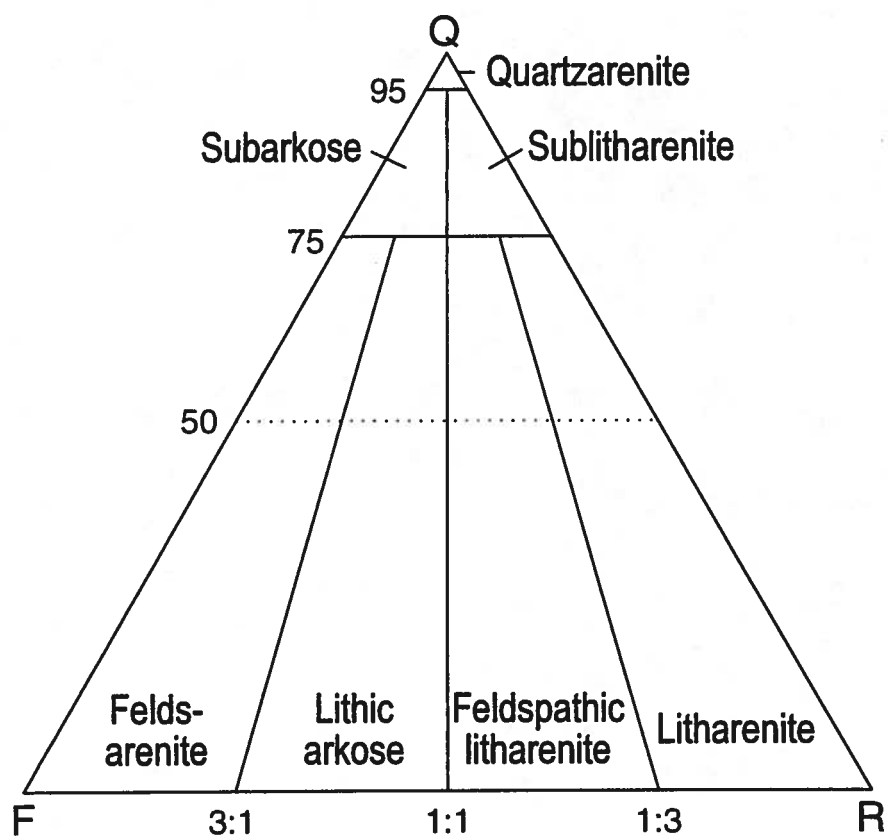


Figure A13. Classification of Sand and Sandstone (from Folk, 1980)

Table A14. Grain Size Scale for Carbonate Sediments and Rocks (modified from Folk, 1962)

	<b>TRANSPORTED CONSTITUENTS</b>	<b>AUTHIGENIC CONSTITUENTS</b>	
256 mm			256 mm
64 mm	<i>Very coarse calcirudite</i>	<i>Extremely coarsely crystalline</i>	
16 mm	<i>Coarse calcirudite</i>		
4 mm	<i>Medium calcirudite</i>		4 mm
1 mm	<i>Fine calcirudite</i>	<i>Very coarsely crystalline</i>	1 mm
0.5 mm	<i>Coarse calcarenite</i>	<i>Coarsely crystalline</i>	
0.25 mm	<i>Medium calcarenite</i>		0.25 mm
	<i>Fine calcarenite</i>	<i>Medium crystalline</i>	
0.125 mm	<i>Very fine calcarenite</i>		
0.062 mm	<i>Coarse calcilutite</i>	<i>Finely crystalline</i>	0.062 mm
0.031 mm	<i>Medium calcilutite</i>		
0.016 mm	<i>Fine calcilutite</i>	<i>Very finely crystalline</i>	0.016 mm
0.008 mm	<i>Very fine calcilutite</i>		
0.004 mm		<i>Aphanocrystalline</i>	0.004 mm
		<i>Cryptocrystalline</i>	0.001 mm

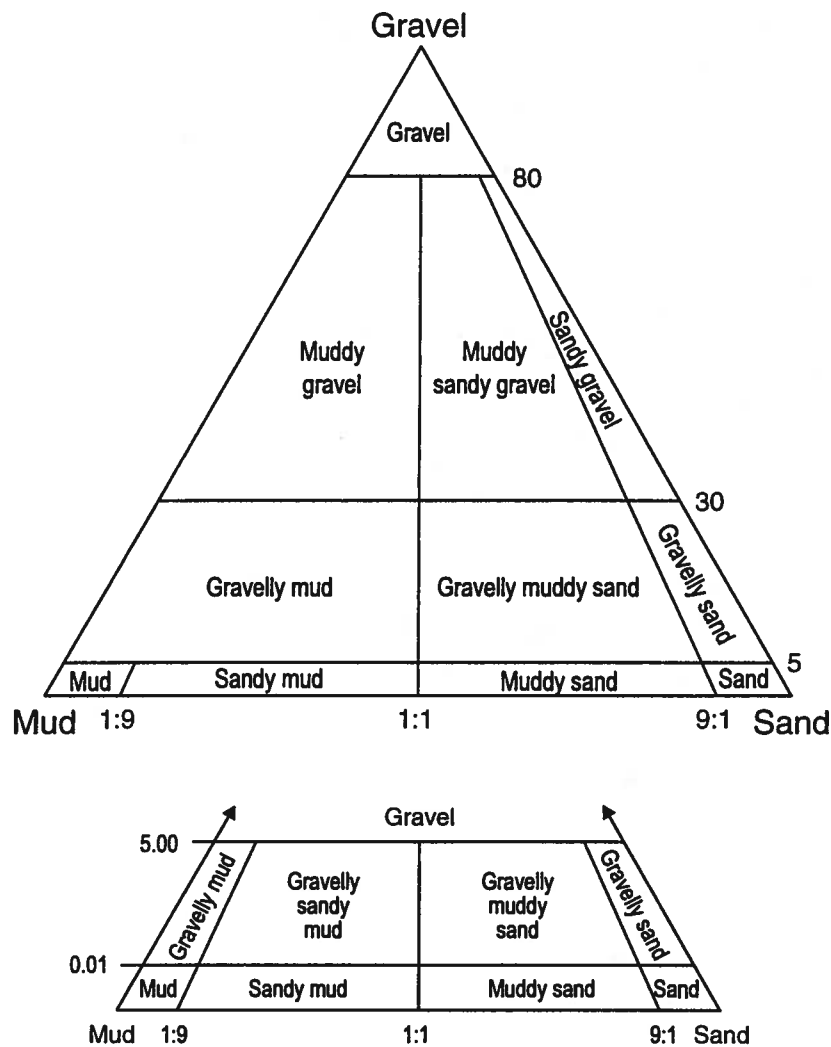


Figure A15. Textural Terminology for Gravel-Bearing Terrigenous Sediments. Specify Clast-Supported or Matrix-Supported when Sand or Mud Fraction is Abundant (modified from Folk, 1954)

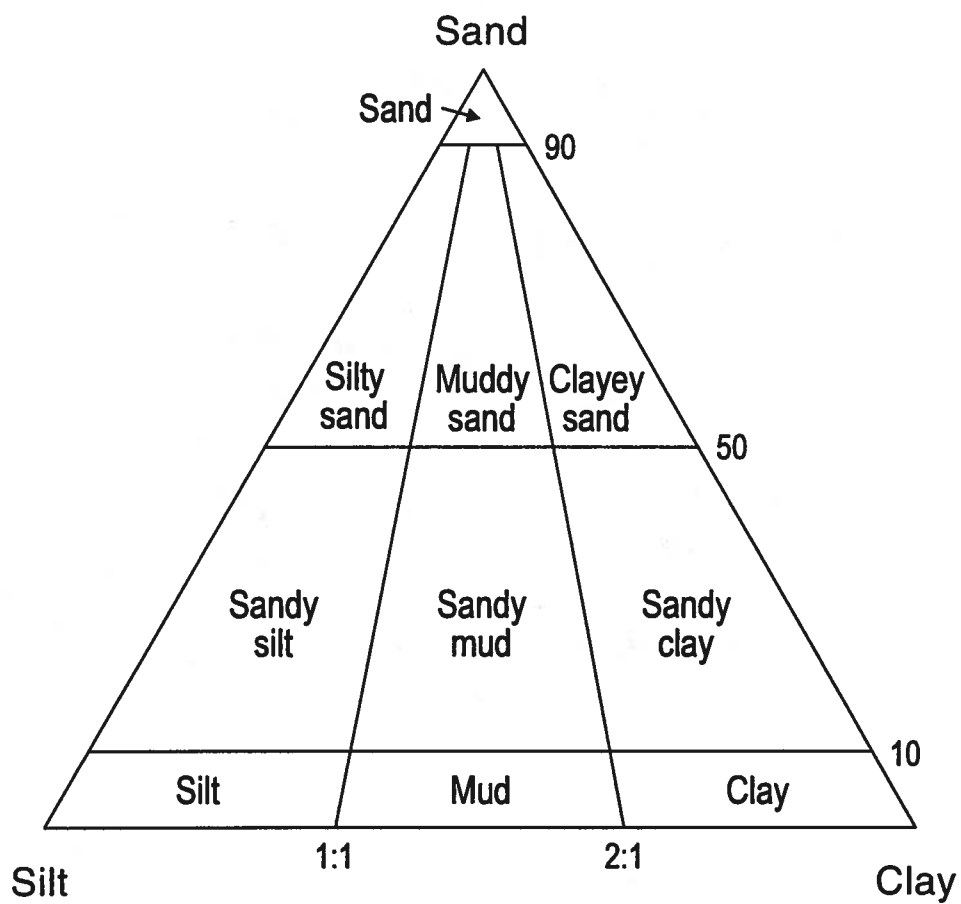


Figure A16. Textural Terminology for Gravel-Free Terrigenous Sediments  
(modified from Folk, 1954)



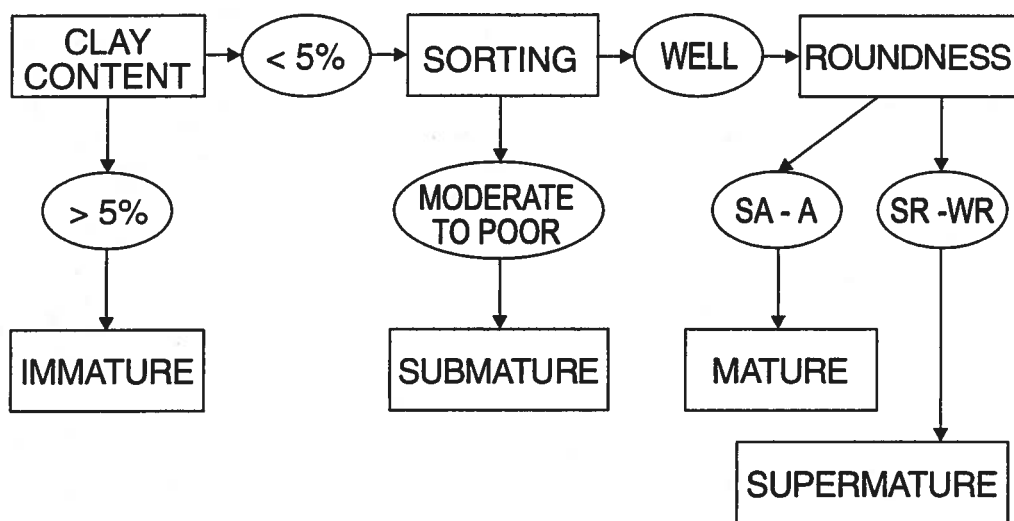















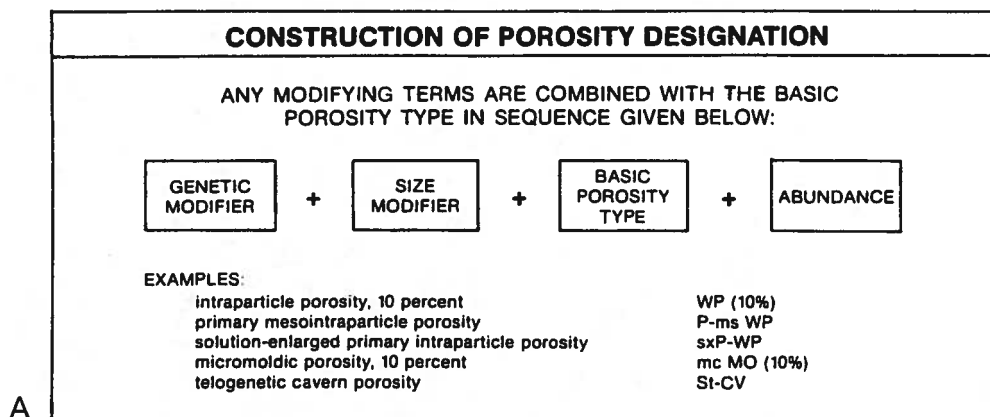
Figure A17. Flow Chart for Determining Textural Maturity of Terrigenous Sand (modified from Folk, 1951)

BASIC POROSITY TYPES			
FABRIC-DEPENDENT/SELECTIVE		NOT FABRIC-SELECTIVE	
	INTERPARTICLE (BP)		VUG (VUG)
	INTRAPARTICLE (WP)		CHANNEL (CH)
	SHELTER (SH)		FRACTURE (FR)
	GROWTH FRAMEWORK (GF)	} CAVERN (CA) (if very large pores)	
	FENESTRAL (FE)		
	MOLDIC (MO)	FABRIC-SELECTIVE OR NOT	
	INTERCRYSTAL (BC)		BURROW/BORING (BU/BO)
			SHRINKAGE (SK)
			BRECCIA (BR)

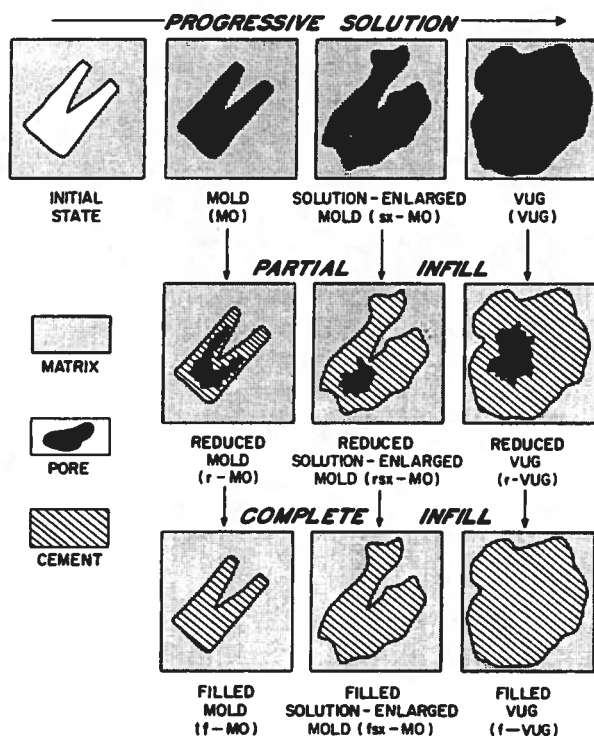
Modified after Choquette & Pray, 1970

MODIFYING TERMS					
GENETIC MODIFIERS				SIZE * MODIFIERS	
PROCESS		DIRECTION OR STAGE		CLASSES	
				mm †	
SOLUTION	s	ENLARGED	x	MEGAPORE mg	large lmg 256
CEMENTATION	c	REDUCED	r		small smg 32
INTERNAL SEDIMENT	i	FILLED	f	MESOPORE ms	large lms 4
					small sms 1/2
TIME OF FORMATION				MICROPORE mc	1/16
PRIMARY		P		Use size prefixes with basic porosity types	
pre-depositional		Pp		mesovug msVUG	
depositional		Pd		small mesomold smsMO	
SECONDARY		S		microinterparticle mcBP	
eogenetic		Se		* For regular-shaped pores smaller than cavern size	
mesogenetic		Sm		† Measures refer to average pore diameter of a single pore or the range in size of a pore assemblage	
telogenetic		St		For tubular pores use average cross-section For platy pores use width and note shape	
Genetic modifiers are combined as follows:					
PROCESS		+	DIRECTION	+	TIME
EXAMPLES		solution-enlarged		sx	
		cement-reduced primary		crP	
		sediment-filled eogenetic		ifSe	
ABUNDANCE MODIFIERS					
percent porosity (15%)					
or					
ratio of porosity types (1:2)					
or					
ratio and percent (1:2) (15%)					

Table A18. Porosity Classification of Choquette and Pray (1970). A. Basic Porosity Types. B. Genetic, Size, and Abundance Modifiers



A



B

Table A19. Porosity Classification of Choquette and Pray (1970). A. Format for Construction of Porosity Name and Code Designations. B. Common Stages in Evolution of Pore, a Mold, Showing Application of Genetic Modifiers and Classification Code

## Appendix B1. Abbreviations for Microfacies Used in this Report

### Lime Mudstone

IM        lime mud (unconsolidated) or mudstone (lithified)  
sdsIM    sandy, skeletal lime mud (unconsolidated) or mudstone (lithified)

### Lime Wackestone

sW       skeletal wackestone  
sdsW    sandy, skeletal wackestone

### Lime Packstone

sdsP    sandy, skeletal packstone

### Lime Grainstone

sdsG    sandy, skeletal grainstone

### Microsparite

R        microsparite  
sdR     sandy microsparite  
sdsR    sandy, skeletal microsparite

### Siliceous Mudstone

sM       siliceous mudstone  
sdsM    sandy, siliceous mudstone  
sksM    skeletal, siliceous mudstone

### Terrigenous Mud

tM       terrigenous mud or mudstone  
stM      sandy, terrigenous mud or mudstone  
sstM    sandy, skeletal terrigenous mud or mudstone

### Terrigenous Sand and Sandstone

mS       muddy sand  
cS       calcareous sand  
ccS      chalcedony- or chert-cemented sandstone  
ocS      opal-cemented sandstone

## **APPENDIX B**

Table B2. Point Count Data for Samples from Aquifer Unit IIA in the General Separations Area, SRS

Constituent	BGX-2B-176	BGX-2B-182	HSB-120A-167	HSB-140-156
Monocrystalline quartz	0.3	39.4	66.7	61.3
Polycrystalline quartz	0.0	0.0	0.0	0.6
Microcline	0.0	0.0	0.0	0.0
Untwinned potassium feldspar	0.0	0.0	0.0	0.0
Plagioclase	0.0	0.0	0.0	0.0
Rock fragment	0.0	0.0	0.0	0.0
Interparticle pore	0.0	n/a	n/a	0.0
Moldic pore	0.0	n/a	n/a	2.0
Intraparticle pore	0.0	n/a	n/a	0.0
Vug pore	0.0	n/a	n/a	0.0
Intercrystal pore	0.0	n/a	n/a	1.7
Terrigenous mud matrix	99.0	48.3	30.3	0.0
Micrite	0.0	0.0	0.0	0.0
Microspar	0.0	0.0	0.0	0.0
Sparry calcite cement & replacement	0.0	0.0	0.0	0.0
Muscovite	0.0	0.3	0.0	0.0
Authigenic zeolite	0.0	1.0	0.0	0.0
Authigenic pyrite	0.7	5.3	0.0	0.0
Authigenic glauconite cement	0.0	0.0	0.0	0.0
Chalcedony / chert cement & replacement	0.0	0.0	1.7	34.3
Opal cement & replacement	0.0	5.7	1.0	0.0
Foraminifer	0.0	0.0	0.0	0.0
Mollusk	0.0	0.0	0.0	0.0
Fragmented skeletal debris	0.0	0.0	0.3	0.0
Echinoderm	0.0	0.0	0.0	0.0
Bryozoan	0.0	0.0	0.0	0.0
Pelecypod	0.0	0.0	0.0	0.0
Gastropod	0.0	0.0	0.0	0.0
Sparry calcite-filled pelecypod mold	0.0	0.0	0.0	0.0
Micritized carbonate grain	0.0	0.0	0.0	0.0
Glauconite grain	0.0	0.0	0.0	0.0
Heavy mineral grain	0.0	0.0	0.0	0.0
Detrital opaque mineral grain	0.0	0.0	0.0	0.0
Collophane	0.0	0.0	0.0	0.0
Sponge spicule	0.0	0.0	0.0	0.0
Carbonate intraclast	0.0	0.0	0.0	0.0
Carbonate pellet	0.0	0.0	0.0	0.0
Total	100.0	100.0	100.0	99.9
Lithology	tM	stM	mS	ccS
Number of grains counted	300	300	300	300
Counting method	PC	L	L	PC

Table B3. Point Count Data for Samples from Confining Unit IIA-IIB in the General Separations Area, SRS

Constituent	BGO-9AA-148	BGO-9AA-150A	BGO-9AA-150B	BGO-9AA-153	BGX-2B-152A	BGX-2B-152B	BGX-2B-155	BGX-2B-156	BGX-2B-161	FSB-115C-118	HMD-1C-125	HPC-1-182
Monocrystalline quartz	29.7	2.0	8.0	10.0	5.0	17.3	18.0	21.7	30.0	53.3	25.0	46.0
Polycrystalline quartz	0.0	0.0	0.0	0.0	0.0	0.0	0.0	0.0	0.0	0.0	0.0	0.0
Microcline	0.0	0.0	0.0	0.0	0.0	0.0	0.0	0.0	0.3	0.3	0.0	0.0
Untwinned potassium feldspar	0.3	0.0	0.0	0.0	0.0	0.0	0.0	0.0	0.0	0.0	0.0	0.0
Plagioclase	0.0	0.0	0.0	0.0	0.0	0.0	0.0	0.0	0.0	0.0	0.0	0.0
Rock fragment	0.0	0.0	0.0	0.0	0.0	0.0	0.0	0.0	0.0	0.0	0.0	0.0
Interparticle pore	0.3	0.3	0.0	0.0	0.7	0.0	0.0	0.0	n/a	3.0	0.0	n/a
Moldic pore	0.0	0.0	0.0	0.0	0.0	5.0	10.0	3.3	n/a	9.3	1.0	n/a
Intraparticle pore	0.0	0.0	0.0	0.0	0.0	0.0	0.0	0.0	n/a	0.0	0.7	n/a
Vug pore	1.7	0.0	0.0	0.0	0.0	7.0	3.0	19.7	n/a	0.0	0.0	n/a
Intercrystal pore	0.0	0.0	0.0	0.0	0.0	0.0	0.0	0.0	n/a	0.0	6.3	n/a
Terrigenous mud matrix	0.0	0.0	0.0	0.0	1.3	0.0	0.0	0.0	50.2	0.0	0.0	51.0
Micrite	48.0	92.3	0.0	0.0	0.0	0.0	0.0	0.0	0.0	0.0	1.3	0.0
Microspar	0.0	0.0	0.0	0.0	0.0	0.0	0.0	0.0	0.0	0.0	0.0	0.0
Sparry calcite cement & replacement	0.0	0.0	0.0	0.0	0.0	0.0	0.0	0.0	0.0	0.0	0.0	0.0
Muscovite	0.0	0.0	0.0	0.0	0.0	0.0	0.0	0.0	0.6	0.0	0.0	0.0
Authigenic pyrite	0.3	0.0	0.0	0.0	0.0	0.0	1.0	0.3	10.8	0.0	3.7	0.0
Authigenic glauconite cement	0.0	0.0	0.0	2.0	0.0	0.0	0.0	0.0	3.4	0.0	0.7	0.0
Chalcedony / chert cement & replacement	0.7	0.0	0.0	2.0	93.0	9.7	6.0	0.0	0.0	32.0	0.0	0.0
Opal cement & replacement	8.0	4.7	56.0	36.0	0.0	60.7	61.0	54.0	0.0	2.0	35.7	0.0
Iron oxide cement & replacement	0.0	0.0	0.0	0.0	0.0	0.0	0.0	0.0	0.0	0.0	0.0	0.0
Foraminifer	1.3	0.0	0.0	2.0	0.0	0.0	0.0	0.0	0.0	0.0	0.3	0.0
Mollusk	0.0	0.0	2.0	6.0	0.0	0.0	0.0	0.0	0.0	0.0	8.0	0.0
Fragmented skeletal debris	1.7	0.3	2.0	0.0	0.0	0.0	0.0	0.0	0.0	0.0	4.0	0.0
Echinoderm	1.3	0.0	0.0	0.0	0.0	0.0	0.0	0.0	0.0	0.0	0.0	0.0
Bryozoan	0.3	0.0	0.0	0.0	0.0	0.0	0.0	0.0	0.0	0.0	0.0	0.0
Pelecypod	4.0	0.0	30.0	36.0	0.0	0.0	0.0	0.0	0.0	0.0	9.0	0.0
Gastropod	1.0	0.0	0.0	4.0	0.0	0.0	0.0	0.0	0.0	0.0	0.0	0.0
Sparry calcite-filled pelecypod mold	0.0	0.0	0.0	0.0	0.0	0.0	0.0	0.0	0.0	0.0	0.0	0.0
Micritized carbonate grain	0.0	0.0	0.0	0.0	0.0	0.0	0.0	0.0	0.0	0.0	2.3	0.0
Glauconite grain	0.3	0.0	0.0	2.0	0.0	0.0	0.0	1.0	4.7	0.0	1.3	0.0
Heavy mineral grain	0.0	0.0	0.0	0.0	0.0	0.3	0.0	0.0	0.0	0.0	0.0	0.7
Detrital opaque mineral grain	0.7	0.3	0.0	0.0	0.0	0.0	0.0	0.0	0.0	0.0	0.0	2.3
Collophane	0.0	0.0	0.0	0.0	0.0	0.0	0.0	0.0	0.0	0.0	0.0	0.0
Sponge spicule	0.0	0.0	0.0	0.0	0.0	0.0	1.0	0.0	0.0	0.0	0.0	0.0
Carbonate intraclast	0.3	0.0	2.0	0.0	0.0	0.0	0.0	0.0	0.0	0.0	0.3	0.0
Carbonate pellet	0.0	0.0	0.0	0.0	0.0	0.0	0.0	0.0	0.0	0.0	0.0	0.0
Total	99.9	99.9	100.0	100.0	100.0	100.0	100.0	100.0	100.0	99.9	99.9	100.0
Lithology	sdsIM	IM	sksM	sksM	sM	sdsM	sdsM	sdsM	stM	ccS	sksM	stM
Number of points counted	300	300	50	50	300	300	100	300	300	300	300	300
Counting method	PC	PC	PC	PC	PC	PC	PC	PC	L	PC	PC	L

Table B3. Point Count Data for Samples from Confining Unit IIA-IIB in the General Separations Area, SRS (Continued)

Constituent	HP-1-186	HSB-TB-157
Monocrystalline quartz	51.7	42.3
Polycrystalline quartz	0.0	0.0
Microcline	0.0	0.0
Untwinned potassium feldspar	0.3	0.0
Plagioclase	0.0	0.0
Rock fragment	0.0	0.0
Interparticle pore	n/a	n/a
Moldic pore	n/a	n/a
Intraparticle pore	n/a	n/a
Vug pore	n/a	n/a
Intercrystal pore	n/a	n/a
Terrigenous mud matrix	34.3	49.0
Micrite	0.0	0.3
Microspar	0.0	0.0
Sparry calcite cement & replacement	0.0	0.0
Muscovite	0.0	0.0
Authigenic pyrite	0.0	0.0
Authigenic glauconite cement	0.0	3.7
Chalcedony / chert cement & replacement	0.3	0.0
Opal cement & replacement	0.0	0.0
Iron oxide cement & replacement	13.0	0.0
Foraminifer	0.0	0.0
Mollusk	0.0	0.0
Fragmented skeletal debris	0.0	2.3
Echinoderm	0.0	0.0
Bryozoan	0.0	0.0
Pelecypod	0.0	0.0
Gastropod	0.0	0.0
Sparry calcite-filled pelecypod mold	0.0	0.0
Micritized carbonate grain	0.0	0.0
Glauconite grain	0.0	2.0
Heavy mineral grain	0.0	0.0
Detrital opaque mineral grain	0.3	0.3
Collophane	0.0	0.0
Sponge spicule	0.0	0.0
Carbonate intraclast	0.0	0.0
Carbonate pellet	0.0	0.0
Total	99.9	99.9
Lithology	mS	stM
Number of points counted	300	300
Counting method	L	L



Table B4. Point Count Data for Samples from Aquifer Unit IIB1 in the General Separations Area, SRS

Constituent	BGO-9AA-113	BGO-9AA-119	BGO-9AA-124	BGO-9AA-125A	BGO-9AA-125B	BGO-9AA-127A	BGO-9AA-127B	BGO-9AA-127C	BGO-9AA-128A	BGO-9AA-128B	BGO-9AA-128C	BGO-9AA-132
Monocrystalline quartz	29.6	30.3	31.7	16.0	19.0	19.4	16.6	15.7	26.3	28.6	27.0	23.0
Polycrystalline quartz	0.0	0.0	0.0	0.0	0.0	0.3	0.0	0.0	0.0	0.0	0.0	0.0
Microcline	0.0	0.0	0.0	0.0	0.0	0.0	0.0	0.7	0.3	0.0	0.3	0.3
Untwinned potassium feldspar	0.0	0.0	0.0	0.0	0.0	0.0	0.0	0.3	0.3	0.0	0.0	0.0
Plagioclase	0.0	0.0	0.0	0.0	0.0	0.0	0.0	0.0	0.3	0.0	0.0	0.0
Rock fragment	0.0	0.0	0.0	0.0	0.0	0.0	0.0	0.0	0.0	0.3	0.0	0.0
Interparticle pore	6.3	3.7	2.3	0.3	0.0	0.0	0.3	0.0	1.0	1.7	4.6	7.3
Moldic pore	0.0	0.0	0.0	0.0	2.3	0.3	4.7	0.0	0.0	0.0	0.7	0.3
Intraparticle pore	0.3	0.3	0.3	0.0	0.0	1.0	1.0	0.0	0.0	0.0	1.7	0.0
Vug pore	0.0	0.0	0.0	0.0	15.9	0.7	15.0	0.0	0.0	0.0	0.0	0.0
Intercrystal pore	0.0	0.0	0.3	0.0	0.0	0.0	0.0	0.0	0.0	0.0	0.0	0.0
Terrigenous mud matrix	0.0	0.0	0.0	0.0	0.0	0.0	0.0	0.0	0.0	0.0	0.0	0.0
Micrite	38.7	52.7	53.7	57.0	53.5	48.0	54.0	61.0	56.0	48.3	51.7	55.3
Microspar	12.7	0.7	0.7	0.0	0.0	0.3	0.0	0.7	7.0	7.3	0.0	0.0
Sparry calcite cement & replacement	0.3	0.0	0.0	0.0	0.0	0.3	0.3	0.0	3.7	5.3	0.0	0.0
Muscovite	0.0	0.0	0.0	0.0	0.0	0.0	0.0	0.3	0.3	0.0	0.0	0.0
Authigenic pyrite	0.0	0.0	0.0	0.0	0.4	0.3	0.0	0.0	0.0	0.0	0.0	0.0
Authigenic glauconite cement	0.3	0.3	0.0	0.0	0.0	0.0	0.0	0.0	0.0	0.0	0.0	0.3
Chalcedony / chert cement & replacement	0.0	0.0	0.0	12.3	0.0	12.3	0.0	3.3	0.0	0.0	0.0	0.3
Opal cement & replacement	0.0	0.0	0.0	2.3	0.8	0.0	0.0	0.3	0.0	0.0	0.0	0.0
Foraminifer	0.7	0.0	0.0	1.7	2.3	3.0	1.3	0.7	0.3	0.7	1.0	0.7
Mollusk	1.0	0.0	0.0	3.0	1.2	2.0	1.7	0.0	0.0	0.0	0.7	0.0
Fragmented skeletal debris	2.3	2.7	5.0	3.0	2.7	4.0	1.7	4.7	2.0	2.7	5.3	3.3
Echinoderm	7.0	6.7	4.3	3.3	1.6	7.7	2.3	6.3	1.7	4.0	3.0	3.0
Bryozoan	0.0	0.0	0.0	0.0	0.0	0.0	0.0	0.0	0.0	0.0	0.3	0.3
Pelecypod	0.7	1.3	1.0	0.0	0.0	0.0	0.0	0.7	0.7	0.0	1.7	4.0
Gastropod	0.0	0.0	0.0	0.0	0.0	0.0	0.0	0.0	0.0	0.0	1.0	0.0
Sparry calcite-filled pelecypod mold	0.0	0.0	0.0	0.0	0.0	0.0	0.0	0.0	0.0	0.0	0.0	0.0
Micritized carbonate grain	0.0	0.0	0.0	0.0	0.0	0.0	0.0	0.3	0.0	0.0	0.0	0.0
Glauconite grain	0.0	0.0	0.0	0.3	0.0	0.3	0.7	0.0	0.0	0.0	0.3	1.3
Heavy mineral grain	0.0	0.0	0.0	0.0	0.4	0.0	0.3	0.0	0.0	0.7	0.0	0.0
Detrital opaque mineral grain	0.0	0.0	0.3	0.0	0.0	0.0	0.0	0.7	0.0	0.3	0.0	0.3
Collophane	0.0	0.3	0.0	0.3	0.0	0.0	0.0	0.0	0.0	0.0	0.0	0.0
Sponge spicule	0.0	0.0	0.0	0.3	0.0	0.0	0.0	4.3	0.0	0.0	0.3	0.0
Carbonate intraclast	0.0	0.7	0.0	0.0	0.0	0.0	0.0	0.0	0.0	0.0	0.0	0.0
Carbonate pellet	0.0	0.3	0.3	0.0	0.0	0.0	0.0	0.0	0.0	0.0	0.3	0.0
Total	99.9	100.0	99.9	99.8	100.1	99.9	99.9	100.0	99.9	99.9	99.9	99.7
Lithology	sdsW	sdsW	sdsW	sdsP	sdsP	sdsP	sdsP	sdsP	sdsW	sdsW	sdsW	sdsW
Number of grains counted	300	300	300	300	258	300	300	300	300	300	300	300
Counting method	PC	PC	PC	PC	PC	PC	PC	PC	PC	PC	PC	PC

Table B4 (Continued)

Constituent	BGO-9AA-134A	BGO-9AA-134B	BGO-9AA-134C	BGO-9AA-134D	BGO-9AA-135	BGO-9AA-140	BGO-9AA-141A	BGO-9AA-141B	BGO-9AA-144	BGO-9AA-145A	BGO-9AA-145B	BGO-10A-130
Monocrystalline quartz	18.4	12.0	12.0	12.7	18.7	5.3	4.0	4.7	15.0	6.6	4.4	32.3
Polycrystalline quartz	0.0	0.0	0.0	0.0	0.0	0.0	0.0	0.0	0.0	0.0	0.0	0.0
Microcline	0.0	0.0	0.0	0.0	0.3	0.0	0.0	0.0	0.0	0.0	0.0	0.7
Untwinned potassium feldspar	0.0	0.0	0.0	0.0	0.0	0.0	0.0	0.0	0.0	0.0	0.0	0.0
Plagioclase	0.3	0.3	0.0	0.3	0.0	0.0	0.0	0.0	0.0	0.0	0.0	0.0
Rock fragment	0.0	0.0	0.0	0.0	0.0	0.0	0.0	0.0	0.0	0.0	0.0	0.0
Interparticle pore	4.0	2.7	0.3	0.7	0.0	10.3	2.0	1.7	0.0	1.7	0.7	12.7
Moldic pore	2.7	0.3	0.3	0.3	8.7	0.3	1.0	0.3	6.3	5.0	0.7	1.0
Intraparticle pore	0.0	0.0	0.0	0.3	0.0	0.3	0.0	0.0	2.0	0.7	0.3	0.7
Vug pore	0.0	0.3	1.7	0.0	4.3	0.0	0.3	0.0	5.0	0.7	0.3	0.7
Intercrystal pore	0.0	0.0	0.0	0.0	0.3	0.0	0.0	0.0	0.0	0.0	0.0	0.0
Terrigenous mud matrix	0.0	0.0	0.0	0.0	0.0	0.0	0.0	0.0	0.0	0.0	0.0	0.0
Micrite	60.2	17.7	20.0	66.7	18.7	28.0	47.7	60.3	14.3	47.0	23.7	28.3
Microspar	4.0	53.3	49.3	7.3	37.7	37.3	24.3	15.7	0.0	2.7	20.0	0.3
Sparry calcite cement & replacement	0.0	2.3	2.7	0.3	1.3	1.7	7.0	5.3	0.0	12.0	29.7	0.0
Muscovite	0.0	0.0	0.0	0.0	0.0	0.0	0.0	0.0	0.3	0.0	0.0	0.0
Authigenic pyrite	0.0	0.7	0.3	0.0	0.0	0.0	1.3	0.0	0.0	0.0	0.0	1.7
Authigenic glauconite cement	0.0	0.0	0.0	0.0	0.3	0.0	1.0	0.0	0.0	0.7	1.0	1.3
Chalcedony / chert cement & replacement	0.0	0.0	0.0	0.0	0.3	0.0	0.0	0.0	0.0	0.0	0.0	0.0
Opal cement & replacement	0.0	0.0	0.3	0.0	0.0	0.0	0.0	0.0	42.0	0.0	0.0	0.0
Foraminifer	0.3	1.0	0.3	1.7	0.0	1.3	1.7	1.0	3.3	0.7	2.0	2.0
Mollusk	0.0	1.3	3.7	0.0	0.7	0.3	1.0	0.7	4.7	7.3	2.0	1.3
Fragmented skeletal debris	5.4	2.7	2.3	5.7	2.3	7.3	2.7	6.0	3.3	0.0	2.0	5.3
Echinoderm	2.3	1.3	3.0	2.0	1.3	3.7	2.0	1.3	2.0	4.0	4.0	10.0
Bryozoan	0.0	0.3	0.0	0.0	0.0	0.0	0.3	0.0	0.0	1.7	0.0	0.0
Pelecypod	2.0	0.0	2.0	1.0	3.0	1.7	2.3	1.3	0.3	6.7	5.0	0.0
Gastropod	0.0	0.0	0.0	0.0	0.0	0.0	0.0	0.7	0.0	0.0	0.7	0.0
Sparry calcite-filled pelecypod mold	0.0	0.0	0.0	0.0	0.0	0.0	0.0	0.0	0.0	0.0	1.0	0.0
Micritized carbonate grain	0.0	0.3	0.0	0.0	0.0	0.0	0.0	0.0	0.0	0.0	0.3	1.7
Glauconite grain	0.3	0.0	0.3	0.0	1.0	1.7	0.3	0.0	0.7	1.7	2.3	0.0
Heavy mineral grain	0.0	0.7	0.0	0.3	0.3	0.0	0.0	0.0	0.3	0.0	0.0	0.0
Detrital opaque mineral grain	0.0	0.3	1.0	0.0	0.0	0.3	0.0	0.0	0.0	0.0	0.0	0.0
Collophane	0.0	0.0	0.0	0.0	0.0	0.0	0.0	0.0	0.3	0.0	0.0	0.0
Sponge spicule	0.0	0.0	0.0	0.0	0.0	0.0	0.0	0.0	0.0	0.0	0.0	0.0
Carbonate intraclast	0.0	2.3	0.0	0.7	0.3	0.3	0.0	1.0	0.0	0.7	0.0	0.0
Carbonate pellet	0.0	0.0	0.3	0.0	0.3	0.0	1.0	0.0	0.0	0.3	0.0	0.0
Total	99.9	99.8	99.8	100.0	99.8	99.8	99.9	100.0	99.8	100.2	100.1	100.0
Lithology	sdsW	sdsR	sdsR	sdsW	sdsW	sW	sW	sW	sdsM	sW	sW	sdsW
Number of grains counted	300	300	300	300	300	300	300	300	300	300	300	300
Counting method	PC	PC	PC	PC	PC	PC	PC	PC	PC	PC	PC	PC

Table B4 (Continued)

Constituent	BGO-10A-132	BGO-10A-136	BGO-10A-144	BGO-10A-147	BGO-10A-161	BGO-10A-163	BGO-14A-122	BGO-14A-126	BGO-14A-126Q	BGO-14A-133	BGO-14A-148	BGO-14A-156
Monocrystalline quartz	27.0	34.0	24.7	18.4	6.0	2.6	9.0	39.3	23.3	34.7	39.3	41.3
Polycrystalline quartz	0.3	0.3	0.0	0.0	0.0	0.0	0.0	0.0	0.0	0.0	0.0	0.3
Microcline	0.0	0.0	0.0	0.0	0.0	0.0	0.0	0.3	0.0	0.0	0.0	0.3
Untwinned potassium feldspar	0.0	0.0	0.0	0.0	0.0	0.0	0.0	0.3	0.0	0.0	0.0	0.0
Plagioclase	0.0	0.0	0.0	0.0	0.0	0.0	0.0	0.0	0.0	0.0	0.0	0.0
Rock fragment	0.0	0.0	0.0	0.0	0.0	0.0	0.0	0.0	0.0	0.0	0.0	0.0
Interparticle pore	9.7	4.3	0.3	6.7	2.7	0.3	0.0	0.0	0.0	0.3	2.7	5.0
Moldic pore	12.3	1.3	1.0	0.3	5.3	4.3	15.0	0.0	0.3	0.0	1.7	4.0
Intraparticle pore	0.3	0.0	0.0	1.0	1.0	0.3	0.0	0.0	0.0	0.0	0.0	0.0
Vug pore	0.7	0.0	2.3	0.0	0.7	0.0	0.0	0.0	1.3	0.0	0.0	0.0
Intercrystal pore	0.0	5.0	0.0	8.7	1.0	2.3	0.3	0.0	0.0	0.0	0.0	0.0
Terrigenous mud matrix	0.0	0.0	39.5	0.0	0.0	0.0	0.0	0.0	0.0	0.0	0.0	0.0
Micrite	31.7	4.7	3.5	3.3	43.7	39.3	4.0	52.3	36.7	44.7	24.0	34.3
Microspar	0.0	33.3	0.3	24.7	20.7	13.0	3.3	1.3	22.7	14.0	19.3	0.0
Sparry calcite cement & replacement	0.0	0.0	0.3	2.3	1.7	19.0	55.0	0.0	12.7	0.0	1.0	0.0
Muscovite	0.0	0.0	0.0	0.0	0.0	0.0	0.0	0.0	0.0	0.0	0.0	0.0
Authigenic pyrite	1.0	0.7	0.0	0.0	1.7	1.0	0.0	0.0	0.0	0.0	0.3	0.0
Authigenic glauconite cement	0.3	1.7	0.0	0.3	1.0	2.0	3.0	1.3	0.0	1.0	1.0	1.3
Chalcedony / chert cement & replacement	0.0	0.0	2.7	0.0	0.0	0.7	0.0	0.0	0.0	0.0	0.0	0.0
Opal cement & replacement	0.0	0.0	18.0	0.0	0.0	0.0	0.0	0.0	0.0	0.3	0.0	0.0
Foraminifer	2.3	1.3	1.7	1.7	1.7	2.0	0.0	0.0	0.3	1.7	0.7	0.7
Mollusk	3.0	2.3	0.3	1.7	3.0	3.3	0.0	0.3	0.0	1.3	1.3	3.7
Fragmented skeletal debris	4.7	2.3	1.3	2.3	3.7	0.7	0.3	3.7	0.7	0.3	2.0	4.3
Echinoderm	4.7	5.3	2.0	21.3	1.7	4.0	4.3	0.3	2.0	0.0	0.0	3.0
Bryozoan	0.3	0.0	0.3	0.0	0.7	0.0	0.0	0.0	0.0	0.0	4.7	0.0
Pelecypod	0.0	1.7	0.0	0.0	1.3	2.0	1.7	0.0	0.0	0.0	0.0	0.0
Gastropod	0.0	0.0	0.0	0.0	0.0	0.0	0.0	0.0	0.0	0.0	0.0	0.0
Sparry calcite-filled pelecypod mold	0.0	0.0	0.0	0.0	0.0	0.0	0.0	0.0	0.0	0.0	0.0	0.0
Micritized carbonate grain	1.3	0.7	0.0	7.3	2.3	3.0	4.0	0.7	0.0	1.3	0.0	1.7
Glauconite grain	0.0	1.0	0.0	0.0	0.0	0.0	0.0	0.0	0.0	0.0	1.7	0.0
Heavy mineral grain	0.0	0.0	0.0	0.0	0.0	0.0	0.0	0.0	0.0	0.3	0.0	0.0
Detrital opaque mineral grain	0.0	0.0	0.0	0.0	0.3	0.0	0.0	0.0	0.0	0.0	0.3	0.0
Collophane	0.3	0.0	0.0	0.0	0.0	0.0	0.0	0.0	0.0	0.0	0.0	0.0
Sponge spicule	0.0	0.0	1.7	0.0	0.0	0.0	0.0	0.0	0.0	0.0	0.0	0.0
Carbonate intraclast	0.0	0.0	0.0	0.0	0.0	0.0	0.0	0.0	0.0	0.0	0.0	0.0
Carbonate pellet	0.0	0.0	0.0	0.0	0.0	0.0	0.0	0.0	0.0	0.0	0.0	0.0
Total	99.9	99.9	99.9	100.0	100.2	99.8	99.9	99.8	100.0	99.9	100.0	99.9
Lithology	sdsW	sdsW	sdsM	sdsG	sW	sW	sdsR	sdIM	sdIM	sdIM	sdsW	sdsW
Number of grains counted	300	300	300	300	300	300	300	300	300	300	300	300
Counting method	PC	PC	PC	PC	PC	PC	PC	PC	PC	PC	PC	PC

Table B4 (Continued)

Constituent	BGO-14A-160	BGO-25A-119	BGO-29A-126	BGX-2B-122	BGX-2B-123	BGX-2B-124	BGX-2B-131	BGX-4A-126	BGX-4A-127	BGX-4A-128	BGX-4A-132	BGX-4A-135
Monocrystalline quartz	29.7	21.0	55.4	48.7	19.4	5.0	14.0	39.6	60.3	39.7	23.0	30.6
Polycrystalline quartz	0.0	0.0	0.0	0.3	0.5	0.0	0.0	0.0	1.6	0.6	0.0	0.3
Microcline	0.0	0.0	0.0	0.0	0.0	0.0	0.0	0.3	0.0	0.7	0.3	0.0
Untwinned potassium feldspar	0.0	0.0	0.0	0.0	0.0	0.0	0.0	0.3	0.0	0.0	0.0	0.0
Plagioclase	0.0	0.0	0.0	0.0	0.0	0.0	0.0	0.0	0.0	0.0	0.0	0.0
Rock fragment	0.0	0.0	0.0	0.0	0.0	0.0	0.0	0.0	0.0	0.0	0.0	0.0
Interparticle pore	0.7	0.0	0.0	n/a	0.0	0.0	0.0	0.0	n/a	1.7	1.0	n/a
Moldic pore	1.7	2.0	0.0	n/a	0.0	0.0	6.0	0.0	n/a	2.7	4.7	n/a
Intraparticle pore	0.3	0.0	0.0	n/a	0.0	0.0	0.0	0.0	n/a	0.3	0.0	n/a
Vug pore	0.0	15.0	1.0	n/a	0.0	0.0	0.0	0.0	n/a	3.0	0.0	n/a
Intercrystal pore	2.7	0.0	0.0	n/a	1.1	0.0	0.0	0.0	n/a	6.7	0.3	n/a
Terrigenous mud matrix	0.0	0.0	0.0	50.0	1.1	0.0	0.0	0.0	37.7	0.0	0.0	0.0
Micrite	1.7	37.0	0.0	0.3	0.0	1.0	0.0	0.0	0.0	28.3	24.0	43.0
Microspar	11.7	10.0	0.0	0.0	7.5	64.0	34.0	1.3	0.0	0.3	29.7	0.3
Sparry calcite cement & replacement	34.7	9.0	0.0	0.0	60.2	19.0	20.0	52.0	0.0	1.0	0.0	0.0
Muscovite	0.0	0.0	0.0	0.0	0.0	0.0	0.0	0.0	0.0	0.3	0.0	0.0
Authigenic pyrite	0.0	0.0	0.0	0.0	0.0	0.0	0.0	0.0	0.0	0.0	0.0	0.0
Authigenic glauconite cement	1.3	0.0	0.0	0.0	0.0	0.0	0.0	1.3	0.0	0.7	3.0	5.0
Chalcedony / chert cement & replacement	0.3	0.0	0.0	0.0	0.0	0.0	18.0	0.0	0.0	0.0	0.0	0.0
Opal cement & replacement	0.0	0.0	43.7	0.0	0.0	0.0	2.0	0.0	0.0	0.0	0.0	0.0
Foraminifer	2.0	0.0	0.0	0.0	0.0	0.0	0.0	0.0	0.0	2.0	1.7	3.0
Mollusk	2.0	0.0	0.0	0.0	0.5	0.0	0.0	0.3	0.0	3.3	1.7	2.3
Fragmented skeletal debris	1.7	1.0	0.0	0.0	0.5	0.0	0.0	3.7	0.0	5.0	2.7	4.7
Echinoderm	6.0	3.0	0.0	0.0	0.5	0.0	0.0	0.3	0.0	2.7	4.0	6.0
Bryozoan	0.0	0.0	0.0	0.0	0.0	0.0	0.0	0.0	0.0	0.0	0.0	0.0
Pelecypod	0.7	2.0	0.0	0.0	8.6	11.0	6.0	0.0	0.0	0.3	1.7	2.3
Gastropod	0.0	0.0	0.0	0.0	0.0	0.0	0.0	0.0	0.0	0.0	0.0	0.0
Sparry calcite-filled pelecypod mold	0.0	0.0	0.0	0.0	0.0	0.0	0.0	0.0	0.0	0.0	0.3	0.0
Micritized carbonate grain	3.0	0.0	0.0	0.0	0.0	0.0	0.0	0.7	0.0	0.3	2.0	2.3
Glauconite grain	0.0	0.0	0.0	0.0	0.0	0.0	0.0	0.0	0.0	0.3	0.0	0.0
Heavy mineral grain	0.0	0.0	0.0	0.7	0.0	0.0	0.0	0.0	0.3	0.0	0.0	0.0
Detrital opaque mineral grain	0.0	0.0	0.0	0.0	0.0	0.0	0.0	0.0	0.0	0.0	0.0	0.0
Collophane	0.0	0.0	0.0	0.0	0.0	0.0	0.0	0.0	0.0	0.0	0.0	0.0
Sponge spicule	0.0	0.0	0.0	0.0	0.0	0.0	0.0	0.0	0.0	0.0	0.0	0.0
Carbonate intraclast	0.0	0.0	0.0	0.0	0.0	0.0	0.0	0.0	0.0	0.0	0.0	0.0
Carbonate pellet	0.0	0.0	0.0	0.0	0.0	0.0	0.0	0.0	0.0	0.0	0.0	0.0
Total	100.2	100.0	100.1	100.0	99.9	100.0	100.0	99.8	99.9	99.9	100.1	99.8
Lithology	sdsW	sdsW	ocS	stM	sdsR	sdsR	sdsR	sdsR	mS	sdsW	sdsW	sdsW
Number of grains counted	300	100	300	300	186	100	50	300	300	300	300	300
Counting method	PC	PC	PC	L	PC	PC	PC	PC	L	PC	PC	L

Table B4 (Continued)

Constituent	BGX-4A-140	BGX-4A-141	BGX-4A-142	BGX-4A-144	BGX-4A-146	BGX-4A-146A	BGX-4A-146B	BGX-4A-147	BGX-4A-148	BGX-4A-148Q	BGX-4A-149	BGX-4A-150
Monocrystalline quartz	17.0	35.0	21.4	30.3	22.3	22.6	26.3	15.3	39.6	12.0	11.7	13.0
Polycrystalline quartz	0.0	0.3	0.0	0.3	0.0	0.0	0.3	0.0	0.0	0.0	0.0	0.0
Microcline	0.0	0.0	0.3	0.7	0.0	0.0	0.0	0.0	0.0	0.0	0.0	0.0
Untwinned potassium feldspar	0.0	0.0	0.0	0.0	0.0	0.0	0.3	0.0	0.0	0.0	0.0	0.0
Plagioclase	0.0	0.0	0.0	0.0	0.0	0.0	0.0	0.0	0.0	0.0	0.0	0.0
Rock fragment	0.0	0.0	0.3	0.0	0.0	0.0	0.0	0.0	0.0	0.0	0.0	0.0
Interparticle pore	0.0	0.7	0.0	0.0	4.7	7.5	0.0	0.0	2.7	1.0	0.0	1.3
Moldic pore	5.0	7.0	4.0	0.0	2.7	14.6	6.7	3.7	1.7	14.7	1.3	19.3
Intraparticle pore	0.3	1.0	0.0	0.0	1.3	0.0	0.0	0.0	0.0	0.3	0.0	0.0
Vug pore	0.0	1.3	0.0	0.0	0.3	0.0	0.0	0.0	0.0	0.0	0.0	0.0
Intercrystal pore	3.0	0.0	0.0	0.3	0.0	0.0	0.0	0.7	0.0	0.7	1.0	0.3
Terrigenous mud matrix	0.0	0.0	0.0	0.0	0.0	0.0	0.0	0.0	0.0	0.0	0.0	0.0
Micrite	15.7	31.0	10.3	0.0	5.7	3.0	0.0	0.0	23.7	40.7	26.0	43.0
Microspar	43.0	0.7	49.7	0.3	28.0	25.1	0.0	58.2	19.3	1.7	38.0	0.0
Sparry calcite cement & replacement	1.7	0.0	0.0	0.0	0.0	0.0	0.3	7.7	1.0	0.0	0.0	0.0
Muscovite	0.0	0.0	0.0	0.0	0.0	0.5	0.0	0.0	0.0	0.0	0.0	0.3
Authigenic pyrite	0.7	0.0	0.0	4.0	1.7	0.5	2.7	1.3	0.3	2.7	0.3	0.3
Authigenic glauconite cement	0.3	2.7	2.3	0.3	1.3	0.5	0.0	0.0	1.0	1.0	2.0	2.0
Chalcedony / chert cement & replacement	0.0	0.0	0.0	0.0	0.0	0.5	17.3	0.0	0.0	0.0	0.0	0.0
Opal cement & replacement	0.0	0.0	0.0	35.0	0.0	0.0	28.3	0.0	0.0	0.0	0.0	0.0
Foraminifer	0.3	0.7	1.7	4.0	3.0	3.5	0.0	0.3	0.7	3.7	3.0	1.0
Mollusk	1.7	4.0	1.0	5.7	3.3	5.0	3.0	0.7	1.3	5.0	4.3	5.7
Fragmented skeletal debris	7.7	5.0	2.7	4.0	8.0	12.6	7.3	4.7	2.0	7.0	5.7	9.0
Echinoderm	2.7	2.7	3.0	2.0	0.7	0.5	0.0	1.7	4.7	3.3	2.7	3.0
Bryozoan	0.0	0.0	0.0	0.0	0.3	0.0	0.0	0.0	0.0	0.3	0.0	0.0
Pelecypod	0.3	6.7	2.7	7.0	15.0	2.0	4.7	4.0	0.0	2.3	3.3	0.7
Gastropod	0.0	0.0	0.0	0.0	0.0	0.0	0.0	0.0	0.0	0.0	0.0	0.0
Sparry calcite-filled pelecypod mold	0.0	0.0	0.0	0.0	0.0	0.0	0.0	0.0	0.0	0.0	0.0	0.0
Micritized carbonate grain	0.3	1.3	0.7	4.0	1.7	1.5	2.0	1.7	1.7	3.0	0.7	1.0
Glauconite grain	0.0	0.0	0.0	0.3	0.0	0.0	0.0	0.0	0.0	0.0	0.0	0.0
Heavy mineral grain	0.0	0.0	0.0	0.7	0.0	0.0	0.3	0.0	0.0	0.3	0.0	0.0
Detrital opaque mineral grain	0.0	0.0	0.0	1.0	0.0	0.0	0.0	0.0	0.3	0.0	0.0	0.0
Collophane	0.3	0.0	0.0	0.0	0.0	0.0	0.0	0.0	0.0	0.3	0.0	0.0
Sponge spicule	0.0	0.0	0.0	0.0	0.0	0.0	0.3	0.0	0.0	0.0	0.0	0.0
Carbonate intraclast	0.0	0.0	0.0	0.0	0.0	0.0	0.0	0.0	0.0	0.0	0.0	0.0
Carbonate pellet	0.0	0.0	0.0	0.0	0.0	0.0	0.0	0.0	0.0	0.0	0.0	0.0
Total	100.0	100.1	100.1	99.9	100.0	99.9	99.8	100.0	100.0	100.0	100.0	99.9
Lithology	sdsR	sdsW	sdsR	sdsM	sdsW	sdsP	sdsM	sdsR	sdsW	sdsW	sdsW	sdsW
Number of grains counted	300	300	300	300	300	199	300	299	300	300	300	300
Counting method	PC	PC	PC	PC	PC	PC	PC	PC	PC	PC	PC	PC

Table B4 (Continued)

Constituent	BGX-4A-151	BGX-9A-139	FSB-100A-140	FSB-100A-151	FSB-114A-109	FSB-116C-86	HMD-1C-114	HMD-1C-117	HMD-1C-121	HMD-3C-93	HPC-1-138	HPC-1-144
Monocrystalline quartz	12.4	6.0	45.3	25.3	8.6	16.7	8.0	19.3	12.7	4.4	35.4	33.3
Polycrystalline quartz	0.0	0.0	0.0	0.0	0.0	0.0	0.0	0.0	0.0	0.0	0.0	0.0
Microcline	0.0	2.0	0.0	0.0	0.0	0.0	0.0	0.0	0.0	0.0	0.7	0.3
Untwinned potassium feldspar	0.0	0.0	0.3	0.0	0.0	0.0	0.0	0.0	0.0	0.0	0.3	0.0
Plagioclase	0.0	0.0	0.0	0.0	0.0	0.0	0.0	0.3	0.0	0.0	0.0	0.0
Rock fragment	0.0	0.0	0.0	0.0	0.0	0.0	0.0	0.0	0.0	0.0	0.0	0.0
Interparticle pore	4.3	0.0	14.3	2.3	0.0	0.0	1.0	0.0	0.0	0.7	n/a	n/a
Moldic pore	19.7	4.0	0.0	0.0	0.0	0.7	1.0	0.7	0.3	0.3	n/a	n/a
Intraparticle pore	1.0	0.0	0.0	0.0	0.0	0.0	0.0	0.7	0.0	0.0	n/a	n/a
Vug pore	1.7	20.0	0.0	1.3	11.7	10.0	4.0	15.7	1.0	0.0	n/a	n/a
Intercrystal pore	0.0	0.0	0.0	0.0	1.0	0.7	0.0	0.0	0.3	0.0	n/a	n/a
Terrigenous mud matrix	0.0	0.0	0.0	0.0	0.3	0.0	0.0	0.0	0.0	0.0	62.3	65.0
Micrite	39.7	0.0	31.7	13.0	13.4	28.0	52.0	21.0	43.3	9.3	0.0	0.0
Microspar	0.0	0.0	1.7	47.0	60.3	32.0	13.0	1.0	19.0	54.0	0.0	0.0
Sparry calcite cement & replacement	0.0	0.0	1.0	3.7	0.0	3.7	4.0	0.3	10.3	28.0	0.0	0.0
Muscovite	0.0	0.0	0.0	0.0	0.7	0.0	0.0	0.3	0.0	0.0	0.0	0.0
Authigenic pyrite	0.3	0.0	0.0	0.0	0.0	0.0	0.0	0.0	0.0	0.0	0.7	0.0
Authigenic glauconite cement	2.7	0.0	0.0	0.0	0.3	0.0	2.0	0.0	0.0	0.0	0.0	0.0
Chalcedony / chert cement & replacement	0.0	10.0	0.0	0.0	0.0	0.0	0.0	0.0	0.0	0.0	0.0	0.0
Opal cement & replacement	0.0	58.0	0.0	0.0	0.0	0.0	0.0	27.3	0.0	0.0	0.0	0.0
Foraminifer	2.7	0.0	0.0	0.3	0.0	0.3	2.0	0.7	1.3	0.0	0.0	0.0
Mollusk	4.7	0.0	0.0	0.3	0.0	0.0	0.0	0.0	0.0	0.0	0.0	0.0
Fragmented skeletal debris	6.3	0.0	0.7	0.0	0.0	0.7	3.0	9.7	3.0	0.3	0.0	0.0
Echinoderm	2.7	0.0	4.3	3.7	1.4	2.0	5.0	2.0	1.0	0.0	0.0	0.0
Bryozoan	0.0	0.0	0.0	0.0	0.0	0.0	0.0	0.0	0.0	0.0	0.0	0.0
Pelecypod	1.3	0.0	0.0	3.0	0.7	5.3	4.0	0.7	6.3	3.0	0.0	0.0
Gastropod	0.0	0.0	0.0	0.0	0.3	0.0	0.0	0.0	0.0	0.0	0.0	0.0
Sparry calcite-filled pelecypod mold	0.0	0.0	0.0	0.0	0.0	0.0	0.0	0.0	0.0	0.0	0.0	0.0
Micritized carbonate grain	0.3	0.0	0.0	0.0	0.0	0.0	0.0	0.0	0.0	0.0	0.0	0.0
Glauconite grain	0.0	0.0	0.0	0.0	1.0	0.0	0.0	0.0	1.0	0.0	0.0	0.0
Heavy mineral grain	0.0	0.0	0.3	0.0	0.0	0.0	0.0	0.0	0.0	0.0	0.7	0.7
Detrital opaque mineral grain	0.3	0.0	0.3	0.0	0.0	0.0	0.0	0.3	0.3	0.0	0.0	0.7
Collophane	0.0	0.0	0.0	0.0	0.0	0.0	0.0	0.0	0.0	0.0	0.0	0.0
Sponge spicule	0.0	0.0	0.0	0.0	0.0	0.0	1.0	0.0	0.0	0.0	0.0	0.0
Carbonate intraclast	0.0	0.0	0.0	0.0	0.0	0.0	0.0	0.0	0.0	0.0	0.0	0.0
Carbonate pellet	0.0	0.0	0.0	0.0	0.0	0.0	0.0	0.0	0.0	0.0	0.0	0.0
Total	100.1	100.0	99.9	99.9	99.7	100.1	100.0	100.0	99.8	100.0	100.1	100.0
Lithology	sdsW	sM	cS	sdR	sdR	sdsW	sW	sdsM	sdsW	R	stM	stM
Number of grains counted	300	50	300	300	290	300	100	300	300	300	300	300
Counting method	PC	PC	PC	PC	PC	PC	PC	PC	PC	PC	L	L

Table B4 (Continued)

Constituent	HPC-1-167	HPT-2A-105	HPT-2A-108	HPT-2A-113	HPT-2A-123	HPT-2A-126	HPT-2A-129	HSB-118-103	HSB-122A-138	HSB-123A-117	HSB-123A-133	HSB-140-100
Monocrystalline quartz	51.4	16.4	21.3	60.4	25.6	15.3	5.3	39.0	21.7	19.4	14.0	12.4
Polycrystalline quartz	0.0	0.0	0.0	0.3	0.3	0.0	0.0	0.0	0.0	0.3	0.0	0.0
Microcline	0.3	0.0	0.0	0.3	0.0	0.0	0.0	0.0	0.0	0.0	0.0	0.0
Untwinned potassium feldspar	0.3	0.0	0.0	0.0	0.0	0.0	0.0	0.0	0.0	0.0	0.0	0.0
Plagioclase	0.3	0.0	0.0	0.0	0.0	0.3	0.0	0.0	0.0	0.0	0.0	0.0
Rock fragment	0.0	0.0	0.0	0.0	0.0	0.0	0.0	0.0	0.0	0.0	0.0	0.0
Interparticle pore	21.0	0.0	0.3	n/a	0.0	0.0	0.0	2.0	4.7	0.0	0.0	0.0
Moldic pore	0.0	2.7	4.0	n/a	8.3	1.0	1.3	0.0	9.3	1.0	0.0	0.3
Intraparticle pore	0.0	0.0	0.0	n/a	0.0	0.7	0.0	0.0	0.0	0.0	0.0	0.0
Vug pore	0.0	0.0	0.3	n/a	0.6	0.0	0.0	0.0	2.0	7.7	14.0	6.4
Intercrystal pore	0.0	3.3	7.3	n/a	6.0	3.7	0.7	1.0	4.3	0.0	0.0	0.0
Terrigenous mud matrix	20.3	0.0	0.0	31.7	0.0	0.0	0.0	0.0	0.0	0.0	0.3	0.0
Micrite	2.3	1.7	2.3	0.0	15.7	0.0	0.7	43.0	44.0	26.0	36.0	63.5
Microspar	0.0	3.3	3.0	0.0	29.7	65.3	86.0	3.0	1.0	35.7	25.3	4.3
Sparry calcite cement & replacement	0.0	70.7	56.3	0.0	1.3	2.3	0.7	0.3	0.0	1.0	1.0	0.0
Muscovite	0.0	0.0	0.0	0.3	0.0	0.0	0.0	0.0	0.0	0.0	0.0	0.0
Authigenic pyrite	3.7	0.0	0.0	5.3	0.0	0.3	0.3	0.0	0.0	0.0	0.0	0.0
Authigenic glauconite cement	0.0	0.0	0.0	0.0	1.7	1.0	0.0	1.0	0.3	0.0	0.0	0.0
Chalcedony / chert cement & replacement	0.0	0.0	0.0	0.0	0.0	0.0	0.0	0.0	0.0	0.0	0.0	0.0
Opal cement & replacement	0.0	0.0	0.0	0.0	0.0	0.0	0.0	0.0	0.0	0.0	0.0	0.0
Foraminifer	0.0	0.3	0.0	0.0	1.7	0.7	0.7	0.0	0.3	0.0	0.7	0.0
Mollusk	0.0	0.3	1.7	0.0	1.0	1.0	0.3	2.0	3.3	0.0	0.3	0.3
Fragmented skeletal debris	0.0	0.0	1.0	0.0	0.3	1.3	0.0	5.0	1.7	0.0	0.3	0.3
Echinoderm	0.0	0.0	0.0	0.0	5.7	2.3	2.0	2.7	3.0	1.3	2.0	3.7
Bryozoan	0.0	0.0	0.0	0.0	0.0	0.0	0.0	0.0	0.0	0.0	0.0	0.0
Pelecypod	0.0	0.3	0.0	0.0	0.0	0.0	0.0	0.3	3.3	7.7	6.0	8.7
Gastropod	0.0	0.0	0.0	0.0	0.0	0.0	0.0	0.0	0.0	0.0	0.0	0.0
Sparry calcite-filled pelecypod mold	0.0	0.0	0.0	0.0	0.0	0.0	0.0	0.0	0.0	0.0	0.0	0.0
Micritized carbonate grain	0.0	1.0	2.3	0.0	1.3	4.0	2.0	0.7	1.0	0.0	0.0	0.0
Glauconite grain	0.0	0.0	0.0	0.7	0.3	0.3	0.0	0.0	0.0	0.0	0.0	0.0
Heavy mineral grain	0.0	0.0	0.0	0.3	0.0	0.0	0.0	0.0	0.0	0.0	0.0	0.0
Detrital opaque mineral grain	0.0	0.0	0.0	0.7	0.0	0.3	0.0	0.0	0.0	0.0	0.0	0.0
Collophane	0.0	0.0	0.0	0.0	0.3	0.0	0.0	0.0	0.0	0.0	0.0	0.0
Sponge spicule	0.0	0.0	0.0	0.0	0.0	0.0	0.0	0.0	0.0	0.0	0.0	0.0
Carbonate intraclast	0.3	0.0	0.0	0.0	0.0	0.0	0.0	0.0	0.0	0.0	0.0	0.0
Carbonate pellet	0.0	0.0	0.0	0.0	0.0	0.0	0.0	0.0	0.0	0.0	0.0	0.0
Total	99.9	100.0	99.8	100.0	99.8	99.8	100.0	100.0	99.9	100.1	99.9	99.9
Lithology	mS	sdR	sdR	mS	sdsW	sdsR	R	sdsW	sdsW	sdsW	sdsW	sdsW
Number of grains counted	300	300	300	300	300	300	300	300	300	300	300	300
Counting method	PC	PC	PC	L	PC	PC	PC	PC	PC	PC	PC	PC

Table B4 (Continued)

Constituent	HSB-140-115	HSB-TB-112	HSB-TB-118	HSB-TB-118Q	HSB-TB-123	HSB-TB-128	HSB-TB-134	HSB-TB-143	HSB-TB-144	HSB-TB-149	HSB-TB-152A	HSB-TB-152B
Monocrystalline quartz	23.3	42.7	40.0	29.7	28.0	21.7	22.0	46.0	22.6	17.6	23.7	10.0
Polycrystalline quartz	0.0	0.0	0.0	0.0	0.3	0.3	0.0	0.0	0.0	0.3	0.0	0.0
Microcline	0.3	0.0	0.3	0.0	0.3	0.0	0.0	0.0	0.0	0.0	0.0	0.0
Untwinned potassium feldspar	0.0	0.3	0.0	0.0	0.3	0.0	0.0	0.0	0.0	0.0	0.0	0.0
Plagioclase	0.0	0.0	0.0	0.0	0.0	0.0	0.0	0.0	0.0	0.0	0.0	0.0
Rock fragment	0.0	0.0	0.0	0.0	0.0	0.0	0.0	0.0	0.0	0.0	0.0	0.0
Interparticle pore	0.3	10.0	1.3	0.0	0.3	4.0	2.7	n/a	n/a	4.7	1.3	7.7
Moldic pore	1.0	0.3	13.0	0.7	5.0	5.3	6.3	n/a	n/a	9.7	5.3	2.7
Intraparticle pore	0.0	0.0	0.0	0.0	0.0	0.0	0.3	n/a	n/a	0.3	1.0	1.7
Vug pore	2.7	0.0	1.3	8.7	0.0	0.7	1.0	n/a	n/a	2.0	0.0	0.0
Intercrystal pore	0.0	0.0	1.7	0.0	3.3	0.0	0.0	n/a	n/a	0.0	0.0	0.0
Terrigenous mud matrix	0.0	0.3	0.0	0.0	0.0	0.0	0.0	41.3	0.0	0.0	0.0	36.7
Micrite	0.0	34.0	23.0	37.3	42.7	44.0	50.6	5.0	40.1	38.7	48.3	0.3
Microspar	0.0	3.0	9.3	19.3	8.3	9.3	0.0	0.0	1.0	0.0	0.0	0.3
Sparry calcite cement & replacement	0.0	0.0	0.0	0.0	1.7	0.0	0.0	0.0	0.0	0.0	0.0	0.0
Muscovite	0.0	0.0	0.0	0.0	0.0	0.0	0.0	0.0	0.0	0.0	0.0	0.0
Authigenic pyrite	0.0	0.0	0.0	0.0	0.7	0.7	0.0	0.0	0.7	1.0	0.3	0.0
Authigenic glauconite cement	0.0	0.0	0.0	0.0	1.0	0.0	0.7	2.3	14.4	0.0	1.3	6.0
Chalcedony / chert cement & replacement	4.0	0.0	0.0	0.0	0.3	0.0	0.0	0.0	0.0	0.0	0.0	0.0
Opal cement & replacement	68.3	0.0	0.0	0.0	0.0	0.0	0.0	0.0	0.0	0.0	0.0	0.0
Foraminifer	0.0	0.3	0.3	0.0	0.0	0.7	0.7	0.0	1.4	9.7	7.0	1.7
Mollusk	0.0	1.3	1.3	0.3	0.3	3.0	7.0	0.0	4.8	0.3	0.0	3.3
Fragmented skeletal debris	0.0	0.7	0.3	0.3	0.3	4.7	5.0	0.7	5.1	9.3	10.3	4.0
Echinoderm	0.0	2.7	5.3	3.0	5.7	3.3	1.0	0.0	1.4	2.0	0.0	0.3
Bryozoan	0.0	0.0	0.0	0.0	0.0	0.0	0.0	0.0	0.0	0.0	0.0	0.0
Pelecypod	0.0	0.3	1.3	0.7	0.0	0.0	0.0	0.0	0.3	0.0	0.0	21.0
Gastropod	0.0	0.0	0.0	0.0	0.0	0.0	0.0	0.0	0.0	0.0	0.0	0.0
Sparry calcite-filled pelecypod mold	0.0	0.0	0.0	0.0	0.0	0.0	0.0	0.0	0.0	0.0	0.0	0.0
Micritized carbonate grain	0.0	3.3	1.0	0.0	1.3	1.3	1.7	0.7	5.8	1.3	0.3	1.3
Glauconite grain	0.0	0.3	0.3	0.0	0.0	0.7	1.0	2.3	2.1	2.7	0.7	3.0
Heavy mineral grain	0.0	0.0	0.0	0.0	0.0	0.3	0.0	0.7	0.3	0.0	0.0	0.0
Detrital opaque mineral grain	0.0	0.0	0.0	0.0	0.0	0.0	0.0	1.0	0.0	0.0	0.3	0.0
Collophane	0.0	0.3	0.0	0.0	0.0	0.0	0.0	0.0	0.0	0.0	0.0	0.0
Sponge spicule	0.0	0.0	0.0	0.0	0.0	0.0	0.0	0.0	0.0	0.0	0.0	0.0
Carbonate intraclast	0.0	0.0	0.0	0.0	0.0	0.0	0.0	0.0	0.0	0.3	0.0	0.0
Carbonate pellet	0.0	0.0	0.0	0.0	0.0	0.0	0.0	0.0	0.0	0.0	0.0	0.0
Total	99.9	99.8	99.7	100.0	99.8	100.0	100.0	100.0	100.0	99.9	99.8	100.0
Lithology	sdsM	sdsW	sdsW	sdIM	sdsW	sdsW	sdsW	stM	sdsW	sdsW	sdsW	sstM
Number of grains counted	300	300	300	300	300	300	300	300	300	300	300	300
Counting method	PC	PC	PC	PC	PC	PC	PC	L	L	PC	PC	PC



Table B4 (Continued)

Constituent	HSB-TB-153	HSB-TB-155	P-18TA-130	P-18TA-148	YSC-2A-109	YSC-4A-114	YSC-4A-121	YSC-5A-99	YSC-5A-106	YSC-5A-111	YSC-5A-116
Monocrystalline quartz	21.7	10.3	30.0	11.0	62.0	0.6	1.0	13.0	35.3	29.6	34.3
Polycrystalline quartz	0.0	0.3	0.0	0.0	0.0	0.0	0.0	0.0	0.0	0.0	0.0
Microcline	0.0	0.0	1.0	0.0	0.3	0.0	0.0	0.3	0.0	0.0	0.3
Untwinned potassium feldspar	0.0	0.0	0.0	0.0	0.0	0.0	0.0	0.0	0.0	0.0	0.0
Plagioclase	0.0	0.0	0.0	0.0	0.0	0.0	0.0	0.0	0.0	0.0	0.0
Rock fragment	0.0	0.0	0.0	0.0	0.0	0.0	0.0	0.0	0.0	0.0	0.0
Interparticle pore	1.6	0.0	0.0	0.0	0.0	0.0	0.0	n/a	0.0	0.0	0.0
Moldic pore	0.0	0.3	0.0	0.0	2.0	0.0	0.0	n/a	2.3	2.7	1.7
Intraparticle pore	0.0	0.3	0.0	0.0	0.3	0.0	0.0	n/a	0.0	0.0	0.0
Vug pore	0.0	0.3	0.0	0.0	13.0	0.0	0.0	n/a	5.7	7.0	15.0
Intercrystal pore	0.0	0.3	0.0	0.0	0.3	0.3	0.3	n/a	0.0	0.0	0.0
Terrigenous mud matrix	0.0	0.0	0.0	0.0	0.0	0.0	0.0	0.0	0.0	0.0	26.7
Micrite	39.0	26.0	52.0	67.0	0.0	0.7	1.7	7.7	3.3	56.7	0.0
Microspar	0.0	0.0	2.0	7.0	0.0	97.6	33.7	62.0	0.0	0.7	0.0
Sparry calcite cement & replacement	0.0	0.0	2.0	0.0	0.0	0.0	63.3	14.3	0.0	0.7	0.3
Muscovite	0.0	0.0	0.0	0.0	0.0	0.0	0.0	0.0	0.0	0.0	0.0
Authigenic pyrite	4.3	5.3	0.0	0.0	0.0	0.0	0.0	0.0	0.0	0.0	0.0
Authigenic glauconite cement	0.0	6.7	0.0	3.0	0.0	0.0	0.0	0.0	0.7	0.0	0.0
Chalcedony / chert cement & replacement	0.0	0.0	0.0	0.0	19.3	0.0	0.0	0.0	0.0	0.0	0.0
Opal cement & replacement	0.0	0.0	0.0	0.0	1.0	0.0	0.0	0.0	50.0	0.0	19.7
Foraminifer	11.7	2.0	0.0	0.0	0.0	0.0	0.0	1.3	0.0	0.3	0.0
Mollusk	2.3	20.7	0.0	0.0	0.0	0.0	0.0	0.0	0.0	0.3	0.0
Fragmented skeletal debris	13.3	7.0	2.0	0.0	0.0	0.7	0.0	0.3	0.3	0.3	0.0
Echinoderm	0.0	0.0	2.0	0.0	0.3	0.0	0.0	0.0	0.7	1.0	1.7
Bryozoan	0.0	0.0	5.0	0.0	0.0	0.0	0.0	0.0	0.0	0.0	0.0
Pelecypod	0.0	11.0	6.0	12.0	0.0	0.0	0.0	0.3	0.0	0.0	0.0
Gastropod	0.0	0.0	0.0	0.0	0.0	0.0	0.0	0.0	0.0	0.0	0.0
Sparry calcite-filled pelecypod mold	0.0	0.0	0.0	0.0	0.0	0.0	0.0	0.0	0.0	0.0	0.0
Micritized carbonate grain	4.0	4.0	0.0	0.0	0.0	0.0	0.0	0.0	0.0	0.3	0.0
Glauconite grain	1.7	4.3	0.0	0.0	0.0	0.0	0.0	0.0	1.0	0.3	0.0
Heavy mineral grain	0.0	0.0	0.0	0.0	0.3	0.0	0.0	0.3	0.0	0.0	0.0
Detrital opaque mineral grain	0.0	1.0	0.0	0.0	0.7	0.0	0.0	0.3	0.3	0.0	0.3
Collophane	0.0	0.0	0.0	0.0	0.3	0.0	0.0	0.0	0.0	0.0	0.0
Sponge spicule	0.3	0.0	0.0	0.0	0.0	0.0	0.0	0.0	0.3	0.0	0.0
Carbonate intraclast	0.0	0.0	0.0	0.0	0.0	0.0	0.0	0.0	0.0	0.0	0.0
Carbonate pellet	0.0	0.0	0.0	0.0	0.0	0.0	0.0	0.0	0.0	0.0	0.0
Total	99.9	99.8	100.0	100.0	99.8	99.9	100.0	99.8	99.9	99.9	100.0
Lithology	sdsW	sdsP	sdsW	sdsW	ccS	R	cS	sdR	sdsM	sdsIM	sdsM
Number of grains counted	300	300	100	100	300	300	300	300	300	300	300
Counting method	PC	PC	PC	PC	PC	PC	PC	L	PC	PC	PC

Table B5. Textural Data for Samples from Aquifer Zone IIA in the General Separations Area, SRS

Parameter	BGX-2B-176	BGX-2B-182	HSB-120A-167	HSB-140-156
Sample depth (feet)	176	182	167	156
Average quartz grain size (mm)	0.003	0.75	0.75	0.38
Maximum quartz grain size (mm)	0.30	5.00	1.75	2.00
Average carbonate allochem grain size (mm)	N/A	N/A	N/A	N/A
Maximum carbonate allochem grain size (mm)	N/A	N/A	N/A	N/A
Average carbonate crystal size (microns)	N/A	N/A	N/A	N/A
Carbonate grain roundness	N/A	N/A	N/A	N/A
Carbonate allochem sorting	N/A	N/A	N/A	N/A
Average quartz grain roundness	SA	SR	SA	SA
Terrigenous sorting	N/A	N/A	MW	MW
Textural maturity	N/A	N/A	SM	SM
Hydrostratigraphic unit	IIA	IIA	IIA	IIA
Lithology	tM	stM	mS	ccS

Table B6. Textural Data for Samples from Confining Unit IIA-IIB in the General Separations Area, SRS

Parameter	BGO-9AA-148	BGO-9AA-150A	BGO-9AA-150B	BGO-9AA-153	BGX-2B-152A	BGX-2B-152B	BGX-2B-155	BGX-2B-156	BGX-2B-161	FSB-115C-118	HMD-1C-125	HPC-1-1-182	HPC-1-1-186	HSB-TB-157
Sample depth (feet)	147.6	149.5	149.5	152.2	151.2	151.2	155.0	156.0	161.0	118.0	125.0	182.0	186.0	157.0
Average quartz grain size (mm)	0.30	0.05	0.30	0.30	0.30	0.20	0.10	0.15	0.75	0.35	0.19	0.005	0.75	0.38
Maximum quartz grain size (mm)	1.75	1.20	4.10	2.25	0.75	0.40	5.00	0.20	6.00	1.80	4.00	0.13	5.00	3.80
Average carbonate allochem grain size (mm)	0.40	N/A	3.00	3.00	N/A	N/A	N/A	N/A	N/A	N/A	1.50	N/A	N/A	N/A
Maximum carbonate allochem grain size (mm)	6.00	6.00	10.00	10.00	N/A	N/A	N/A	N/A	N/A	N/A	9.00	N/A	N/A	N/A
Average carbonate crystal size (microns)	N/A	N/A	N/A	N/A	N/A	N/A	N/A	N/A	N/A	N/A	4	N/A	N/A	N/A
Carbonate grain roundness	SR	R	R	R	N/A	N/A	N/A	N/A	N/A	N/A	SR	N/A	N/A	N/A
Carbonate allochem sorting	P	P	P	P	N/A	N/A	N/A	N/A	N/A	N/A	P	N/A	N/A	N/A
Average quartz grain roundness	SA	SA	SA	SA	A	A	SA	SA	SR	SA	SA	SA	SA	SA
Terrigenous sorting	N/A	N/A	N/A	N/A	N/A	N/A	N/A	N/A	N/A	M	N/A	N/A	P	N/A
Textural maturity	N/A	N/A	N/A	N/A	N/A	N/A	N/A	N/A	N/A	SM	N/A	N/A	SM	N/A
Hydrostratigraphic unit	IIA-B	IIA-B	IIA-B	IIA-B	IIA-B	IIA-B	IIA-B	IIA-B	IIA-B	IIA-B	IIA-B	IIA-B	IIA-B	IIA-B
Lithology	sdsIM	IM	sksM	sksM	sM	sdsM	sdsM	sdsM	stM	ccS	sksM	stM	mS	stM

Table B7. Textural Data for Samples from Aquifer Zone IIB1 in the General Separations Area, SRS

Parameter	BGO-9AA-113	BGO-9AA-119	BGO-9AA-124	BGO-9AA-125A	BGO-9AA-125B	BGO-9AA-127A	BGO-9AA-127B	BGO-9AA-127C	BGO-9AA-128A	BGO-9AA-128B	BGO-9AA-128C	BGO-9AA-132	BGO-9AA-134A	BGO-9AA-134B	BGO-9AA-134C	BGO-9AA-134D	BGO-9AA-135	BGO-9AA-140	BGO-9AA-141A	BGO-9AA-141B
Sample depth (feet)	112.9	118.6	123.3	125.0	125.0	126.2	126.2	126.4	127.2	127.3	127.5	131.2	134.0	134T	134B	134.0	134.6	139.8	140.6	140.7
Average quartz grain size (mm)	0.20	0.20	0.20	0.10	0.10	0.10	0.10	0.20	0.20	0.30	0.30	0.30	0.20	0.40	0.20	0.20	0.40	0.15	0.20	0.10
Maximum quartz grain size (mm)	0.90	0.60	1.25	0.40	0.40	0.60	0.60	0.60	1.75	1.25	1.50	1.50	1.50	1.75	1.50	1.50	1.25	2.10	5.00	1.25
Average carbonate allochem grain size (mm)	0.2	0.01	0.01	0.20	0.25	0.20	0.20	0.15	0.20	0.25	0.20	0.20	0.25	0.30	0.20	0.20	0.75	0.20	0.40	0.15
Maximum carbonate allochem grain size (mm)	6.00	1.25	2.10	1.50	1.50	3.00	3.00	0.30	5.00	3.00	3.00	5.00	2.00	12.00	5.00	2.00	8.00	5.00	1.25	6.00
Average carbonate crystal size (microns)	8	8	N/A	N/A	N/A	N/A	N/A	N/A	8	20	N/A	N/A	8	8	800	8	10	6	6	8
Carbonate grain roundness	SR	R	R	R	R	SR	SR	R	R	R	R	R	SR	SR	SR	SR	R	SR	R	R
Carbonate allochem sorting	P	P	P	P	P	P	P	M	P	P	P	P	P	P	P	P	P	P	P	P
Average quartz grain roundness	SA	SA	SA	SA	SA	SA	SA	SA	SA	SA	SA	SA	SA	SA	SA	SA	SA	SA	SA	SA
Terrigenous sorting	N/A	N/A	N/A	N/A	N/A	N/A	N/A	N/A	N/A	N/A	N/A	N/A	N/A	N/A	N/A	N/A	N/A	N/A	N/A	N/A
Textural maturity	N/A	N/A	N/A	N/A	N/A	N/A	N/A	N/A	N/A	N/A	N/A	N/A	N/A	N/A	N/A	N/A	N/A	N/A	N/A	N/A
Hydrostratigraphic unit	IIB1	IIB1	IIB1	IIB1	IIB1	IIB1	IIB1	IIB1	IIB1	IIB1	IIB1	IIB1	IIB1	IIB1	IIB1	IIB1	IIB1	IIB1	IIB1	IIB1
Lithology	sdsW	sdsW	sdsW	sdsP	sdsP	sdsP	sdsP	sdsP	sdsW	sdsW	sdsW	sdsW	sdsW	sdsC	sdsC	sdsW	sdsW	sW	sW	sW

Table B7. (Continued)

Parameter	BGO-9AA-144	BGO-9AA-145A	BGO-9AA-145B	BGO-10A-130	BGO-10A-132	BGO-10A-136	BGO-10A-144	BGO-10A-147	BGO-10A-161	BGO-10A-163	BGO-14A-122	BGO-14A-126	BGO-14A-133	BGO-14A-148	BGO-14A-156	BGO-14A-160	BGO-25A-119	BGO-29A-126	BGX-2B-122	BGX-2B-123
Sample depth (feet)	144.0	144.8	144.8	130.0	131.0	136.0	144.0	147.0	161.0	163.0	122.0	126.0	133.0	148.0	156.0	159.5	119.0	125.0	122.0	123.0
Average quartz grain size (mm)	0.10	0.20	0.20	0.20	0.30	0.40	0.40	0.20	0.20	0.38	0.40	0.20	0.20	0.38	0.75	0.38	0.40	0.20	0.15	0.20
Maximum quartz grain size (mm)	0.40	0.95	0.80	0.70	0.70	1.50	0.75	0.35	2.00	1.00	2.00	0.50	1.00	3.00	1.00	2.00	1.50	3.50	3.00	1.50
Average carbonate allochem grain size (mm)	0.15	0.40	0.75	0.35	0.39	0.38	0.20	0.20	0.75	1.50	0.38	0.25	0.38	0.80	2.00	1.50	1.25	N/A	N/A	0.25
Maximum carbonate allochem grain size (mm)	8.00	8.50	3.00	3.00	4.00	3.00	0.75	0.50	6.00	5.00	5.00	1.00	4.00	1.50	6.00	4.00	12.00	N/A	N/A	4.50
Average carbonate crystal size (microns)	N/A	60	10	4	4	6	4	10	4	4	100	31	16	16	4	31	8	N/A	N/A	20
Carbonate grain roundness	SR	R	R	R	R	R	R	R	R	R	R	R	R	R	R	R	R	N/A	N/A	R
Carbonate allochem sorting	P	P	P	M	P	M	M	W	P	P	P	M	P	P	P	P	P	N/A	N/A	P
Average quartz grain roundness	SA	SA	SA	SA	SA	SA	SA	SA	SA	SA	SA	SA	SA	SA	SA	SA	SA	SA	A	A
Terrigenous sorting	N/A	N/A	N/A	N/A	N/A	N/A	N/A	N/A	N/A	N/A	N/A	N/A	N/A	N/A	N/A	N/A	N/A	P	N/A	N/A
Textural maturity	N/A	N/A	N/A	N/A	N/A	N/A	N/A	N/A	N/A	N/A	N/A	N/A	N/A	N/A	N/A	N/A	N/A	SM	N/A	N/A
Hydrostratigraphic unit	IIB1	IIB1	IIB1	IIB1	IIB1	IIB1	IIB1	IIB1	IIB1	IIB1	IIB1	IIB1	IIB1	IIB1	IIB1	IIB1	IIB1	IIB1	IIB1	IIB1
Lithology	sdsM	sW	sW	sdsW	sdsW	sdsW	sdsM	sdsG	sW	sW	sdsR	sdsIM	sdsIM	sdsW	sdsW	sdsW	sdsW	ocS	stM	sdsR

Table B7. (Continued)

Parameter	BGX-2B-124	BGX-2B-131	BGX-4A-126	BGX-4A-127	BGX-4A-128	BGX-4A-132	BGX-4A-135	BGX-4A-140	BGX-4A-141	BGX-4A-142	BGX-4A-144	BGX-4A-146	BGX-4A-146A	BGX-4A-146B	BGX-4A-147	BGX-4A-148	BGX-4A-149	BGX-4A-150	BGX-4A-151	BGX-9A-139
Sample depth (feet)	124.0	130.5	126.0	127.0	128.0	131.0	135.0	139.0	141.3	141.3	144.0	145.5	146.0	146.0	147.0	148.0	149.0	150.0	151.0	139.0
Average quartz grain size (mm)	0.10	0.30	0.75	0.75	0.20	0.25	0.19	0.19	0.38	0.38	0.38	0.38	0.19	0.19	0.25	0.13	0.10	0.13	0.10	0.40
Maximum quartz grain size (mm)	1.75	1.25	N/A	1.00	1.00	1.00	0.75	2.00	2.00	2.00	4.00	2.00	0.50	1.00	2.00	1.00	2.00	1.00	3.00	1.10
Average carbonate allochem grain size (mm)	0.22	0.15	N/A	N/A	0.40	0.38	0.40	0.50	0.38	1.00	0.75	1.50	0.20	0.50	0.38	0.38	0.38	0.75	0.50	N/A
Maximum carbonate allochem grain size (mm)	15.00	12.00	N/A	N/A	4.00	2.00	5.00	4.00	2.00	4.00	11.00	8.00	3.50	4.00	10.00	4.00	2.00	4.00	5.00	N/A
Average carbonate crystal size (microns)	8	8	N/A	N/A	8	8	8	16	16	4	8	8	8	6	16	8	16	6	4	N/A
Carbonate grain roundness	R	R	N/A	N/A	R	R	R	R	R	R	R	R	R	R	R	R	R	R	R	N/A
Carbonate allochem sorting	P	P	N/A	N/A	P	P	P	P	P	P	P	P	P	P	P	P	P	P	P	N/A
Average quartz grain roundness	A	A	SA	SA	SA	SA	SA	SR	SA	SA	SA	SA	SA	SR	SA	SA	SA	SA	SA	SA
Terrigenous sorting	N/A	N/A	N/A	N/A	N/A	N/A	N/A	N/A	N/A	N/A	N/A	N/A	N/A	N/A	N/A	N/A	N/A	N/A	N/A	N/A
Textural maturity	N/A	N/A	N/A	N/A	N/A	N/A	N/A	N/A	N/A	N/A	N/A	N/A	N/A	N/A	N/A	N/A	N/A	N/A	N/A	N/A
Hydrostratigraphic unit	IIB1	IIB1	IIB1	IIB1	IIB1	IIB1	IIB1	IIB1	IIB1	IIB1	IIB1	IIB1	IIB1	IIB1	IIB1	IIB1	IIB1	IIB1	IIB1	IIB1
Lithology	sdsR	sdsR	sdsR	mS	sdsW	sdsW	sdsW	sdsR	sdsW	sdsR	sdsM	sdsW	sdsP	sdsM	sdsR	sdsW	sdsW	sdsW	sdsW	sM

Table B7. (Continued)

Parameter	FSB-100A-140	FSB-100A-151	FSB-114A-109	FSB-116C-066	HMD-1C-114	HMD-1C-117	HMD-1C-121	HMD-3C-093	HPC-1-138	HPC-1-144	HPC-1-167	HPT-2A-105	HPT-2A-108	HPT-2A-113	HPT-2A-123	HPT-2A-126	HPT-2A-129	HSB-118-103	HSB-122A-138	HSB-123A-117
Sample depth (feet)	139.3	151.0	109.0	66.0	114.0	117.0	121.0	93.0	138.0	144.0	167.0	105.0	108.0	112.0	123.0	125.0	128.0	103.0	138.0	117.0
Average quartz grain size (mm)	0.20	0.20	0.40	0.20	0.10	0.15	0.20	0.15	0.00	0.00	0.30	0.19	0.19	0.19	0.19	0.19	0.38	0.75	0.75	0.20
Maximum quartz grain size (mm)	1.25	1.75	0.80	1.50	8.00	0.75	3.00	1.50	0.80	1.50	1.50	0.35	0.75	1.75	0.75	0.38	0.75	1.50	2.00	2.50
Average carbonate allochem grain size (mm)	0.01	0.00	N/A	?	0.15	N/A	0.10	N/A	N/A	N/A	N/A	0.19	0.19	N/A	0.28	0.37	0.38	1.50	1.00	0.05
Maximum carbonate allochem grain size (mm)	0.75	2.50	N/A	3.50	9.00	N/A	6.00	3.50	N/A	N/A	N/A	6.00	2.00	N/A	1.00	1.00	2.00	3.00	3.00	12.00
Average carbonate crystal size (microns)	N/A	8	1500	8	N/A	N/A	N/A	15	N/A	N/A	N/A	31	31	N/A	31	8	31	8	8	N/A
Carbonate grain roundness	N/A	R	N/A	R	R	N/A	R	R	N/A	N/A	N/A	R	R	N/A	R	R	R	R	R	R
Carbonate allochem sorting	P	P	N/A	P	P	N/A	P	N/A	N/A	N/A	N/A	M	M	N/A	M	W	M	P	P	P
Average quartz grain roundness	SA	SA	SA	SA	SA	SA	SA	SA	A	SA	SA	SA	SA	SA	SA	SA	SA	SA	SA	SA
Terrigenous sorting	M	N/A	N/A	N/A	N/A	N/A	N/A	N/A	N/A	N/A	N/A	N/A	N/A	P	N/A	N/A	N/A	N/A	N/A	N/A
Textural maturity	I	N/A	N/A	N/A	N/A	N/A	N/A	N/A	N/A	N/A	N/A	N/A	N/A	IM	N/A	N/A	N/A	N/A	N/A	N/A
Hydrostratigraphic unit	IIB1	IIB1	IIB1	IIB1	IIB1	IIB1	IIB1	IIB1	IIB1	IIB1	IIB1	IIB1	IIB1	IIB1	IIB1	IIB1	IIB1	IIB1	IIB1	IIB1
Lithology	cS	sdR	sdR	sdsW	sW	sdsM	sdsW	R	stM	stM	mS	sdR	sdR	mS	sdsW	sdsR	R	sdsW	sdsW	sdsW

Table B7. (Continued)

Parameter	HSB-123A-133	HSB-140-100	HSB-140-115	HSB-TB-112	HSB-TB-118	HSB-TB-123	HSB-TB-128	HSB-TB-134	HSB-TB-143	HSB-TB-144	HSB-TB-149	HSB-TB-152A	HSB-TB-152B	HSB-TB-153	HSB-TB-155	P-18TA-130	P-18TA-148	YSC-2A-109	YSC-4A-114	YSC-4A-121
Sample depth (feet)	133.0	100.0	115.0	112.0	118.0	123.0	128.0	134.0	143.0	143.5	149.0	152.0	152.0	153.0	155.0	130.0	148.0	109.0	114.0	121.0
Average quartz grain size (mm)	0.40	0.30	0.15	0.19	0.19	0.19	0.38	0.38	0.38	0.18	0.06	0.05	0.38	0.10	0.17	0.40	0.30	0.30	0.08	0.10
Maximum quartz grain size (mm)	0.85	1.50	0.75	1.00	0.75	1.00	2.00	2.00	2.00	2.00	0.19	0.25	1.90	0.14	1.00	1.75	3.00	0.90	0.20	0.20
Average carbonate allochem grain size (mm)	0.05	N/A	N/A	0.38	0.38	0.80	0.80	0.38	N/A	0.75	0.19	0.06	0.75	0.10	4.00	N/A	1.25	N/A	N/A	N/A
Maximum carbonate allochem grain size (mm)	9.00	6.00	N/A	4.00	4.00	4.00	4.00	4.00	N/A	13.00	1.00	0.50	1.00	4.00	6.50	12.00	10.00	N/A	N/A	N/A
Average carbonate crystal size (microns)	N/A	N/A	N/A	16	4	16	16	4	N/A	4	4	4	4	4	4	8	8	N/A	50	10
Carbonate grain roundness	R	R	N/A	SR	SR	R	SR	SR	N/A	SR	SR	R	R	SR	SR	R	R	N/A	N/A	N/A
Carbonate allochem sorting	P	P	N/A	P	P	P	P	P	N/A	P	W	W	P	W	M	P	P	N/A	N/A	N/A
Average quartz grain roundness	SA	SA	SA	SA	SA	SA	SA	SA	A	SA	SA	SR	SR	SA	SA	SA	SA	SR	SA	SA
Terrigenous sorting	N/A	N/A	N/A	N/A	N/A	N/A	N/A	N/A	N/A	N/A	N/A	N/A	N/A	N/A	N/A	N/A	N/A	M	N/A	M
Textural maturity	N/A	N/A	N/A	N/A	N/A	N/A	N/A	N/A	N/A	N/A	N/A	N/A	N/A	N/A	N/A	N/A	N/A	SM	N/A	SM
Hydrostratigraphic unit	IIB1	IIB1	IIB1	IIB1	IIB1	IIB1	IIB1	IIB1	IIB1	IIB1	IIB1	IIB1	IIB1	IIB1	IIB1	IIB1	IIB1	IIB1	IIB1	IIB1
Lithology	sdsW	sdsW	sdsM	sdsW	sdsW	sdsW	sdsW	sdsW	stM	sdsW	sdsW	sdsW	sstM	sdsW	sdsP	sdsW	sdsW	ccS	R	cS



Table B7. (Continued)

Parameter	YSC-5A-099	YSC-5A-106	YSC-5A-111	YSC-5A-116
Sample depth (feet)	99.0	105.5	111.0	116.0
Average quartz grain size (mm)	0.20	0.10	0.20	0.20
Maximum quartz grain size (mm)	2.10	1.75	0.75	0.75
Average carbonate allochem grain size (mm)	N/A	N/A	0.01	N/A
Maximum carbonate allochem grain size (mm)	0.75	N/A	0.75	0.90
Average carbonate crystal size (microns)	8	N/A	N/A	N/A
Carbonate grain roundness	R	N/A	N/A	R
Carbonate allochem sorting	N/A	N/A	N/A	P
Average quartz grain roundness	SA	A	SA	SA
Terrigenous sorting	N/A	N/A	N/A	N/A
Textural maturity	N/A	N/A	N/A	N/A
Hydrostratigraphic unit	IIB1	IIB1	IIB1	IIB1
Lithology	sdR	sdsM	sdW	sdsM

Table B8. Acid Insoluble Residue Data for General Separations Area "Calcareous Zone" Samples

Well	Depth (ft)	Hydro Unit	Sampled Interval			Weight (g)			Percent Carbonate
			Sample Designator	Top	Bottom	Initial Sample	Filter Paper	Filter + Residue	
BGO-9AA	104	IIB1	BGO-9AA-104	103.7	104.0	71.34	5.80	76.54	0.8
BGO-9AA	108	IIB1	BGO-9AA-108	107.7	108.0	57.27	5.75	62.82	0.3
BGO-9AA	110	IIB1	BGO-9AA-110	109.7	110.0	55.87	5.74	61.24	0.7
BGO-9AA	111	IIB1	BGO-9AA-111	110.5	110.8	53.45	5.74	57.47	3.2
BGO-9AA	113	IIB1	BGO-9AA-113	112.7	113.0	114.20	5.75	72.76	41.3
BGO-9AA	114	IIB1	BGO-9AA-114	113.7	114.0	123.45	5.80	71.23	47.0
BGO-9AA	115	IIB1	BGO-9AA-115	114.7	115.0	96.76	5.85	66.18	37.6
BGO-9AA	116	IIB1	BGO-9AA-116	115.7	116.0	135.76	5.64	78.41	46.4
BGO-9AA	117	IIB1	BGO-9AA-117	116.5	116.8	125.94	5.69	77.64	42.9
BGO-9AA	118	IIB1	BGO-9AA-118	117.7	118.0	148.83	5.74	96.19	39.2
BGO-9AA	119	IIB1	BGO-9AA-119	118.7	119.0	110.60	5.77	70.61	41.4
BGO-9AA	120	IIB1	BGO-9AA-120	119.7	120.0	112.31	5.71	76.37	37.1
BGO-9AA	121	IIB1	BGO-9AA-121	120.7	121.0	102.26	5.78	72.46	34.8
BGO-9AA	122	IIB1	BGO-9AA-122	121.7	122.0	99.59	5.73	66.27	39.2
BGO-9AA	123	IIB1	BGO-9AA-123	122.7	123.0	107.39	5.72	73.42	37.0
BGO-9AA	124	IIB1	BGO-9AA-124	123.7	124.0	102.08	5.79	68.07	39.0
BGO-9AA	125	IIB1	BGO-9AA-125	124.7	125.0	91.44	5.70	56.96	43.9
BGO-9AA	127	IIB1	BGO-9AA-127	126.0	126.2	61.11	5.75	46.36	33.5
BGO-9AA	128	IIB1	BGO-9AA-128	127.7	128.0	101.89	5.78	61.18	45.6
BGO-9AA	129	IIB1	BGO-9AA-129	128.7	129.0	105.33	5.75	61.06	47.5
BGO-9AA	130	IIB1	BGO-9AA-130	129.7	130.0	105.14	5.70	60.29	48.1
BGO-9AA	132	IIB1	BGO-9AA-132	131.0	131.3	105.54	5.79	56.34	52.1

B-8-1

Table B8. (Continued)

Well	Depth (ft)	Hydro Unit	Sampled Interval			Weight (g)			Percent Carbonate
			Sample Designator	Top	Bottom	Initial Sample	Filter Paper	Filter + Residue	
BGO-9AA	133	IIB1	BGO-9AA-133	132.7	133.0	104.58	4.80	39.84	66.5
BGO-9AA	134	IIB1	BGO-9AA-134	133.7	134.0	123.35	5.79	37.73	74.1
BGO-9AA	135	IIB1	BGO-9AA-135	134.4	134.6	118.53	5.81	39.55	71.5
BGO-9AA	138	IIB1	BGO-9AA-138	137.0	137.3	88.33	4.88	47.04	52.3
BGO-9AA	139	IIB1	BGO-9AA-139	138.7	139.0	147.84	5.66	52.17	68.5
BGO-9AA	140	IIB1	BGO-9AA-140	139.7	140.0	152.53	5.72	48.54	71.9
BGO-9AA	141	IIB1	BGO-9AA-141	140.3	140.6	153.08	4.82	28.09	84.8
BGO-9AA	142	IIB1	BGO-9AA-142	140.8	141.1	152.56	4.81	31.16	82.7
BGO-9AA	143	IIB1	BGO-9AA-143	142.7	143.0	92.19	5.75	68.38	32.1
BGO-9AA	144	IIB1	BGO-9AA-144	143.7	144.0	76.56	5.80	58.04	31.8
BGO-9AA	145	IIB1	BGO-9AA-145	144.5	144.8	189.50	4.82	30.05	86.7
BGO-9AA	148	IIB1	BGO-9AA-148	147.7	148.0	111.24	5.76	93.97	20.7
BGO-9AA	149	IIA-IIB	BGO-9AA-149	148.7	149.0	73.40	5.74	66.34	17.4
BGO-9AA	150	IIA-IIB	BGO-9AA-150	149.3	149.5	81.30	5.74	66.14	25.7
BGO-9AA	151	IIA-IIB	BGO-9AA-152	150.8	151.1	108.08	5.80	68.53	42.0
BGO-9AA	153	IIA-IIB	BGO-9AA-153	152.7	153.0	95.63	5.75	68.65	34.2
BGO-9AA	154	IIA-IIB	BGO-9AA-154	153.7	154.0	126.42	5.75	121.04	8.8
BGO-9AA	155	IIA-IIB	BGO-9AA-155	154.7	155.0	43.44	5.75	47.27	4.4
BGO-9AA	158	IIA-IIB	BGO-9AA-158	157.6	157.8	52.68	5.71	55.67	5.2
BGO-9AA	163	IIA	BGO-9AA-163	162.0	162.3	54.85	5.67	59.29	2.2
BGO-9AA	168	IIA	BGO-9AA-168	167.0	167.3	58.65	5.80	64.11	0.6
FSB-116C	51	IIB1	FSB-116C-51	50.7	51.0	57.75	4.82	62.29	0.5

Table B8. (Continued)

Well	Depth (ft)	Hydro Unit	Sampled Interval			Weight (g)			Percent Carbonate
			Sample Designator	Top	Bottom	Initial Sample	Filter Paper	Filter + Residue	
FSB-116C	52	IIB1	FSB-116C-52	51.7	52.0	57.17	4.82	61.29	1.2
FSB-116C	53	IIB1	FSB-116C-53	52.7	53.0	60.47	4.81	64.28	1.6
FSB-116C	55	IIB1	FSB-116C-55	54.7	55.0	57.04	4.82	61.53	0.6
FSB-116C	56	IIB1	FSB-116C-56	55.7	56.0	56.50	4.80	60.92	0.7
FSB-116C	57	IIB1	FSB-116C-57	56.5	56.7	82.08	4.82	64.15	27.7
FSB-116C	58	IIB1	FSB-116C-58	57.7	58.0	60.98	4.81	40.18	42.0
FSB-116C	61	IIB1	FSB-116C-61	60.7	61.0	103.02	4.82	59.73	46.7
FSB-116C	62	IIB1	FSB-116C-62	61.7	62.0	72.48	4.84	42.90	47.5
FSB-116C	63	IIB1	FSB-116C-63	62.7	63.0	158.34	4.82	97.34	41.6
FSB-116C	64	IIB1	FSB-116C-64	63.1	63.3	89.48	4.82	59.40	39.0
FSB-116C	65	IIB1	FSB-116C-65	64.0	64.3	110.41	4.84	72.98	38.3
FSB-116C	66	IIB1	FSB-116C-66	65.2	65.5	90.13	4.79	35.55	65.9
FSB-116C	68	IIB1	FSB-116C-68	67.7	68.0	58.27	4.80	34.25	49.5
FSB-116C	69	IIB1	FSB-116C-69	68.8	69.0	53.17	4.82	56.34	3.1
FSB-116C	70	IIB1	FSB-116C-70	69.7	70.0	59.61	4.84	63.29	2.0
FSB-116C	71	IIB1	FSB-116C-71	70.7	71.0	63.18	4.83	67.86	0.2
FSB-116C	72	IIB1	FSB-116C-72	71.3	71.5	65.14	4.87	62.31	11.8
FSB-116C	75	IIB1	FSB-116C-75	74.0	74.3	81.37	4.85	83.76	3.0
FSB-116C	77	IIB1	FSB-116C-77	76.7	77.0	76.59	4.91	76.13	7.0
FSB-116C	78	IIB1	FSB-116C-78	77.7	78.0	81.82	4.82	84.60	2.5
FSB-116C	79	IIB1	FSB-116C-79	78.7	79.0	62.01	4.89	65.33	2.5
FSB-116C	80	IIB1	FSB-116C-80	79.7	80.0	74.07	4.82	70.32	11.6

B-8-3

Table B8. (Continued)

Well	Depth (ft)	Hydro Unit	Sampled Interval			Weight (g)			Percent Carbonate
			Sample Designator	Top	Bottom	Initial Sample	Filter Paper	Filter + Residue	
HPT-2A	91	IIB1	HPT-2A-091	90.7	91.0	56.82	4.85	61.12	1.0
HPT-2A	92	IIB1	HPT-2A-092	91.7	92.0	60.11	4.87	64.28	1.2
HPT-2A	93	IIB1	HPT-2A-093	92.7	93.0	71.76	4.86	75.25	1.9
HPT-2A	94	IIB1	HPT-2A-094	93.7	94.0	55.65	4.83	59.72	1.4
HPT-2A	99	IIB1	HPT-2A-099	98.7	99.0	87.38	4.83	88.53	4.2
HPT-2A	100	IIB1	HPT-2A-100	99.7	100.0	67.75	4.78	70.89	2.4
HPT-2A	101	IIB1	HPT-2A-101	100.7	101.0	81.48	4.81	76.18	12.4
HPT-2A	102	IIB1	HPT-2A-102	101.7	102.0	81.18	4.85	71.76	17.6
HPT-2A	103	IIB1	HPT-2A-103	102.2	102.4	64.67	4.83	42.61	41.6
HPT-2A	109	IIB1	HPT-2A-109	108.7	109.0	70.60	4.82	59.55	22.5
HPT-2A	110	IIB1	HPT-2A-110	109.7	110.0	64.17	4.81	60.98	12.5
HPT-2A	111	IIB1	HPT-2A-111	110.7	111.0	62.30	4.90	62.70	7.2
HPT-2A	113	IIB1	HPT-2A-113	112.7	113.0	58.47	4.76	56.35	11.8
HPT-2A	114	IIB1	HPT-2A-114	113.7	114.0	53.44	4.80	54.73	6.6
HPT-2A	115	IIB1	HPT-2A-115	114.7	115.0	59.10	4.80	60.19	6.3
HPT-2A	116	IIB1	HPT-2A-116	115.7	116.0	55.47	4.77	57.63	4.7
HPT-2A	117	IIB1	HPT-2A-117	116.7	117.0	57.96	4.82	60.74	3.5
HPT-2A	118	IIB1	HPT-2A-118	117.7	118.0	53.83	4.77	56.58	3.7
HPT-2A	119	IIB1	HPT-2A-119	118.7	119.0	57.04	4.92	59.60	4.1
HPT-2A	120	IIB1	HPT-2A-120	119.7	120.0	54.88	4.83	55.39	7.9
HPT-2A	121	IIB1	HPT-2A-121	120.7	121.0	58.95	4.86	50.95	21.8
HPT-2A	122	IIB1	HPT-2A-122	121.7	122.0	58.27	4.85	49.73	23.0

B-84

Table B8. (Continued)

Well	Depth (ft)	Hydro Unit	Sampled Interval			Weight (g)			Percent Carbonate
			Sample Designator	Top	Bottom	Initial Sample	Filter Paper	Filter + Residue	
HPT-2A	123	IIB1	HPT-2A-123	122.7	123.0	75.34	4.81	64.63	20.6
HPT-2A	124	IIB1	HPT-2A-124	123.7	124.0	72.14	4.84	60.43	23.0
HPT-2A	125	IIB1	HPT-2A-125	124.7	125.0	74.77	4.83	51.48	37.6
HPT-2A	126	IIB1	HPT-2A-126	125.7	126.0	79.09	4.83	55.06	36.5
HPT-2A	128	IIB1	HPT-2A-128	127.7	128.0	78.97	4.74	29.78	68.3
HPT-2A	129	IIB1	HPT-2A-129	128.7	129.0	79.25	4.82	58.40	32.4
HPT-2A	130	IIB1	HPT-2A-130	129.7	130.0	74.43	4.84	59.66	26.3
HPT-2A	131	IIB1	HPT-2A-131	130.7	131.0	62.37	4.81	54.89	19.7
HPT-2A	132	IIB1	HPT-2A-132	131.7	132.0	70.86	4.86	71.10	6.5
HPT-2A	133	IIB1	HPT-2A-133	132.7	133.0	56.98	4.83	56.67	9.0
HPT-2A	134	IIB1	HPT-2A-134	133.7	134.0	58.85	4.87	58.12	9.5
HPT-2A	135	IIB1	HPT-2A-135	134.7	135.0	66.13	4.83	63.24	11.7
HPT-2A	136	IIB1	HPT-2A-136	135.7	136.0	60.47	4.84	58.26	11.7
HPT-2A	138	IIA-IIB	HPT-2A-138	137.7	138.0	66.97	4.87	62.93	13.3
HPT-2A	139	IIA-IIB	HPT-2A-139	138.7	139.0	87.32	4.80	83.07	10.4
HPT-2A	140	IIA-IIB	HPT-2A-140	139.7	140.0	182.22	4.85	153.13	18.6
HSB-TB	92	IIB1	HSB-TB-092	91.0	91.3	57.21	5.82	62.75	0.5
HSB-TB	94	IIB1	HSB-TB-094	93.0	93.3	58.22	5.74	61.80	3.7
HSB-TB	96	IIB1	HSB-TB-096	95.0	95.3	61.13	5.81	65.18	2.9
HSB-TB	98	IIB1	HSB-TB-098	97.7	98.0	60.22	5.76	64.76	2.0
HSB-TB	100	IIB1	HSB-TB-100	99.0	99.3	61.39	5.79	62.01	8.4
HSB-TB	103	IIB1	HSB-TB-103	102.7	103.0	59.25	5.70	60.29	7.9

Table B8. (Continued)

Well	Depth (ft)	Hydro Unit	Sampled Interval			Weight (g)			Percent Carbonate
			Sample Designator	Top	Bottom	Initial Sample	Filter Paper	Filter + Residue	
HSB-TB	104	IIB1	HSB-TB-104	103.7	104.0	63.90	5.74	66.17	5.4
HSB-TB	105	IIB1	HSB-TB-105A	104.3	104.5	59.42	5.72	58.25	11.6
HSB-TB	105	IIB1	HSB-TB-105B	104.8	105.0	58.87	5.83	57.11	12.9
HSB-TB	110	IIB1	HSB-TB-110	109.5	109.7	90.83	5.82	37.48	65.2
HSB-TB	111	IIB1	HSB-TB-111	110.0	110.3	91.46	5.79	50.35	51.3
HSB-TB	112	IIB1	HSB-TB-112	111.5	111.7	83.51	5.84	50.57	46.4
HSB-TB	113	IIB1	HSB-TB-113	112.7	113.0	84.35	5.80	57.49	38.7
HSB-TB	114	IIB1	HSB-TB-114	113.7	114.0	86.74	5.83	59.03	38.7
HSB-TB	115	IIB1	HSB-TB-115	114.7	115.0	92.25	5.72	61.98	39.0
HSB-TB	116	IIB1	HSB-TB-116	115.7	116.0	86.50	5.75	54.27	43.9
HSB-TB	118	IIB1	HSB-TB-118	117.5	117.7	88.19	5.88	58.27	40.6
HSB-TB	119	IIB1	HSB-TB-119	118.3	118.5	92.34	5.72	68.60	31.9
HSB-TB	120	IIB1	HSB-TB-120	119.0	119.3	80.83	5.76	54.08	40.2
HSB-TB	123	IIB1	HSB-TB-123	122.4	122.6	159.39	5.81	87.72	48.6
HSB-TB	124	IIB1	HSB-TB-124	123.0	123.2	81.21	5.80	40.60	57.1
HSB-TB	125	IIB1	HSB-TB-125	124.7	124.9	134.73	5.66	60.68	59.2
HSB-TB	128	IIB1	HSB-TB-128	127.7	128.0	103.04	5.83	50.07	57.1
HSB-TB	129	IIB1	HSB-TB-129	128.7	129.0	131.82	5.72	49.41	66.9
HSB-TB	130	IIB1	HSB-TB-130	129.7	130.0	101.33	5.70	49.11	57.2
HSB-TB	131	IIB1	HSB-TB-131	130.7	131.0	181.27	5.81	65.32	67.2
HSB-TB	133	IIB1	HSB-TB-133	132.0	132.3	102.05	5.72	39.39	67.0
HSB-TB	134	IIB1	HSB-TB-134	133.2	133.5	149.00	5.73	67.18	58.8

Table B8. (Continued)

Well	Depth (ft)	Hydro Unit	Sampled Interval			Weight (g)			Percent Carbonate
			Sample Designator	Top	Bottom	Initial Sample	Filter Paper	Filter + Residue	
HSB-TB	138	IIB1	HSB-TB-138	137.7	138.0	58.88	5.77	63.25	2.4
HSB-TB	139	IIB1	HSB-TB-139	138.7	139.0	60.17	5.84	57.91	13.5
HSB-TB	140	IIB1	HSB-TB-140	139.7	140.0	60.04	5.75	54.25	19.2
HSB-TB	143	IIB1	HSB-TB-143	142.0	142.3	88.58	5.78	85.93	9.5
HSB-TB	143	IIB1	HSB-TB-143B	142.8	143.0	94.73	5.77	35.74	68.4
HSB-TB	145	IIB1	HSB-TB-145	144.0	144.3	135.61	5.78	62.00	58.5
HSB-TB	146	IIB1	HSB-TB-146	145.7	146.0	165.71	5.74	83.74	52.9
HSB-TB	147	IIB1	HSB-TB-147	146.7	147.0	87.43	5.77	84.59	9.8
HSB-TB	148	IIB1	HSB-TB-148	147.7	148.0	54.64	5.81	20.10	73.9
HSB-TB	149	IIB1	HSB-TB-149	148.7	149.0	112.16	5.67	52.34	58.4
HSB-TB	150	IIB1	HSB-TB-150	149.8	150.0	106.15	5.77	61.12	47.9
HSB-TB	152	IIB1	HSB-TB-152	151.6	151.7	72.42	5.77	53.02	34.8
HSB-TB	153	IIB1	HSB-TB-153	152.4	152.6	94.43	5.72	47.41	55.8
HSB-TB	154	IIB1	HSB-TB-154	153.5	153.6	97.70	5.73	32.95	72.1
HSB-TB	155	IIB1	HSB-TB-155	154.7	154.8	106.40	5.80	26.13	80.9
HSB-TB	156	IIB1	HSB-TB-156	155.5	155.6	77.25	5.69	24.47	75.7
HSB-TB	157	IIB1	HSB-TB-157	156.0	156.3	86.82	5.70	29.09	73.1
HSB-TB	158	IIA-IIIB	HSB-TB-158	157.3	157.6	149.63	5.89	140.78	9.9
HSB-TB	159	IIA-IIIB	HSB-TB-159	158.7	159.0	73.45	5.82	77.77	2.0
HSB-TB	160	IIA-IIIB	HSB-TB-160	159.7	160.0	136.98	5.80	138.36	3.2
HSB-TB	161	IIA-IIIB	HSB-TB-161	160.6	160.8	78.93	5.82	82.91	2.3
HSB-TB	162	IIA	HSB-TB-162	161.7	162.0	71.85	5.81	72.47	7.2



Table B8. (Continued)

Well	Depth (ft)	Hydro Unit	Sampled Interval			Weight (g)			Percent Carbonate
			Sample Designator	Top	Bottom	Initial Sample	Filter Paper	Filter + Residue	
HSB-TB	165	IIA	HSB-TB-165	164.7	165.0	59.98	5.80	64.49	2.1
HSB-TB	166	IIA	HSB-TB-166	165.7	166.0	57.18	5.85	61.75	2.2
HSB-TB	168	IIA	HSB-TB-168	167.7	168.0	55.06	5.74	59.59	2.2
HSB-TB	170	IIA	HSB-TB-170	169.7	170.0	54.63	5.73	60.05	0.6
YSC-5A	91	IIB1	YSC-5A-091	90.0	90.3	74.50	4.77	77.96	1.8
YSC-5A	92	IIB1	YSC-5A-092	91.2	91.4	133.07	4.77	134.38	2.6
YSC-5A	94	IIB1	YSC-5A-094	93.7	94.0	79.94	4.79	80.10	5.8
YSC-5A	95	IIB1	YSC-5A-095	94.7	95.0	71.28	4.78	64.43	16.3
YSC-5A	96	IIB1	YSC-5A-096	95.7	96.0	69.40	5.66	69.16	8.5
YSC-5A	97	IIB1	YSC-5A-097	96.7	97.0	76.51	4.67	77.23	5.2
YSC-5A	98	IIB1	YSC-5A-098	97.4	97.7	74.10	4.72	75.31	4.7
YSC-5A	99	IIB1	YSC-5A-099	98.7	99.0	69.40	4.76	54.14	28.8
YSC-5A	100	IIB1	YSC-5A-100	99.7	100.0	74.58	4.76	58.57	27.9
YSC-5A	101	IIB1	YSC-5A-101	100.7	101.0	58.90	4.77	61.50	3.7
YSC-5A	102	IIB1	YSC-5A-102	101.7	102.0	61.83	4.80	58.71	12.8
YSC-5A	103	IIB1	YSC-5A-103	102.3	102.5	52.74	4.77	56.41	2.1
YSC-5A	104	IIB1	YSC-5A-104	103.7	104.0	52.89	4.71	54.09	6.6
YSC-5A	105	IIB1	YSC-5A-105	104.7	105.0	58.27	4.71	57.78	8.9
YSC-5A	106	IIB1	YSC-5A-106	105.5	105.8	66.72	5.66	67.17	7.8
YSC-5A	107	IIB1	YSC-5A-107	106.3	106.5	64.14	4.80	62.63	9.8
YSC-5A	109	IIB1	YSC-5A-109	108.0	108.3	75.55	5.58	56.95	32.0
YSC-5A	110	IIB1	YSC-5A-110	109.0	109.2	76.05	5.62	44.39	49.0

B-8-8

Table B8. (Continued)

Well	Depth (ft)	Hydro Unit	Sampled Interval			Weight (g)			Percent Carbonate
			Sample Designator	Top	Bottom	Initial Sample	Filter Paper	Filter + Residue	
YSC-5A	111	IIB1	YSC-5A-111	110.0	110.3	64.36	5.67	60.55	14.7
YSC-5A	112	IIB1	YSC-5A-112	111.0	111.3	64.08	4.79	59.81	14.1
YSC-5A	113	IIB1	YSC-5A-113	112.0	112.3	69.46	4.79	65.09	13.2
YSC-5A	114	IIB1	YSC-5A-114	113.2	113.4	64.70	4.87	60.13	14.6
YSC-5A	115	IIB1	YSC-5A-115	114.0	114.3	63.55	5.58	50.46	29.4
YSC-5A	117	IIB1	YSC-5A-117	116.7	117.0	56.65	4.75	59.90	2.7
YSC-5A	118	IIB1	YSC-5A-118	117.7	118.0	58.82	4.85	60.93	4.7
YSC-5A	119	IIB1	YSC-5A-119	118.7	119.0	66.92	4.78	68.40	4.9
YSC-5A	120	IIB1	YSC-5A-120	119.7	120.0	54.64	4.72	56.98	4.4
YSC-5A	121	IIB1	YSC-5A-121	120.7	121.0	56.68	5.44	58.85	5.8
YSC-5A	122	IIB1	YSC-5A-122	121.7	122.0	54.80	4.74	56.61	5.3
YSC-5A	123	IIB1	YSC-5A-123	122.7	123.0	55.91	4.64	57.74	5.0
YSC-5A	124	IIB1	YSC-5A-124	123.7	124.0	48.43	4.75	50.83	4.9
YSC-5A	125	IIB1	YSC-5A-125	124.7	125.0	57.34	4.76	59.24	5.0
YSC-5A	126	IIB1	YSC-5A-126	125.7	126.0	48.46	5.73	51.30	6.0
YSC-5A	127	IIB1	YSC-5A-127	126.7	127.0	57.05	5.61	58.92	6.6
YSC-5A	128	IIB1	YSC-5A-128	127.7	128.0	54.54	4.80	53.32	11.0
YSC-5A	129	IIB1	YSC-5A-129	128.5	128.7	44.41	4.86	39.48	22.0
YSC-5A	130	IIB1	YSC-5A-130	129.5	129.8	54.34	5.57	57.16	5.0
YSC-5A	132	IIB1	YSC-5A-132	131.7	132.0	57.29	4.65	59.90	3.5
YSC-5A	133	IIB1	YSC-5A-133	132.7	133.0	60.12	4.67	61.74	5.1
YSC-5A	134	IIB1	YSC-5A-134	133.7	134.0	72.13	4.69	68.37	11.7

B-8-9

Table B8. (Continued)

Well	Depth (ft)	Hydro Unit	Sampled Interval			Weight (g)			Percent Carbonate
			Sample Designator	Top	Bottom	Initial Sample	Filter Paper	Filter + Residue	
YSC-5A	135	IIB1	YSC-5A-135	134.7	135.0	44.88	4.74	46.62	6.7
YSC-5A	138	IIA-IIIB	YSC-5A-138	137.7	138.0	77.82	5.65	74.93	11.0
YSC-5A	139	IIA-IIIB	YSC-5A-139	138.7	139.0	78.78	5.65	74.54	12.6
YSC-5A	140	IIA-IIIB	YSC-5A-140	139.7	140.0	77.26	4.79	71.55	13.6

Table B9. Insoluble Residue Data and Folk and Ward Grain-Size Statistics for the Greater than 62 Micron Insoluble Fra of GSA samples (from Richardson, 1991)

Well	Depth	Unit	% Carbonate	% Terrigenous		Mean (Phi)	Sorting (Phi)	Skewness	Graphic	Transformed
				%Sand	%Mud				Kurtosis	Kurtosis
BGO010A	129.0	IIB1	3.31	78.20	18.49	2.70	0.68	-0.01	0.94	0.49
BGO010A	130.0	IIB1	39.14	47.50	13.36	2.80	0.70	-0.13	0.93	0.48
BGO010A	131.0	IIB1	43.51	40.63	15.86	2.67	0.68	0.01	0.96	0.49
BGO010A	136.0	IIB1	40.58	44.92	14.50	2.47	0.47	0.09	1.09	0.52
BGO010A	137.0	IIB1	53.07	38.96	7.97	2.89	1.20	-0.45	3.19	0.76
BGO010A	147.0	IIB1	33.70	60.08	6.22	-0.76	2.48	0.88	0.49	0.33
BGO010A	151.6	IIB1	60.66	27.97	11.37	2.39	0.66	-0.13	1.23	0.55
BGO010A	153.8	IIB1	73.38	17.74	8.88	2.24	0.79	-0.03	1.17	0.54
BGO010A	157.0	IIB1	64.53	8.17	27.30	3.10	0.97	-0.51	1.03	0.51
BGO010A	160.0	IIB1	75.78	6.43	17.79	3.03	1.06	-0.35	0.99	0.50
BGO010A	163.0	IIB1	84.12	5.81	10.07	2.49	0.94	-0.10	1.29	0.56
BGO010A	165.0	IIB1	43.11	26.63	30.26	2.66	0.82	-0.20	1.57	0.61
BGO010A	165.5	IIB1	81.99	6.84	11.17	2.19	1.22	-0.31	1.09	0.52
BGO010A	167.5	IIB1	42.85	30.04	27.11	1.45	1.73	-0.13	0.73	0.42
BGO010A	168.5	IIA-IIB	27.44	55.08	17.48	0.04	1.95	-0.21	0.97	0.49
BGO010A	169.5	IIA-IIB	0.00	67.79	32.21	1.12	1.58	-0.09	0.92	0.48
BGO014A	120.0	IIB1	4.82	82.56	12.62	2.09	0.68	-0.23	1.33	0.57
BGO014A	122.5	IIB1	80.84	15.71	3.45	1.15	1.16	-0.27	0.77	0.44
BGO014A	126.0	IIB1	57.90	35.63	6.47	2.61	0.58	-0.11	1.27	0.56
BGO014A	130.0	IIB1	36.61	55.58	7.81	2.40	1.10	-0.30	3.85	0.79
BGO014A	133.5	IIB1	23.10	54.50	22.40	2.82	0.77	-0.20	1.05	0.51
BGO014A	140.0	IIB1	33.08	45.16	21.76	2.98	0.65	-0.21	0.98	0.49
BGO014A	148.0	IIB1	42.32	46.50	11.18	2.47	0.56	0.21	1.16	0.54
BGO014A	150.0	IIB1	27.45	59.89	12.66	2.38	0.46	0.27	1.64	0.62
BGO014A	156.0	IIB1	36.11	56.82	7.07	2.37	0.42	0.24	1.59	0.61
BGO014A	159.5	IIB1	65.91	27.64	6.45	2.56	0.58	0.14	1.05	0.51
BGO014A	160.0	IIB1	37.18	43.35	19.47	2.49	0.43	0.08	1.02	0.50

B-9-1

Table B9. (Continued)

Well	Depth	Unit	% Carbonate	% Terrigenous		Mean (Phi)	Sorting (Phi)	Skewness	Graphic	Transformed
				%Sand	%Mud				Kurtosis	Kurtosis
BGO014A	163.0	IIB1	6.12	69.22	24.66	2.30	0.49	0.03	1.09	0.52
BGO014A	164.0	IIB1	0.00	74.81	25.19	2.31	0.55	-0.03	1.22	0.55
BGO018A	139.0	IIB1	0.26	89.32	10.42	2.02	1.01	-0.28	1.24	0.55
BGO018A	140.0	IIB1	38.65	43.30	18.05	2.89	0.72	-0.21	0.94	0.48
BGO018A	145.0	IIB1	40.75	42.75	16.50	2.73	0.68	-0.07	0.89	0.47
BGO018A	150.0	IIB1	18.81	68.71	12.48	1.82	1.70	-0.52	2.11	0.68
BGO025A	119.0	IIB1	74.27	23.87	1.86	1.98	0.55	-0.02	1.17	0.54
BGO025A	124.0	IIB1	71.33	24.21	4.46	2.38	0.82	-0.31	1.56	0.61
BGO026A	184.0	IIA	3.36	56.91	39.73	2.15	0.37	-0.07	1.23	0.55
BGO026A	185.0	IIA	1.35	91.44	7.21	2.16	0.39	-0.09	1.28	0.56
BGO029A	125.0	IIB1	4.93	90.49	4.58	-1.49	1.75	0.82	1.19	0.54
BGO029A	127.0	IIB1	2.50	87.95	9.55	2.07	0.93	0.03	1.21	0.55
BGO029A	131.0	IIB1	1.07	91.92	7.01	1.76	0.37	0.01	1.39	0.58
BGO029A	136.0	IIB1	0.00	75.05	24.95	2.34	0.69	-0.13	1.07	0.52
BGO029A	140.0	IIA-IIB	0.00	80.58	19.42	0.13	2.33	-0.15	0.54	0.35
BGO029A	150.0	IIA-IIB	0.00	47.37	52.63	1.65	1.34	0.20	1.31	0.57
BGX002B	123.0	IIB1	73.16	24.48	2.36	2.02	0.99	-0.51	0.95	0.49
BGX002B	124.0	IIB1	77.05	19.69	3.26	1.85	1.02	-0.30	0.97	0.49
BGX002B	130.5	IIB1	57.57	38.67	3.76	0.90	1.13	0.88	0.35	0.26
BGX002B	161.0	IIA-IIB	11.74	61.71	26.55	0.94	1.32	-0.15	1.03	0.51
BGX002B	182.0	IIA	8.68	67.58	23.74	1.16	0.69	0.11	1.43	0.59
BGX004A	121.0	IIB1	0.67	93.37	5.96	2.99	0.44	0.03	1.00	0.50
BGX004A	127.0	IIB1	38.95	53.58	7.47	2.62	0.56	-0.05	1.10	0.52
BGX004A	128.0	IIB1	46.06	31.40	22.54	2.61	0.49	-0.11	1.25	0.56
BGX004A	131.0	IIB1	52.71	30.11	17.18	2.49	0.52	-0.19	1.06	0.51
BGX004A	135.0	IIB1	44.39	41.76	13.85	2.78	0.35	-0.06	1.31	0.57
BGX004A	139.0	IIB1	44.10	48.72	7.18	2.75	0.67	-0.09	0.94	0.48

Table B9. (Continued)

Well	Depth	Unit	% Carbonate	% Terrigenous		Mean (Phi)	Sorting (Phi)	Skewness	Graphic	Transformed
				%Sand	%Mud				Kurtosis	Kurtosis
BGX004A	141.3	IIB1	42.08	36.92	21.00	2.42	0.53	-0.25	1.02	0.51
BGX004A	143.3	IIB1	50.63	34.21	15.16	2.54	0.61	-0.09	1.15	0.53
BGX004A	144.0	IIB1	38.54	39.54	21.92	2.68	0.84	-0.02	1.07	0.52
BGX004A	145.5	IIB1	42.75	38.00	19.25	2.28	1.24	-0.21	1.20	0.55
BGX004A	146.0	IIB1	23.19	63.18	13.63	0.74	1.05	1.00	0.53	0.35
BGX004A	147.0	IIB1	75.70	15.59	8.71	2.56	0.74	-0.15	0.90	0.47
BGX004A	148.0	IIB1	63.99	17.17	18.84	2.82	1.61	-0.50	1.83	0.65
BGX004A	149.0	IIB1	68.89	8.06	23.05	2.94	0.92	-0.29	0.89	0.47
BGX004A	150.0	IIB1	63.65	12.07	24.28	2.96	1.05	-0.24	0.85	0.46
BGX004A	151.0	IIB1	70.10	9.35	20.55	2.86	1.04	-0.42	1.00	0.50
BGX004A	151.5	IIB1	4.55	44.55	50.90	2.99	0.64	0.00	1.03	0.51
BGX004A	160.5	IIA-IIB	15.01	43.53	41.46	2.23	1.46	-0.37	1.02	0.50
BGX004A	165.0	IIA-IIB	3.16	27.86	68.98	2.18	1.36	-0.59	2.25	0.69
BGX004A	169.0	IIA	1.66	89.66	8.68	0.18	1.33	0.23	1.17	0.54
BGX009A	137.0	IIB1	0.00	49.59	50.41	2.70	1.11	-0.03	0.89	0.47
FSB100A	127.5	IIB1	13.13	79.68	7.19	1.63	0.71	0.26	0.81	0.45
FSB100A	130.0	IIB1	36.87	33.92	29.21	2.37	0.87	0.12	0.90	0.47
FSB100A	138.5	IIB1	33.08	59.39	7.53	2.32	0.69	-0.09	0.99	0.50
FSB100A	138.9	IIB1	44.08	50.84	5.08	2.42	0.64	-0.12	1.08	0.52
FSB100A	139.3	IIB1	54.88	41.48	3.64	2.63	0.60	-0.14	1.13	0.53
FSB100A	144.0	IIB1	64.41	25.89	9.70	1.65	1.02	-0.18	1.21	0.55
FSB100A	150.0	IIB1	44.03	49.79	6.18	2.32	0.63	0.01	0.99	0.50
FSB100A	153.0	IIB1	0.00	80.35	19.65	2.10	0.74	0.27	1.26	0.56
FSB114A	103.0	IIB1	2.70	87.65	9.65	1.02	1.11	-0.12	1.14	0.53
FSB114A	104.0	IIB1	37.44	37.59	24.97	1.92	0.69	-0.44	1.38	0.58
FSB114A	106.0	IIB1	59.16	33.97	6.87	2.02	0.53	-0.24	1.35	0.57
FSB114A	109.0	IIB1	85.82	12.66	1.52	2.12	0.46	-0.17	1.26	0.56

Table B9. (Continued)

Well	Depth	Unit	% Carbonate	% Terrigenous		Mean (Phi)	Sorting (Phi)	Skewness	Graphic	Transformed
				%Sand	%Mud				Kurtosis	Kurtosis
FSB114A	110.0	IIB1	81.67	15.44	2.89	1.96	0.46	-0.03	1.09	0.52
FSB114A	114.0	IIB1	0.00	88.82	11.18	1.88	1.09	-0.46	1.93	0.66
FSB116C	56.0	IIB1	0.00	88.95	11.05	2.04	0.38	-0.07	0.91	0.48
FSB116C	57.0	IIB1	24.16	72.58	3.26	1.77	0.58	-0.24	1.03	0.51
FSB116C	61.0	IIB1	39.26	50.49	10.25	2.51	0.58	0.12	1.15	0.53
FSB116C	66.0	IIB1	28.25	62.80	8.95	2.46	0.64	-0.23	1.14	0.53
FSB116C	69.0	IIB1	1.78	88.12	10.10	2.63	0.91	-0.23	1.61	0.62
HMD001C	88.0	IIB1	0.71	91.36	7.93	2.86	0.90	-0.32	2.38	0.70
HMD001C	90.0	IIB1	46.91	45.49	7.60	2.66	0.57	-0.07	1.07	0.52
HMD001C	95.0	IIB1	46.98	34.94	18.08	2.83	0.45	-0.02	1.01	0.50
HMD001C	101.0	IIB1	40.23	39.55	20.22	2.58	0.56	-0.10	1.05	0.51
HMD001C	104.0	IIB1	42.62	43.41	13.97	2.46	0.56	-0.15	1.14	0.53
HMD001C	108.0	IIB1	37.01	32.00	30.99	3.10	0.78	-0.13	1.06	0.51
HMD001C	114.0	IIB1	84.78	5.45	9.77	2.60	1.11	-0.15	0.98	0.50
HMD001C	120.0	IIB1	29.00	50.08	20.92	1.60	2.69	-0.74	0.66	0.40
HMD001C	121.0	IIB1	78.22	12.76	9.02	2.42	1.18	-0.34	1.09	0.52
HMD001C	124.0	IIB1	30.79	38.79	30.42	2.97	0.90	-0.30	1.69	0.63
HMD001C	125.0	IIA-IIB	39.68	35.23	25.09	1.39	1.61	-0.18	0.67	0.40
HMD001C	128.0	IIA-IIB	32.88	54.74	12.38	0.53	1.77	-0.10	1.01	0.50
HMD003C	93.0	IIB1	33.65	47.65	18.70	2.64	0.56	-0.06	1.03	0.51
HPT002A	101.0	IIB1	0.00	89.47	10.53	2.01	0.55	-0.24	1.35	0.57
HPT002A	102.0	IIB1	27.88	60.66	11.46	2.23	0.80	-0.02	1.19	0.54
HPT002A	104.0	IIB1	39.22	46.24	14.54	2.40	0.93	0.06	0.92	0.48
HPT002A	108.0	IIB1	73.49	19.50	7.01	2.81	0.78	-0.31	1.21	0.55
HPT002A	111.0	IIB1	26.30	55.47	18.23	3.05	0.68	-0.16	1.15	0.53
HPT002A	112.0	IIB1	7.00	85.47	7.53	2.34	1.20	-0.41	0.80	0.44
HPT002A	117.0	IIB1	0.00	89.09	10.91	1.42	1.31	-0.16	0.83	0.45

Table B9. (Continued)

Well	Depth	Unit	% Carbonate	% Terrigenous		Mean (Phi)	Sorting (Phi)	Skewness	Graphic	Transformed
				%Sand	%Mud				Kurtosis	Kurtosis
HPT002A	119.0	IIB1	11.88	67.63	20.49	1.61	2.04	-0.59	0.99	0.50
HPT002A	122.0	IIB1	0.00	70.22	29.78	2.18	1.53	-0.50	1.28	0.56
HPT002A	123.0	IIB1	30.37	56.19	13.44	2.65	0.36	-0.10	1.29	0.56
HPT002A	125.0	IIB1	30.81	45.73	23.46	2.69	0.88	-0.39	3.44	0.77
HPT002A	128.0	IIB1	21.62	60.55	17.83	2.55	0.51	-0.16	1.18	0.54
HPT002A	133.0	IIB1	4.78	72.52	22.70	2.64	0.73	0.07	1.08	0.52
HPT002A	135.0	IIB1	1.39	68.29	30.32	2.55	0.81	0.03	0.99	0.50
HPT002A	138.0	IIA-IIB	1.61	50.31	48.08	2.25	1.09	0.04	1.07	0.52
HSB085A	132.0	IIB1	62.06	31.15	6.79	2.69	0.72	-0.09	0.98	0.49
HSB085A	137.0	IIB1	5.45	81.75	12.80	2.41	1.04	-0.35	1.20	0.55
HSB085A	144.0	IIB1	14.50	65.63	19.87	3.02	0.66	-0.12	1.12	0.53
HSB085A	151.0	IIB1	38.91	45.79	15.30	2.49	0.84	-0.07	1.26	0.56
HSB085A	151.5	IIB1	15.15	79.89	4.96	1.71	0.90	-0.24	1.40	0.58
HSB085A	152.0	IIB1	42.43	43.07	14.50	1.92	0.77	0.01	1.21	0.55
HSB085A	157.0	IIB1	9.31	87.14	3.55	2.05	0.60	0.07	1.16	0.54
HSB085A	160.0	IIB1	1.28	87.10	11.62	2.31	0.36	0.09	1.50	0.60
HSB085A	161.0	IIB1	0.00	85.32	14.68	2.26	0.42	-0.04	1.70	0.63
HSB118A	100.0	IIB1	7.52	82.86	9.62	2.08	0.56	-0.02	1.24	0.55
HSB118A	103.0	IIB1	34.01	57.22	8.77	2.39	0.55	0.00	1.04	0.51
HSB118A	105.0	IIB1	2.49	85.06	12.45	2.52	0.66	0.03	1.06	0.51
HSB120A	160.0	IIA	0.00	89.24	10.76	2.30	0.81	-0.02	0.93	0.48
HSB120A	164.0	IIA	3.35	90.32	6.33	2.42	0.74	-0.20	1.16	0.54
HSB120A	165.0	IIA	3.07	94.81	2.12	2.05	0.76	0.04	0.99	0.50
HSB120A	167.0	IIA	10.13	86.85	3.02	1.37	1.33	-0.05	1.63	0.62
HSB120A	173.0	IIA	2.59	94.19	3.22	1.57	1.37	-0.18	0.81	0.45
HSB120A	176.0	IIA	1.67	97.11	1.22	1.19	0.65	0.18	1.06	0.51
HSB120A	180.0	IIA	0.72	97.71	1.57	1.78	0.54	-0.01	1.17	0.54



Table B9. (Continued)

Well	Depth	Unit	% Carbonate	% Terrigenous		Mean (Phi)	Sorting (Phi)	Skewness	Graphic Transformed	
				%Sand	%Mud				Kurtosis	Kurtosis
HSB120A	181.0	IIA	8.08	90.75	1.17	0.71	0.98	0.06	0.89	0.47
HSB120A	185.0	IIA	0.07	95.96	3.97	1.86	0.83	-0.29	2.42	0.71
HSB140A	88.0	IIB1	0.00	68.47	31.53	1.71	1.04	-0.42	1.88	0.65
HSB140A	89.0	IIB1	17.39	63.76	18.85	2.01	0.50	-0.11	1.16	0.54
HSB140A	93.0	IIB1	47.49	43.02	9.49	3.08	0.48	-0.21	1.21	0.55
HSB140A	96.0	IIB1	68.68	25.23	6.09	2.27	0.78	-0.21	1.14	0.53
HSB140A	98.0	IIB1	49.09	41.39	9.52	2.21	0.70	-0.01	1.15	0.54
HSB140A	100.0	IIB1	65.34	27.43	7.23	2.09	0.75	-0.06	1.34	0.57
HSB145C	76.0	IIB1	9.96	68.15	21.89	1.94	0.57	-0.36	1.22	0.55
HSB145C	80.0	IIB1	0.51	86.79	12.70	1.39	1.18	-0.17	0.87	0.46
HSB145C	87.0	IIB1	6.81	84.53	8.66	1.93	1.32	-0.51	1.86	0.65
HSB145C	90.0	IIB1	59.63	34.62	5.75	1.99	0.75	-0.11	1.13	0.53
HSB145C	95.0	IIB1	53.46	40.37	6.17	2.25	0.81	-0.07	1.00	0.50
HSB145C	100.0	IIB1	19.51	75.64	4.85	2.13	0.83	-0.07	1.03	0.51
HSBTB	111.0	IIB1	42.83	47.06	10.11	2.52	0.75	-0.06	0.99	0.50
HSBTB	117.0	IIB1	44.29	48.31	7.40	2.47	0.72	0.04	1.00	0.50
HSBTB	120.0	IIB1	29.82	62.64	7.54	2.61	0.68	0.01	0.94	0.48
HSBTB	123.0	IIB1	55.55	37.43	7.02	2.39	0.80	0.05	0.88	0.47
HSBTB	127.0	IIB1	65.01	28.52	6.47	2.08	0.72	0.16	1.24	0.55
HSBTB	131.0	IIB1	62.20	29.35	8.45	2.46	0.77	-0.10	1.09	0.52
HSBTB	134.0	IIB1	70.58	23.56	5.86	2.56	0.83	-0.11	0.97	0.49
HSBTB	137.0	IIB1	11.36	81.37	7.27	1.82	0.60	-0.24	1.33	0.57
HSBTB	138.0	IIB1	7.04	80.60	12.36	2.51	0.88	-0.16	1.08	0.52
HSBTB	140.0	IIB1	7.46	89.64	2.90	1.80	0.54	-0.17	1.25	0.56
HSBTB	146.0	IIB1	57.65	24.18	18.17	2.03	0.83	-0.23	1.02	0.51
HSBTB	147.0	IIB1	0.00	78.58	21.42	1.87	0.64	-0.21	1.24	0.55
HSBTB	149.0	IIB1	38.20	7.59	54.21	3.11	1.22	-0.69	1.37	0.58

Table B9. (Continued)

Well	Depth	Unit	% Carbonate	% Terrigenous		Mean (Phi)	Sorting (Phi)	Skewness	Graphic	Transformed
				%Sand	%Mud				Kurtosis	Kurtosis
HSBTB	151.9	IIB1	43.61	43.18	13.21	3.46	0.70	-0.54	1.96	0.66
HSBTB	152.0	IIB1	33.09	2.67	64.24	-0.84	2.32	0.74	0.60	0.37
HSBTB	153.0	IIB1	36.34	2.90	60.76	3.04	1.41	-0.73	1.54	0.61
HSBTB	155.0	IIB1	82.17	4.82	13.01	1.75	1.18	-0.10	1.26	0.56
HSBTB	159.0	IIA-IIB	2.65	79.77	17.58	2.69	0.34	-0.06	1.38	0.58
P018TA	125.0	TC	0.00	76.73	23.27	1.38	0.96	-0.14	1.20	0.54
P018TA	126.5	IIB1	46.81	34.01	19.18	1.33	1.24	-0.21	0.94	0.48
P018TA	130.0	IIB1	53.49	35.82	10.69	1.60	0.96	0.06	0.96	0.49
P018TA	138.0	IIB1	62.88	22.93	14.19	2.37	1.10	-0.42	1.74	0.64
P018TA	143.0	IIB1	24.19	66.75	9.06	1.09	0.96	0.05	0.98	0.50
P018TA	148.0	IIB1	71.14	21.71	7.15	1.11	1.11	-0.21	1.02	0.50
P018TA	152.0	IIB1	3.02	90.55	6.43	1.35	0.88	0.02	1.04	0.51
P018TA	157.0	IIA-IIB	0.00	93.99	6.01	1.25	0.47	0.00	0.96	0.49
YSC002A	94.0	IIB1	0.00	76.66	23.34	3.17	0.56	-0.10	1.01	0.50
YSC002A	95.0	IIB1	37.95	48.28	13.77	2.98	0.67	-0.19	1.18	0.54
YSC002A	103.0	IIB1	17.68	77.51	4.81	2.80	0.47	0.10	1.21	0.55
YSC002A	108.0	IIB1	21.85	53.08	25.07	3.00	1.22	-0.30	1.99	0.67
YSC002A	113.0	IIB1	47.82	33.03	19.15	2.05	1.02	-0.03	1.33	0.57
YSC002A	117.0	IIB1	73.09	17.19	9.72	1.37	1.63	-0.24	0.79	0.44
YSC002A	119.0	IIB1	0.00	73.69	26.31	2.18	1.30	-0.32	0.92	0.48
YSC004A	107.0	IIB1	0.65	88.07	11.28	3.21	0.41	-0.04	1.25	0.56
YSC004A	109.0	IIB1	23.21	60.93	15.86	3.18	0.55	-0.11	1.10	0.52
YSC004A	114.0	IIB1	47.04	31.38	21.58	2.93	1.45	-0.59	2.34	0.70
YSC004A	125.0	IIB1	65.09	23.23	11.68	2.41	0.97	-0.16	1.10	0.52
YSC004A	133.0	IIA-IIB	79.56	8.78	11.66	1.34	1.46	-0.20	0.89	0.47
YSC004A	138.0	IIA-IIB	9.95	55.27	34.78	1.45	1.64	0.13	0.69	0.41
YSC004A	139.0	IIA-IIB	0.00	7.09	92.91	2.85	1.24	-0.62	1.30	0.57

Table B9. (Continued)

Well	Depth	Unit	% Carbonate	% Terrigenous		Mean (Phi)	Sorting (Phi)	Skewness	Graphic Kurtosis	Transformed Kurtosis
				%Sand	%Mud					
YSC005A	97.0	IIB1	0.00	70.73	29.27	3.15	0.58	-0.19	1.33	0.57
YSC005A	98.0	IIB1	27.68	49.66	22.66	2.90	0.68	-0.25	1.16	0.54
YSC005A	101.0	IIB1	0.00	75.87	24.13	2.50	0.80	-0.10	1.13	0.53
YSC005A	105.0	IIB1	0.00	59.51	40.49	2.90	0.87	-0.30	1.02	0.50
YSC005A	108.0	IIB1	32.79	50.55	16.66	2.56	1.01	-0.29	1.10	0.52
YSC005A	116.0	IIB1	11.96	73.88	14.16	1.28	2.57	-0.74	1.20	0.55